SYNTHESIS, CHARACTERIZATION, AND EVALUATION OF DIHYDROXYACETONE BASED POLYMERS FOR USE AS RAPIDLY DEGRADING FUNCTIONAL BIOMATERIALS

A Dissertation

Presented to the Faculty of the Graduate School

of Cornell University

In Partial Fulfillment of the Requirements for the Degree of

Doctor of Philosophy

By

Nicole Grace Ricapito

August 2016

SYNTHESIS, CHARACTERIZATION, AND EVALUATION OF DIHYDROXYACETONE BASED POLYMERS FOR USE AS RAPIDLY DEGRADING FUNCTIONAL BIOMATERIALS

Nicole Grace Ricapito, Ph. D.

Cornell University 2016

Novel polymeric biomaterials are continuously under investigation for the advancement of human health. Biocompatibility and biodegradability are among the most crucial factors to consider when designing materials for biomedical applications. One common method to reduce the risk of inflammation and toxicity is to synthesize macromolecular structures from metabolic synthons. Dihydroxyacetone (DHA) is a triose sugar that plays an important role in the glycolysis cycle. To date, several DHA-based synthetic polymers have been developed that show promise as controlled drug delivery devices, seroma prevention tools, and hemostatic agents. In the present work, two properties of DHA-based materials are studied to shed light on future potential applications: degradation rates in aqueous environments and reactivity with amine-containing compounds.

The present work consists of three main goals. The first was to gain insight into the mechanism of rapid degradation of DHA-based hydrogels in aqueous environments. A new class of DHA-based polycarbonate hydrogels was synthesized and studied in comparison to similar non-DHA containing hydrogels. Comparative degradation studies reveal that the ketone present in DHA is the leading cause for the observed rapid degradation rates. The short carbon chain length between carbonate bonds and neighboring ketone groups is also a contributing factor. The second goal was to exploit the degradation behavior of DHA-based polycarbonates to develop a

new surgical device: a rapidly biodegradable shield to protect abdominal organs, such as the intestines, from injury during abdominal closure after a laparotomy (ex: to prevent inadvertent needle puncture while suturing components of the abdominal wall). The DHA-based hydrogels synthesized for this study were found to uphold rapid degradation rates in a mouse model, demonstrate promising resistance to inadvertent needle puncture, and appeared to not cause inflammation by visual inspection of the abdomen post-degradation. The third goal of the work was to gain insight into the rate of Schiff base formation between the ketone of DHA and amine containing compounds. A model reaction between DHA and ethanolamine was studied using real-time infrared spectroscopy. The kinetic analysis presented herein is a simplistic first step in a broader initiative to gain understanding of the potential for DHA-based materials in amine reactive surface applications.

Overall, DHA-based materials are excellent candidates for applications requiring rapid degradation in aqueous environments, amine reactive functionality, or combinations thereof. Insight into basic material properties that can translate across different polymer compositions will facilitate the rational design of future DHA-based materials and thereby open doors for novel biomaterials.

BIOGRAPHICAL SKETCH

Nicole G. Ricapito was born on June 14,th 1988 to Jo-Anne and Thomas Ricapito. She attended Putnam Valley High School where she was a year-round athlete and graduated as salutatorian in June of 2006. Nicole was awarded the Rensselaer Medal to attend Rensselaer Polytechnic Institute and graduated magna cum laude in 2010 with a B.S. degree in Chemical Engineering. During her time at RPI, she performed undergraduate research under the guidance of Dr. Pankaj Karande and also became a member of Alpha Omega Epsilon, a professional and social sorority dedicated to the advancement of women in engineering and technical sciences. In 2010, Nicole began her doctoral research at Cornell University under the direction of Dr. David Putnam where she was able to pursue a long time interest in polymer chemistry. In addition to her studies, Nicole participated in several educational outreach programs in accordance with her passion for STEM education.

To Jo-Anne and Thomas Ricapito, for a lifetime of boundless support and encouragement

ACKNOWLEDGMENTS

I would first like to thank my advisor, Dr. David Putnam, for welcoming me into his lab and providing support throughout the academic program. I am particularly thankful for his open mind with regard to new research projects and directions, which fostered my growth in creativity and independence.

I would also like to thank my committee members Dr. Geoffrey Coates and Dr. Jeffrey Varner for their advice and guidance on my work.

Thank you to Dr. Jason Spector and his research team for our exciting collaboration, which has provided me an enhanced understanding of the clinical world as well as new perspectives on biomaterial development.

Thank you to Dr. Ivan Keresztes for many long conversations in front of NMR spectra; his expertise, kindness, and eagerness to help have made much of this work possible. Also, thank you to Anthony Condo for his assistance with various additional polymer characterization techniques.

Thank you to Dr. Mark Grinstaff of Boston University for his contributions to our collaborative review article; his involvement helped guide me through the publication process, enhance my knowledge of the field, and strengthen my professional development.

I would especially like to thank all the Putnam Lab members for their insights into my work over the years, their assistance in lab, and for creating the most welcoming of environments. It has been inspiring to work alongside such an intelligent, creative, and hard-working group of individuals. I am extremely grateful for our time both inside and outside the lab as they have helped pull me through all the inevitable challenges of a PhD program.

I would also like to thank my TA Training crew for creating a wonderful outlet where I can share my passion for teaching. Their ideas, opinions, and past experiences will continue to have a positive influence on me for years to come. I would especially like to thank Linda J.

Tompkins for her support during my doctoral program and for creating a funding opportunity that enabled me to deeply strengthen my leadership skills.

Thank you to all my family and friends. Thank you to Kyle Watters for years of love, laughter, and encouragement, as well as countless research-based discussions that have helped me grow as a scientist. Thank you to my family for showing me the meaning of hard work and perseverance; each of their unique challenges and accomplishments has been an inspiration. Thank you to my amazing friends for making my time at Cornell a memorable experience. I will always value my Thursday night pizza club, "awful movies on Netflix" nights, BreakFree dance practices, intramural softball games, and so many more good times.

My dissertation is dedicated to my parents, Jo-Anne and Thomas Ricapito, for everything they've done that has enabled me to go to college. My journey was as new to them as it was to me. Every new college-directed idea that came about was a challenge they did not hesitate to take on. My successes are as much theirs as they are mine. I couldn't have made it here without their never ending love and support – thank you.

TABLE OF CONTENTS

LIST OF FIGURES

LIST OF TABLES

CHAPTER 1

INTRODUCTION

(Contributors: Cynthia Ghobril, Heng Zhang, and Mark W. Grinstaff)

Metabolic synthons have been a subject of interest in the development of biocompatible biomaterials for decades. One of the earliest examples is the development of biodegradable sutures from glycolic acid in the late 1960s and early 1970s.[1,2] The human metabolome contains thousands of metabolites with a diverse set of structures that have proven highly advantageous in a wide range of applications.[3,4] For example, polymeric materials designed from hydroxy acids such as lactic acid, glycolic acid, and 6-hydroxyhexanoic acid have shown use in drug delivery, tissue engineering, and packaging.[5–8] Polymers derived from natural amino acids have been used in the synthesis of cortical neural probe carriers as well as surgical adhesives and sealants.[9–11] Macromolecular structures designed with glycerol have demonstrated use in tumor recurrence reduction, tissue engineering scaffolds, corneal wound repair, and controlled drug delivery.[12–15] Saccharides are also used in polymeric drug delivery vehicles and have been explored for vaccine development and biosensing as well.[16–18]

The premise of using metabolites for the synthesis of biodegradable biomaterials is that the body is equipped with natural pathways to eliminate downstream polymer degradation products, thereby reducing risks of inflammation and toxicity. The present work focuses on one particular metabolic synthon: dihydroxyacetone. The research goal is to shed light on properties of DHA, and polymers thereof, to gain a larger appreciation for potential future applications. Several strategies have been established for the development of DHA-based macromolecules that

*Sections 1.1 through 1.5.4. are reprinted with permission from Ricapito, N. G.; Ghobril, C.; Zhang, H.; Grinstaff, M. W.; Putnam, D. Synthetic Biomaterials from Metabolically Derived Synthons. *Chem. Rev.* **2016,** 116, 2664–2704. Copyright (2016) American Chemical Society.

can be exploited to expand the current library of DHA-based materials. To better understand the opportunities and limitations of current synthetic strategies as well as key features of present technologies, a comprehensive review of DHA-based polymers is provided. Polymerization routes, polymer architectures and linkages, form factors (ex: hydrogels, microparticles, etc.), and applications are discussed.

1.1. Dihydroxyacetone Overview

Dihydroxyacetone (DHA, I, Figure 1.1a), a three-carbon sugar, is an important metabolite in humans, yeast, bacteria, and plants. The awareness of DHA, sometimes called "dioxyacetone," in carbohydrate metabolism dates back to the early 1900s.[19,20] One of the first proposed therapeutic applications of DHA was for the treatment of diabetes. Rabinowitch published reports on the ability of DHA to reduce the dosage of insulin needed by diabetics.[19,21–23] It was not until the late 1950s, however, that DHA gained interest for its first major commercial use: sunless tanning lotions. Eva Wittgenstein noticed that when children accidentally "spit up" an orally administered solution of DHA onto their skin, pigmentation occurred.[24] While it had been previously known that sugars react with primary amines to form brown pigments known as melanoidins, a reaction discovered by Maillard in 1912,[25] and more mechanistically detailed by Hodge in 1953,[26] it was Wittgenstein and Berry who drew a connection between the browning in foods and the browning of skin from DHA.[27] They suggested that the mechanism through which DHA functions as an artificial tanning lotion is a reaction between the carbonyl group of DHA and the basic groups of amino acids in proteins present on the surface of the skin.[27,28] To date, DHA-based artificial tanning lotions are FDA approved for topical use and remain a popular selling item. Although, some controversy has arisen over the unknown long-term health effects

of the inhalation of spray tan products, as well as postapplication UV exposure and the generation of harmful reactive oxygen species,[29–31] DHA-based artificial tanning lotions continue to be accepted as a safe alternative to UV-based tanning.[32–34] A brief review on the safety concerns of DHA-based sunless tanners is covered by Pagoto.[32]

DHA's reactive ketone functionality, two α-hydroxy groups, and metabolic involvement are key reasons why this synthon is of continued interest. From a topical standpoint, DHA shows potential as a treatment for proliferative skin diseases such as psoriasis and eczema, a cosmetic solution to the masking of vitiligo, and as an ingredient for controlled release mosquito-repellent formulations.[35–39] DHA has been studied for internal use in diet formulations as a method to prolong muscle endurance (oral LD_{50} in rats is >16,000 mg/kg) and also as a preventative for cyanide poisoning.[34,40–42] In this section, we will cover macromolecules that are synthesized from DHA and their intended applications.

1.1.1. Dihydroxyacetone Phosphate in Metabolism

As mentioned above, the premise of using metabolites as monomer units for synthesis of biodegradable polymers is that the body is already equipped with pathways to eliminate downstream polymer degradation products. The natural form of DHA in metabolism is dihydroxyacetone phosphate (DHAP). Once DHA enters the bloodstream, it can be phosphorylated by DHA kinases and entered into a metabolic pathway if not otherwise eliminated through natural disposal of excess or foreign material.[43]

Glycolysis, the breakdown of glucose for energy, is the most well-known source of DHAP in the body. DHAP, as well as the structural isomer glyceraldehyde-3-phosphate, are generated during the initial "energy consumption" stages of glycolysis, which is followed by a

series of reactions resulting in pyruvate and a net positive production of ATP: the cellular "energy currency." DHAP is also an intermediate in the breakdown of other common dietary sugars including fructose, mannose, and galactose. During times of starvation, when sugar supply is low, the liver will perform gluconeogenesis, a pathway in which glucose is synthesized so that it can be released into the bloodstream and sent to necessary organs such as the brain. DHAP plays an important role in gluconeogenesis as the pathway operates much like a reverse glycolysis cycle, requiring several of the same intermediates.[44]

In addition to carbohydrate metabolism, DHAP is often involved in the storage of lipids. DHAP is a precursor to the glycerol backbone of triglycerides, the major method of energy storage in the body. DHAP is first generated through glycolysis before use in triacylglycerol synthesis, thus being one of the many molecules that make metabolic processes interdependent.[44]

1.1.2. Structure and Reactivity

Pentose and hexose sugars, such as fructose and glucose, exist as 5- or 6-membered rings due to intramolecular nucleophilic addition reactions between their carbonyl and hydroxyl groups. As a triose, DHA cannot react intramolecularly to form an energetically favorable ring. DHA instead reacts intermolecularly to form a hemi-acetal dimer, the commercially available form of DHA, as shown in Figure 1.1a.[45] Davis observed that in aqueous solutions the dimer dissociates into ketone and gem-diol forms (Figure 1.1b).[46] Lyophilization of a stirred aqueous solution of dimer can be used to obtain a solid form of the keto-monomer.[46,47] Davis also discovered that in solution, the ketone and hydrate exist in a 4:1 ratio, respectively, at room temperature. [46] Infrared and nuclear magnetic resonance studies on DHAP indicate that the ketone:hydrate ratio is temperature dependent with a trend for increasing ketone content with increasing temperature.[48]

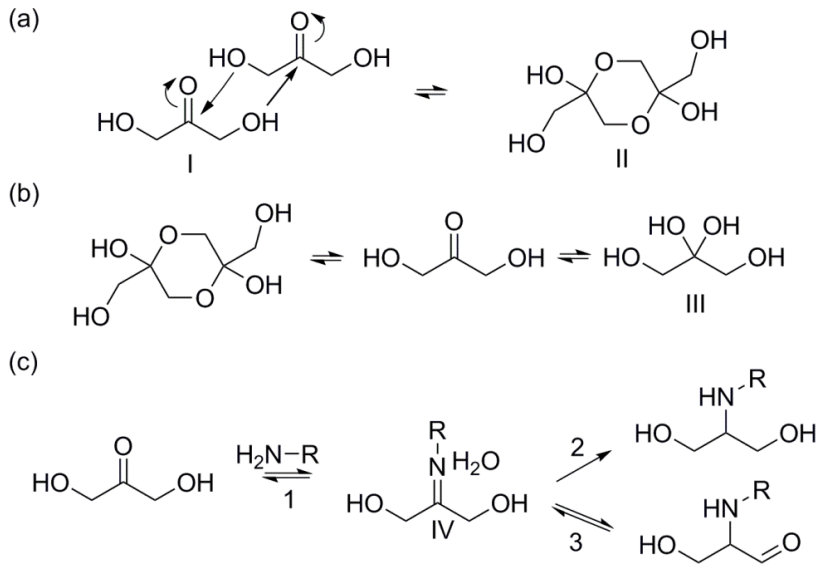

Figure 1.1 DHA structure and reactivity. (a) DHA dimerization mechanism.[45] (b) Dissociation of DHA dimer in aqueous solutions. (c) (1) Reversible reaction of DHA with a primary amine to form a Schiff base, (2) reductive amination to a secondary amine, and (3) Heyns rearrangement. Nomenclature: I, DHA; II, DHA dimer; III, gem-diol (DHA hydrate). Reprinted with permission from reference 4. Copyright (2016) American Chemical Society.

A key feature of DHA is the carbonyl group, which can react with primary and secondary amines. Reactions of DHA with amino compounds are of interest in several diverse fields including biomedical materials, enzyme mechanism determination, and cosmetics.[49–52] When a primary amine reacts with the ketone, an imine is formed, commonly known as a Schiff base (IV, Figure 1.1c). The reaction is reversible (1, Figure 1.1c) but can be made irreversible through reductive amination with a reducing agent such as sodium cyanoborohydride (2, Figure 1.1c).[49,53] A third possible outcome following imine formation is a Heyn's rearrangement (3, Figure 1.1c): a presumed step in a series of rearrangements and reactions leading to Maillard-type products and browning.[54,55] Precise reaction mechanisms leading to melanoidins are difficult to confirm as the Maillard reaction is known to be highly dependent on the specific amine reagent, pH of

solution, temperature, and various other reaction conditions.[56,57]

The high chemical reactivity of the carbonyl group in combination with the ability of DHA to possess multiple forms in solution limits the number of polymerization conditions and catalysts that can be applied to DHA. In this next section, we cover several synthetic procedures used to successfully synthesize polycarbonates and poly(carbonate-esters) of DHA.

1.2 Ring-Opening Polymerization

Ring-opening polymerization (ROP) is a highly effective and widely used technique to generate polyesters, polycarbonates, polyamides, polyethers, and others.[58] Fine tuning of the ratio between cyclic monomers, catalysts, and initiators affords controlled syntheses of high molecular weight polymers with low PDIs, as well as reproducible thermal and mechanical properties. Polycarbonates, in particular, are of interest in biomedical applications due to their strength, biodegradability and versatility. For example, various polycarbonate materials are receiving considerable attention for the development of controlled drug delivery systems[59–63] and regenerative medicine.[64–66] ROP is among the most widely used techniques for generating polycarbonates. Song et al. and Zhang et al. recently reviewed a number of cyclic carbonates used in the ROP of aliphatic polycarbonates as well as their biomedical applications.[67,68]

Cyclic ketone-protected carbonate derivatives of DHA are used to synthesize homopolymers, random copolymers, and diblock copolymers via ROP with a variety of catalyst/initiator combinations. This discussion focuses on the synthesis of cyclic DHA derivatives, catalysts used in the ROP of DHA-based polymers, postpolymerization modification, polymers synthesized through these methods, and applications of the reported polymers.

1.2.1. Ketone Protection

DHA is commercially available as a dimer, which is transformed into a stable monomeric form for subsequent polymerization. The most common methods to generate DHA-based macromolecules involve protection of the reactive ketone group. Ketone protection poses two major advantages: (1) dimerization is no longer feasible, enabling a pure monomeric derivative of DHA to be obtained and (2) the likelihood of unwanted side reactions decreases, offering a greater number of plausible starting materials and catalysts.

Two cyclic ketone-protected DHA derivatives are used for ROP: 2,2-dimethoxypropylene carbonate (MeO_2DHAC)[49] and 2,2-ethylenedioxypropane-1,3-diol carbonate (EOPDC).[69,70] MeO_2DHAC possesses a dimethoxy-acetal protecting group, whereas EOPDC contains a cyclic acetal. The synthesis of MeO_2DHAC occurs in two stages as shown in Figure 1.2a. In the first stage, dimethoxy-protected DHA monomer, 2,2-dimethoxy-propane-1,3-diol (MeO_2DHA), is synthesized by combining the DHA dimer with trimethylorthoformate and *p*-toluenesulfonic acid in methanol. Following treatment with sodium carbonate, the product is isolated via a number of different purification procedures from column chromatography,[71] to distillation,[72] or recrystallization from diethyl ether.[49] We found that purification by crystallization is easily amendable to large batches, generating significant quantities of material, but also has lower overall yield and can be difficult to coax into the solid state from the oil. The second stage in MeO_2DHAC synthesis is the cyclization of MeO_2DHA. Three different methods are presented in the literature to prepare the cyclic carbonate. Putnam et al. reported the successful use of the common reagent triphosgene, which involves addition of the reagent to a stirring solution of MeO_2DHA, pyridine, and dichloromethane at -70 ^{o}C, followed by reaction at

room temperature.[49] Zhuo et al. showed that the reaction could be successfully carried out entirely at room temperature.[73] Putnam et al. also reported a second synthetic method that is attractive, owing to the increased simplicity in the purification procedures. The reaction utilizes an alternative organochloride, ethyl chloroformate, in tetrahydrofuran solvent with triethylamine as the organic base. Purification is accomplished through paper filtration and recrystallization in diethyl ether as opposed to aqueous/organic extraction and flash chromatography.[49] Waymouth et al. demonstrated that oxidative carbonylation is also an effective method to generate the cyclic carbonate. Their method uses the palladium-based reagent (neocuproine)$Pd(OAc)_2$ and offers increased safety compared to a phosgene-type reagent.[74] In the procedure, MeO_2DHA is added to a stirring solution of (neocuproine)$Pd(OAc)_2$ and sodium dichloroisocyanuric acid in acetonitrile. The reaction occurs at 35 ^oC inside a vessel that is vented and pressurized with carbon monoxide, both before and after diol addition.[74] All three methods are adequate synthetic techniques that generate MeO_2DHAC in satisfactory yields.

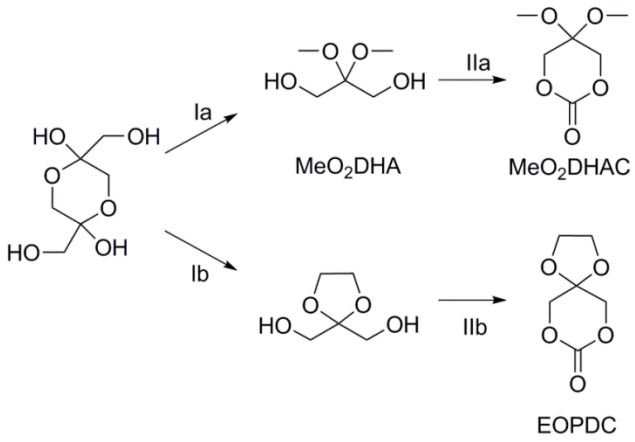

Figure 1.2 Synthetic schemes to MeO_2DHAC and EOPDC. Ia. Trimethyl orthoformate, *p*-toluenesulfonic acid, and methanol, followed by sodium carbonate. IIa. Performed through three different methods involving trisphosgene[49], ethyl chloroformate[49], or oxidative carbonylation[75] Ib. *p*-toluenesulfonic acid, glycol, and benzene IIb. triphosgene, pyridine, and dichloromethane.[69]

Finally, Zhuo et al. introduced a cyclic-acetal protecting group to the field of DHA-based polymers as shown in compound EOPDC (Figure 1.2). Both a two- and four- step process are reported for generating EOPDC.[69,70] The more simplistic two-step process is described in Figure 1.2b. It should be noted that unlike polymers of MeO_2DHAC, which are deprotected and studied in their ketone-containing form, the focus of polymers derived from EOPDC in the current literature is on their ketone-protected form.

1.2.2. Catalysts

Several catalysts are employed for the polymerization of MeO_2DHAC (Table 1.1). The first reported synthesis of p(MeO_2DHAC) (Figure 1.3a) is described by Putnam et al. using the catalyst stannous octoate, which afforded molecular weights of approximately 8-37.5 kDa, as determined by gel permeation chromotography.[49] Zhuo et al. studied variations on reaction temperature, time, and monomer:catalyst ratios, to identify conditions that give molecular weights up to 138.2 kDa.[73]

Table 1.1. Catalysts used in polymerization of MeO_2DHAC. Reprinted with permission from reference 4. Copyright (2016) American Chemical Society.

Catalyst	**T (^{o}C)**	**t (h)**	**Molecular Weight (kDa)**	**Đ**	**Ref**
Metal-Based Catalysts					
$Sn(Oct)_2$	100	1-2	8-37.5[ad]	1.35-1.5	[49]
$Sn(Oct)_2$	110-140	24	14.3-138.2[be]	1.31-1.91	[73]
(BDI)Zn($NTMS_2$)	60, 90	1-2	3-70.2[ae]	1.12-1.79	[76]
Organocatalysts					
BEMP	90	3	14-14.3[ae]	1.53,1.66	[76,77]
DMAP	90	5.5	6.8[ae]	1.23	[76]
TBD	90	3	14.1[ae]	1.71	[76]
TBD	RT	5.5 (min)	6.3[ce]	1.55[a]	[75]
DBU+TU	RT	0.55, 1.17	7.5 and 31[ce]	1.20, 1.24[a]	[75]
(-)-sparteine + TU	RT	7-25	5.8-28[ce]	1.11-1.18[a]	[75]

[a]GPC, THF, Polystyrene Standards, [b]GPC, chloroform, no standards listed. [c]NMR, [d]M_w, [e]M_n

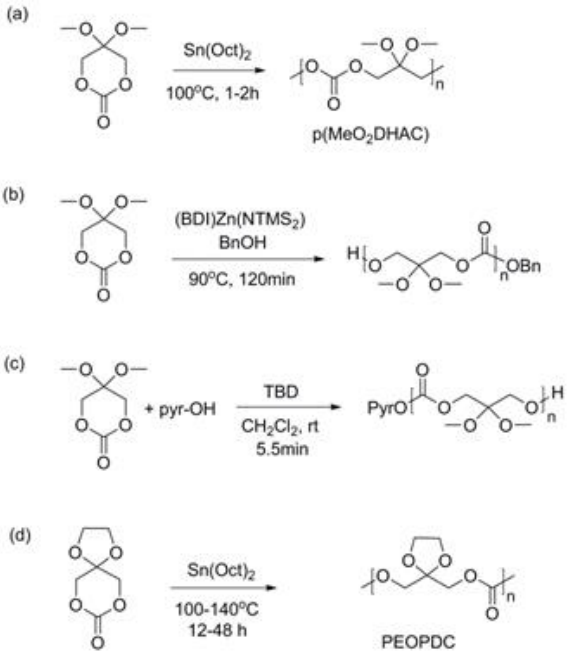

Figure 1.3. Example syntheses of protected-DHA homopolymers performed by: (a) Putnam et al.,[49] (b) Guillaume et al.,[76] (c) Waymouth et al.,[75] and (d) Zhuo et al.[70] Reprinted with permission from reference 4. Copyright (2016) American Chemical Society.

A drawback of the method reported by Putnam et al. is its reliance on trace atmospheric moisture as a polymer initiator. Guillaume and co-workers investigated alternative catalyst systems, which would yield more control over polymer molecular weight. Guillaume et al. found that dimethoxy-acetal-protected DHA homopolymers can be synthesized with molecular weights as high as 70.2 kDa via an "immortal" ROP with the zinc complex [(BDI)Zn($NTMS_2$)] using an alcohol initiator (Figure 1.3b).[76] Guillaume et al. additionally tested several organocatalysts to promote the use of "green" catalytic systems where concerns over trace toxic metals in final products could be eliminated.[76,77] Catalysts 2-*tert*-butylimino-2-diethylamino-1,3-dimethylperhydro-1,3,2-diazaphosphorine (BEMP), 4-*N*,*N*-dimethylaminopyridine (DMAP), and 1,5,7-triazabicyclo-[4.4.0]dec-5-ene (TBD) were all shown to be active in the synthesis of dimethoxy protected DHA polymers.[76,77] Waymouth et al. further investigated the use of organocatalysts in ROP of MeO_2DHAC by evaluating 1,8-diazabicyclo[5.4.0]undec-7-ene

(DBU), 1-(3,5-Bis(trifluoromethyl)phenyl)-3-cyclohexyl-2-thiourea (TU), and (-)-sparteine as well as TBD.[75] TBD is the most efficient organocatalyst reported in their study, as concluded by a monomer conversion of 95% during only 5.5 min of reaction time (Figure 1.3c).[75] A summary of catalysts, reaction conditions, and results from syntheses of MeO_2DHAC homopolymers are shown in Table 1.1. Copolymerizations of MeO_2DHAC with poly(ethylene glycol) (PEG),[78] lactide,[79] ε-CL,[75] and trimethylene carbonate (TMC)[80] are also reported using the catalysts listed in Table 1.1, thus extending the compositions and properties attained with DHA-based polymers.

Zhuo and co-workers first reported polymers of the cylic-ketone-protected DHA (Figure 1.3d).[70] The polymer, poly(2,2-ethylenedioxy-propane-1,3-diol carbonate) (PEOPDC), can be synthesized using two separate catalysts: stannous octoate [$Sn(Oct)_2$] and aluminum isobutanoxide [$Al(O^iBu)_3$]. The use of stannous octoate resulted in higher molecular weights and percent yields with a reported range of 31.9-55 kDa and 79.3-92.6%, respectively.[70] Copolymerizations of EOPDC with lactide,[81] caprolactone,[82] and 1,4-dioxane-2-one[83] are also reported using stannous octoate as a catalyst.

1.2.3. Ketone Deprotection

To date, three methods are established for the deprotection of dimethoxy-acetal protected dihydroxyacetone macromolecules. Putnam et al. demonstrated that the ketone functionality could be recovered after treatment with a trifluoroacetic acid (TFA)/water solution (Figure 1.4a).[49] Deprotection >95% is possible; however, the authors targeted 85% to maintain polymer solubility for structural characterization.[49] Putnam et al. showed that this method is also effective for diblock copolymers of DHA and PEG (Figure 1.4b) and that the acidic nature of the protocol does not result in degradation of the polymer backbone.[78]

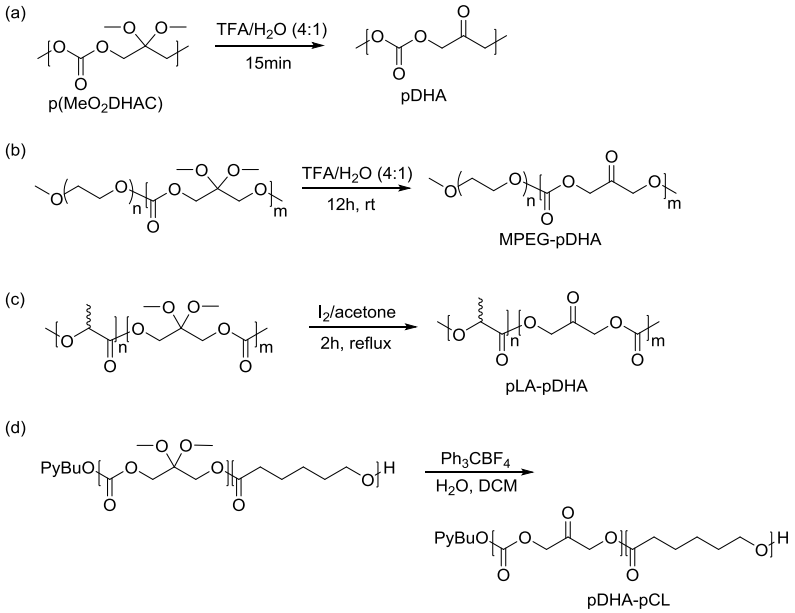

Figure 1.4 Synthetic methods of dimethoxy-acetal deprotection in various DHA-based polymers demonstrated by: (a) Putnam et al.,[49] (b) Putnam et al.,[78] (c) Putnam et al.,[79] and (d) Waymouth et al.[75] Figure 1.4a-c is reprinted with permission from reference[4]. Copyright (2016) American Chemical Society. Figure 1.4(d) is reprinted with permission from reference[75]: Copyright (2012) American Chemical Society.

While polymer degradation is not observed in these specific cases, Putnam et al. investigated an anhydrous deprotection protocol to reduce concern for DHA-based polymers containing additional acid-hydrolyzable bonds.[79] They found that a deprotection procedure developed by Hu et al. in which ketal containing compounds are refluxed in an iodine/acetone solution successfully afforded poly(carbonate-esters) of DHA and lactic acid (pLA-pDHA, Figure 1.4c).[79,84] The extent of deprotection to afford the ketone polymer influences polymer solubility. Increased ketone content (i.e., DHA content) decreases solubility in organic solvents like acetone, and therefore, polymers high in DHA content precipitate from solution prior to reaction completion. Despite this challenge, ≥80% deprotection is possible for all of the polymers tested, encompassing a range of 15-100% DHA content.[79]

Waymouth et al. demonstrated the success of triphenylcarbenium tetrafluoroborate in the deprotection of poly(carbonate-ester) copolymers of DHA and ε-CL (pDHA-pCL, Figure 1.4d).[75] Similar to pLA-pDHA, polymers high in DHA content precipitated from solution during reaction; however, complete deprotection was still observed and reported. Also, the procedure requires only a small quantity of water (one equivalent to each MeO_2DHAC unit) compared to the TFA-based method reported by Putnam et al., thereby offering a second route by which DHA-based polymers can be deprotected with decreased probability for hydrolytic degradation.[49,75]

1.3. Direct Esterification

While ROP affords a large number of possibilities to synthesize DHA-based polymeric materials, protection of DHA is time consuming. Ketone protection generally takes several days depending on the desired level of purity of the final product and generates low yields. In 1969, Schrek et al. and Lasslo et al. showed that esters of DHA which retain the ketone functional group can be synthesized using acyl chloride compounds, such as undecanoyl chloride, in the presence of pyridine.[39,85,86] The goal of their studies was to develop sustained release mosquito repellent technologies in which DHA would anchor the compound to the skin, then degradation would lead to release of the active repellent molecule.[86] The ability to esterify DHA without first protecting the ketone is an attractive feature for the future of DHA-based macromolecules. In 2010, Putnam and Yazdi showed that lipid diesters of DHA synthesized through these methods can be formulated into microparticles and are promising controlled release drug delivery vehicles.[87]

1.4. Cyclic Macromolecules of DHA

Few reports describe the polymerization of the DHA dimer. In 1934, based on a series of X-ray diffraction patterns, Strain and Dore suggested that when the DHA monomer is left in dry form at room temperature for 25-30 days, the molecules would dimerize, and when left for several months, DHA would polymerize further.[88] In 1989, Akar and Talinli reported that the DHA dimer polymerizes into poly(spiro-acetals) by mixing DHA dimer in ethanol with heat and an acid catalyst.[45] The resulting polymers are insoluble in most organic solvents but slightly soluble in dimethyl sulfoxide (DMSO). Several years later, Alder and Reddy reported a transketalization method to synthesize the poly(spiro-acetals).[89]

Putnam et al. reported additional polymers that retain the cyclic nature of the DHA dimer[90,91] (Figure 1.5). In order to prevent dissociation during polymerization, modified forms of the dimer are synthesized, as shown in Figure 1.5. The ethyl derivative, 2,5-diethoxy-1,4-dioxane-2,5-dimethanol (Figure 1.5, R=CH_2CH_3), is used, previously described by Wong et al., as an intermediate in a method for synthesizing DHAP.[92] The molecular weight of the resulting polymers ranged from 28 to 48.4 kDa with dispersities of 1.7 to 2.2. The materials exhibited comparable mechanical properties to that of cancellous bone, with compressive yield strengths of

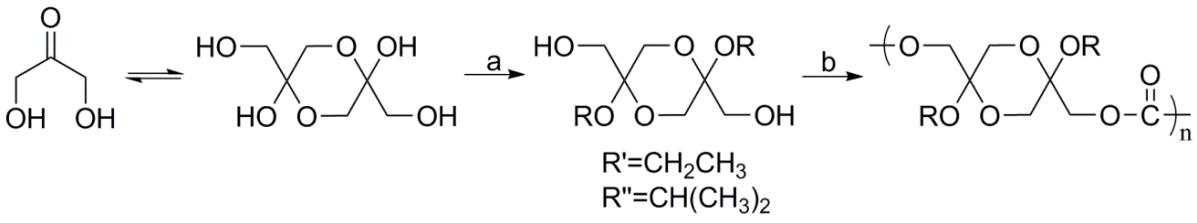

Figure 1.5 Synthetic route to poly(carbonate-acetals) from DHA dimer. (a) R': triethyl orthoformate, EtOH, *p*-TsOH, RT, and R": triisopropyl orthoformate, 2-propanol, *p*-TsOH, and RT and (b) triphosgene, pyridine, and CH_2Cl_2. Adapted with permission from reference[90] Copyright (2005) American Chemical Society.

45 ± 5 MPa and Young's moduli of 0.8 ± 0.01 GPa.[90,93,94] The mechanical properties in combination with confirmed NIH-3T3 cell growth on polymer films suggests that polymers generated from the dimeric form of DHA may have applications in tissue engineering.

1.5. Applications

1.5.1. Functionalizable Surfaces

Surfaces bearing reactive functional groups are of widespread interest for uses including, but not limited to cell adhesion,[95] modifying degradation rates,[96] protein immobilization,[97] drug attachments,[98,99] and layer-by-layer assembly of nanostructures.[100] As previously discussed, DHA reacts with primary amines to form an imine or Schiff base (Figure 1.1c). Therefore, a number of surface modifications of DHA-based materials are possible.

The Schiff base itself is a powerful tool with applications in drug delivery,[99,101,102] bioreactor design,[103,104] biosensors,[105] protein microarrays,[106,107] preparation of nano[108]/microstructures,[109] etc. The imine possesses several unique properties which enable its widespread use including: (1) pH sensitivity, (2) autofluorescence, (3) formation under mild conditions without added reagents, (4) occurrence in both aqueous and organic solvents, and (5) reversibility (with the option of irreversibility through reductive amination).[53] In most biomedical applications, Schiff bases are formed by reactions with aldehydes as opposed to ketones due to the increased reactivity of the carbonyl group. For example, as a tool to prevent infection from medical implants over a prolonged period of time, Meier et al. synthesized polymersomes with outer aldehyde groups that permanently attach to amine-coated silicon surfaces via reductive amination of imine linkages and sustain local release of antibiotics.[110] Li et al. synthesized biodegradable and biocompatible microcapsules containing covalently assembled

layers of chitosan (amine-containing polysaccharide) and derivatized alginate (oxidized to contain aldehyde groups). The Schiff base linkages between layers resulted in autofluoroescence of the microcapsules and pH dependent permeability, indicating their potential use in drug delivery applications with improved *in vivo* tracking capabilities.[111] An extensive review of Schiff base forming technologies based on aldehyde-amine reactions, and their applications, is recently covered by Jia and Li.[53]

Putnam et al. performed several studies to show that the ketone functionality of DHA-based polymers does not lose reactivity upon polymerization of the alpha hydroxyl groups.[49] They spin-coated ketone-protected DHA polymer [p(MeO_2DHAC)] onto glass slides and spotted a TFA/water solution in specified regions to generate areas of deprotected (i.e., ketone-containing) polymer. Subsequent incubation with fluorescently tagged poly(lysine) showed immobilization only in regions containing deprotected polymer, indicating that the ketone is essential to the immobilization mechanism (Figure 1.6a). Similar results are obtained for studies with fluorescently tagged albumin, demonstrating that pDHA is also reactive with proteins. To further verify that Schiff base formation is feasible postpolymerization, Putnam et al. synthesized a small molecular weight analog (I, Figure 1.6b) of pDHA and studied its reaction with phenylethylamine in the presence of a reducing agent. ^{13}C NMR data showed the expected product from reductive amination of a Schiff base formed between the analog and amine compounds (II, Figure 1.6b).[49] The results of Putnam et al. indicate that pDHA, and copolymers thereof, are promising functional biomaterials. In addition, pDHA is reported to possess high strength, similar to that of cancellous bone, and a T_g above physiological temperature (~ 60 ^{o}C). These properties further support the potential for DHA-based materials in medical devices, drug delivery, tissue engineering, and more.[49]

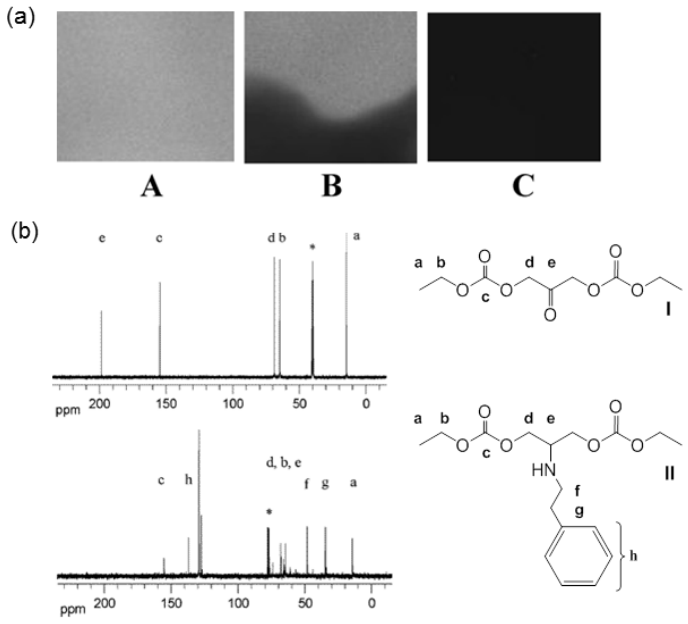

Figure 1.6 (a) Fluorescent imaging of poly(lysine) surface conjugation onto glass microscope slides coated with A: pDHA, B: p(MeO_2DHAC) and pDHA, C: p(MeO_2DHAC) (b) ^{13}C NMR spectra of a small molecular weight analog of pDHA both (I) before and (II) after reaction with phenylethylamine and a reducing agent. Reprinted with permission from reference[49]. Copyright (2006) American Chemical Society.

1.5.2. Hydrogels

Hydrogels are cross-linked polymer networks that swell in aqueous solutions and have varied applications in tissue engineering,[112–114] wound healing,[115–119] and drug delivery.[120–123] Hydrogels are prepared using naturally occurring polymers (cellulose,[124] hyaluronan,[125] alginate,[126] etc.), synthetic materials (poly(vinyl alcohol),[127] poly(ethylene glycol),[128,129] poly(2-hydroxyethyl methacrylate),[130,131] etc.), and genetically engineered protein-based materials created using recombinant DNA technology.[132–134]

Putnam *et al.* reported a new class of synthetic hydrogels using DHA-based polymers.[78,135] They found that diblock copolymers comprised of pDHA, a water-insoluble

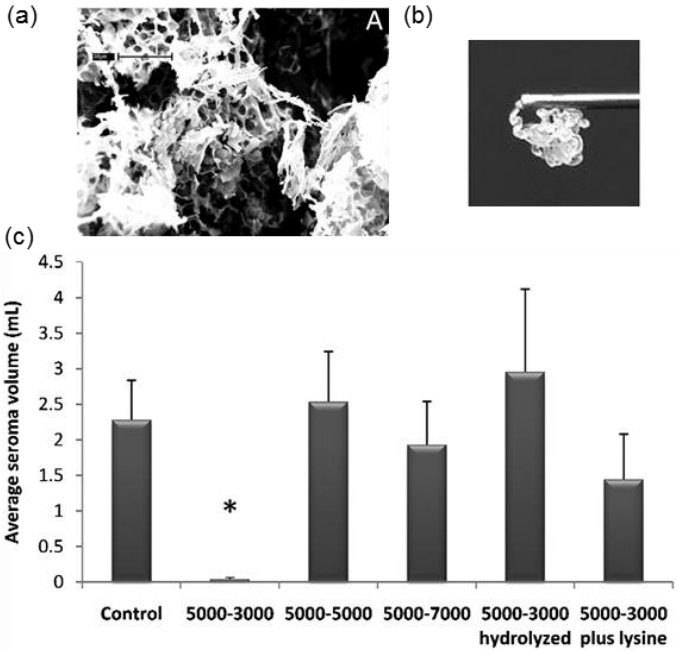

Figure 1.7 (a) SEM image of lyophilized MPEG-pDHA (5000-3000) hydrogel. (b) MPEG-pDHA (5000-5000) hydrogel extrusion through a 26-gauge needle. (c) Seroma volumes measured using a rat mastectomy model following treatment with various MPEG-pDHA formulations and a saline control. Figures are reprinted with permission from reference.[135]

polymer, and the highly hydrophilic polymer PEG afford biocompatible hydrogels with tunable properties (MPEG-pDHA, Figure 1.7a). Studies performed on diblock copolymers with fixed-length MPEG segments (5 kDa) and variable pDHA segments showed that as the pDHA chain increases, hydrogel pore size, swelling, and hydrolytic degradation rates decrease, whereas entanglement density and viscosity increases. Physical cross-linking in MPEG-pDHA hydrogels is hypothesized to occur due to charge interactions arising from the dipole moment of the carbonyl groups on dihydroxyacetone. It is hypothesized that the transient nature of such attractions contribute to the ability to extrude MPEG-pDHA through a 26-gauge needle (Figure 1.7b).[135]

A unique property of DHA-based hydrogels is the relatively rapid degradation rate compared to other polycarbonates [e.g., poly(trimethylene carbonate), (PTMC)]. *In vitro,* under conditions mimicking the physiological media, MPEG-DHA hydrogels degrade within a 24 hour period.[135] The rapid degradation rate of DHA hydrogels, in combination with the ease of extrusion through a needle, is advantageous in the prevention of seromas, accumulation of serous fluid resulting from surgical complications. In an *in vivo* rat model of lymphandenctomy, the polymers with molecular weights ~ 3 kDa in pDHA and ~ 5 kDa in MPEG are highly effective at preventing seroma formation (Figure 1.7c).[135] Three days after treatment, no polymer is observed at the surgical site, indicating that MPEG-pDHA hydrogels are capable of serving a transient distinct function before being eliminated from the body.

The rapid degradation of MPEG-pDHA polymers along with the ability to prevent seroma provides a rationale for investigation of other potential uses, including one as a biodegradable hemostatic agent.[136] With the use of an *in vivo* liver resection rat model, application of the MPEG-pDHA reduced the bleeding time to 97 seconds compared to a saline control (464 seconds) and Instat^{TM}, an industry standard (165 seconds).[136] The total blood loss is not statistically different between MPEG-pDHA and Instat trials, indicating that MPEG-pDHA hydrogels are adequate hemostatic agents with the added bonus of a rapid *in vivo* resorption rate. Histological studies performed 3 weeks postoperation showed a similar inflammatory response of MPEG-pDHA samples to saline controls.[136] The combination of biocompatibility, reduced bleeding time, synthetic origin of the material, and rapid degradation of MPEG-pDHA hydrogels suggest that MPEG-pDHA hemostatic agents would lead to minimized risk of infection and long-term inflammation.

The reactive carbonyl functionality present within DHA hydrogels provides opportunities for chemical cross-linking, drug attachments, or surface modifications, thereby opening doors to additional applications. Furthermore, chemical alterations, such as the introduction of small hydrophobic regions or the use of urethane polymer linkages, may lead to enhanced control in hydrogel swelling and degradation, expanding the potential for DHA-based hydrogels in biomedical applications.

1.5.3. Controlled Drug Delivery

Polymeric materials are of significant interest in the field of controlled drug delivery owing to the vast opportunities in synthetic design leading to various tunable features as well as their ability to form macro, micro, or nanostructures. Several review articles cover polymers used for controlled drug delivery that describe their unique advantages and specific applications in detail, and the reader is referred to these articles.[137–141] DHA-based polymers contain several desirable characteristics for controlled drug release systems. First, the degradation of DHA-based polymers into biocompatible compounds reduces risks of inflammation and toxicity, while also eliminating concerns over invasive post-treatment device removal. Second, through ROP, DHA can be easily copolymerized in a controlled manner with other biocompatible materials such as lactide[79] and caprolactone.[75] By altering initial monomer, comonomer, initiator, and catalyst ratios, the final product composition can be predicted, creating a reliable parameter by which drug release rates are controlled. Overall, there is a large realm of possibilities for DHA-based polymers with regard to hydrophilicity, rigidity, glass-transition temperatures, melting temperatures, rheological properties, and pH sensitivity, depending on the chosen comonomer and reaction conditions. Furthermore, variations in these properties yield opportunities for

different 3D structures. Diblock copolymers of DHA and MPEG afford hydrogels[135] and nanoparticles,[78] whereas random copolymers of DHA and LA give powders that can be compressed into solid tablets.[79] Putnam and Yazdi showed that DHA-based microparticles are also feasible; however, these materials employ a separate synthetic technique, as previously discussed.[87] A third attractive feature of DHA-based materials is the reactive ketone functionality. Although this has yet to be specifically explored, it is an extension of the research and opens up possibilities for the attachment of active agents or affinity-ligands.

Putnam et al. showed that random copolymers of DHA and LA, synthesized via ROP with stannous octoate catalysts, are promising candidates for controlled release of protein therapeutics.[142] Cylindrical tablets, for subsequent drug release studies, are prepared by mixing the powdered polymers containing approximately 50 to 85% DHA with dry powders of model proteins, bovine serum albumin (BSA) or lysozyme, and compressed. Copolymers containing less than 50% DHA are too tough to process into tablets and therefore were not investigated. Thermal studies revealed that for all LA:DHA ratios, glass transition temperature (53 - 68 ^{o}C) and degradation temperatures (T_d, 50 wt%: 230 - 330 ^{o}C) are above physiological temperature, indicating that the tablets will retain structural integrity when subject to *in vivo* temperatures.[79,142]

In vitro controlled release experiments showed a first order release of BSA and lysozyme over 2.5-70 days, depending on the percent drug loading and percent DHA in the polymer backbone.[142] Lysozyme activity tests following release indicated that the protein retained significant activity throughout release and was not highly inactivated due to the environment of the delivery device. For any copolymer composition, at least 50% of the protein activity is retained after one month of release. Protein release rates increased with increasing pDHA

content.[142] This result is not surprising given the results of *in vitro* degradation studies, which showed that polymer erosion occurs more rapidly with increasing DHA content within the polymer backbone. In addition to tablet erosion studies visualized by scanning electron microscopy, degradation of the polymer backbone can be tracked utilizing the bicinchoninic acid assay, which Putnam et al. discovered to be a valuable tool in quantitatively measuring α-hydroxy ketones, such as DHA, in solution.[143] Zhuo et al. report that upon deprotection of the pDHA homopolymer, hydrolytic degradation of the associated carbonate bonds drastically increases.[73] The results suggest that percent deprotection of pDHA in DHA-based materials is a potential control parameter in drug release technologies.

Zhuo and co-workers performed release studies on polymers containing EOPDC (Figure 1.2), a cyclic-acetal protected form of DHA, using the chemotherapeutic agent Tegafur.[81–83] Results from EOPDC:1,4-dioxane-2-one copolymers and EOPDC:caprolactone copolymers show a decreased drug release rate with increasing EOPDC content, resulting in release of less than 4% in 350 hours in any formulation.[82,83]

Diblock copolymers of pDHA and MPEG (Figure 1.4b) are also proposed for controlled release applications; however, no formal testing is reported. Putnam et al. showed that in addition to hydrogels, MPEG-pDHA polymers can be formulated into nanoparticles that take on a micellar shape with a pDHA core and PEG corona.[78] Nanoparticles, prepared by control precipitation (via stirring) from DMSO/polymer solutions in water, ethanol, or dichloromethane, afforded average particle diameters of 45 ± 1nm, 70 ± 1nm, and 94 ± 1nm, respectively, from polymers with molecular weights of 1.8 kDa for pDHA and 4.5 kDa PEG.

1.5.4. Green Thermoplastics

Today, concerns over landfill sizes, depletion of scarce resources, and greenhouse gas production are significant given the increasing world population. These issues spurred the investigation, development, and use of biodegradable plastics from renewable resources, as opposed to traditional petroleum-based materials such as polyethylene or polypropylene. Examples of "green" plastics include those composed of starch, soy protein, cellulose, PLA, and poly(hydroxyalkanoate)s.[8,144–147] Waymouth et al. noticed that the structure of pDHA is similar to Carilon, a polyketone thermoplastic derived from ethylene (E) and carbon monoxide (CO).[75] Since DHA can be synthesized from glycerol,[148,149] a byproduct in the production of biodiesel, the authors investigated the potential use of DHA-based polymers in the field of renewable and biodegradable thermoplastic materials.[75] Similar to E/CO polymers, pDHA possesses a melting temperature, T_m of 246 ^oC, close to the thermal degradation temperature, T_d = 273 ^oC, which is difficult for processing due the high T_m and close T_m and T_d values.[75] As a solution, Waymouth et al. copolymerized DHA with ε-CL, which lowered the T_m of the polymer, with the extent of T_m lowering depending on the percent of caprolactone added to the composition.[75] These results indicate that pDHA-CL copolymers are thermoplastic materials with tunable thermal properties.

Guillaume et al., also interested in creating thermoplastic materials from biorenewable resources, synthesized diblock and triblock copolymers of dimethoxy-acetal protected DHA with the well-known polycarbonate PTMC.[80] It was found that much like PLA, a popular "green" choice for polymers," segments of protected DHA added rigidity to PTMC polymers which is a control parameter for the generation of well performing thermoplastic materials. The results from the Guillaume and Waymouth laboratories, show that DHA-based polymers are not limited to

biomedical applications. The features that make these polymers appeal to biomedical research, their biocompatibility and biodegradability, also open doors to the possibility of producing materials with improved environmental preservation capabilities.

1.6. Research Goals

Several polymeric materials have been synthesized with the natural metabolite dihydroxyacetone including hydrogels, microparticles, powders, nanoparticles, and thermoplastics. Of these DHA-based macromolecules, a subset has successfully demonstrated use in controlled drug delivery, hemostasis, seroma prevention, and tissue engineering. Although a diverse set of DHA-based materials are known and effective in several applications, a number of opportunities remain. The main goal of the study was to gain insight into two characteristic properties of DHA-based materials: degradation in aqueous environments and Schiff base formation with amine containing compounds.

Biodegradable polymers are highly advantageous in biomedical applications owing to the wide variety of functions they can serve in vivo while maintaining the ability to be eliminated from the body non-invasively once they are no longer needed. Although previous studies have highlighted the rapid degradation of one specific DHA-based hydrogel, the focal point in the literature has been on the intended applications, rather than the underlying mechanism of action. To highlight the utility of DHA in the development of novel rapidly degrading biomaterials, we conducted a study to shed light on the underlying mechanism.

As described in Chapter 2, we synthesized a new class of DHA-based polycarbonates: chemically crosslinked hydrogels comprised of a glycerol ethoxylate (GE) backbone and tri(ethylene glycol) bis(chloroformate) (TEGBC) cross-linker. Chemically cross-linked

hydrogels were selected due to facile visualization and testing of hydrogel degradation. Hydrogels swell in aqueous solutions, thereby enabling significant contact of polymer chains with water, while also remaining insoluble, which allows separation from degradation products through basic filtration methods. Degradation rates were compared to those of similarly designed hydrogels that differed in the presence and location of a ketone functional group within the polymer backbone. The results shed light on the structural features of DHA that contribute to the observed rapid degradation rates and suggest that such properties are translatable to additional hydrophilic DHA-based systems.

Following the analysis of degradation rates and products, the chemically crosslinked hydrogels were fabricated into disks and tested for use as a rapidly degradable surgical device to prevent accidental bowel injury during abdominal closure after a laparotomy. Using a mouse model, it was confirmed that the DHA-based hydrogels degrade on a rapid timescale in vivo and do not appear to induce an inflammatory response. The work, as detailed in Chapter 3, provides just one example of how insight into the mechanism by which DHA promotes rapid degradation of polycarbonates can stimulate the innovation of novel medical devices.

In additional to biodegradability, the amine reactive functionality of DHA-based polymers is highly advantageous. A long term goal is to explore the use of DHA-based polymers as amine reactive surfaces for use both inside and outside the realm of biomaterials; however, the present work focuses solely on aqueous solutions. As a first step, we studied the rate at which ethanolamine, a highly water soluble molecule containing a primary amine, can react with free DHA in solution. Our goal in studying this simplified reaction was to eliminate the complications associated with diffusion limitations, etc. of large macromolecules in order to assess what the formation rate of a Schiff base is between a primary amine and DHA in solution.

By measuring the formation rate, we can assess the future feasibility of DHA-based materials in amine reactive surface applications.

Our efforts to measure the degradation rates of DHA hydrogels and the DHA-amine reaction rate are the just the beginning of an improved framework that would be used to develop novel DHA-based biomaterials according to a predict-build-assess approach. In the initial stages of using unexplored monomer units, a blind build-test-refine cycle of polymer synthesis is highly advantageous for gaining information on the capabilities and limitations of the proposed monomer. Transition from pilot studies to wide spread acceptance, however, requires an enhanced ability to predict the behavior of a desired polymer prior to synthesis, with specific goals in mind for a particular application. The work presented herein serves to highlight key features of DHA-based materials to facilitate the wide spread use of DHA in macromolecular materials.

1.7. References

(1) Frazza, E. J.; Schmitt, E. E. A New Absorbable Suture. *J. Biomater. Res.* **1971**, *1*, 43–58.

(2) Schmitt, E. E.; Albert, R. Surgical Sutures. U.S. Patent 3297033, 1967.

(3) Wishart, D. S.; Jewison, T.; Guo, A. C.; Wilson, M.; Knox, C.; Liu, Y.; Djoumbou, Y.; Mandal, R.; Aziat, F.; Dong, E.; Bouatra, S.; Sinelnikov, I.; Arndt, D.; Xia, J.; Liu, P.; Yallou, F.; Bjorndahl, T.; Perez-Pineiro, R.; Eisner, R.; Allen, F.; Neveu, V.; Greiner, R.; Scalbert, A. HMDB 3.0-The Human Metabolome Database in 2013. *Nucleic Acids Res.* **2013**, *41*, D801–D807.

(4) Ricapito, N. G.; Ghobril, C.; Zhang, H.; Grinstaff, M. W.; Putnam, D. Synthetic Biomaterials from Metabolically Derived Synthons. *Chem. Rev.* **2016**, *116*, 2664–2704.

(5) Dash, T. K.; Konkimalla, V. B. Poly-Є-Caprolactone Based Formulations for Drug Delivery and Tissue Engineering: A Review. *J. Control. Release* **2012**, *158*, 15–33.

(6) Bala, I.; Hariharan, S.; Kumar, M. N. V. R. PLGA Nanoparticles in Drug Delivery: The State of the Art. *Crit. Rev. Ther. Drug Carrier Syst.* **2004**, *21*, 387–422.

(7) Makadia, H. K.; Siegel, S. J. Poly Lactic-Co-Glycolic Acid (PLGA) as Biodegradable Controlled Drug Delivery Carrier. *Polymers (Basel).* **2011**, *3*, 1377–1397.

(8) Sudesh, K.; Iwata, T. Sustainability of Biobased and Biodegradable Plastics. *Clean - Soil, Air, Water* **2008**, *36*, 433–442.

(9) Lewitus, D.; Smith, K. L.; Shain, W.; Kohn, J. Ultrafast Resorbing Polymers for Use as Carriers for Cortical Neural Probes. *Acta Biomater.* **2011**, *7*, 2483–2491.

(10) Wathier, M.; Jung, P. J.; Carnahan, M. A.; Kim, T.; Grinstaff, M. W. Dendritic Macromers as in Situ Polymerizing Biomaterials for Securing Cataract Incisions. *J. Am. Chem. Soc.* **2004**, *126*, 12744–12745.

(11) Ghobril, C.; Charoen, K.; Rodriguez, E. K.; Nazarian, A.; Grinstaff, M. W. A Dendritic Thioester Hydrogel Based on Thiol-Thioester Exchange as a Dissolvable Sealant System for Wound Closure. *Angew. Chemie - Int. Ed.* **2013**, *52*, 14070–14074.

(12) Liu, R.; Wolinsky, J. B.; Walpole, J.; Southard, E.; Chirieac, L. R.; Grinstaff, M. W.; Colson, Y. L. Prevention of Local Tumor Recurrence Following Surgery Using Low-Dose Chemotherapeutic Polymer Films. *Ann. Surg. Oncol.* **2010**, *17*, 1203–1213.

(13) Söntjens, S. H. M.; Nettles, D. L.; Carnahan, M. A.; Setton, L. A.; Grinstaff, M. W. Biodendrimer-Based Hydrogel Scaffolds for Cartilage Tissue Repair. *Biomacromolecules* **2006**, *7*, 310–316.

(14) Carnahan, M. A.; Middleton, C.; Kim, J.; Kim, T.; Grinstaff, M. W. Hybrid Dendritic−Linear Polyester−Ethers for in Situ Photopolymerization. *J. Am. Chem. Soc.* **2002**, *124*, 5291–5293.

(15) Morgan, M. T.; Carnahan, M. A.; Immoos, C. E.; Ribeiro, A. A.; Finkelstein, S.; Lee, S. J.; Grinstaff, M. W. Dendritic Molecular Capsules for Hydrophobic Compounds. *J. Am. Chem. Soc.* **2003**, *125*, 15485–15489.

(16) Miura, Y.; Hoshino, Y.; Seto, H. Glycopolymer Nanobiotechnology. *Chem. Rev.* **2016**, *116*, 1673-1692.

(17) Appelhans, D.; Klajnert-Maculewicz, B.; Janaszewska, A.; Lazniewska, J.; Voit, B. Dendritic Glycopolymers Based on Dendritic Polyamine Scaffolds: View on Their Synthetic Approaches, Characteristics and Potential for Biomedical Applications. *Chem. Soc. Rev.* **2015**, *44*, 3968–3996.

(18) Parry, A. L.; Clemson, N. a; Ellis, J.; Bernhard, S. S. R.; Davis, B. G.; Cameron, N. R. "Multicopy Multivalent" Glycopolymer-Stabilised Gold Nanoparticles as Potential Synthetic Cancer Vaccines. *J. Am. Chem. Soc.* **2013**, *135*, 9362–9365.

(19) Rabinowitch, I. M. Observations on the Use of Dihydroxyacetone in the Treatment of Diabetes Mellitus. *Can. Med. Assoc. J.* **1925**, *15*, 374–381.

(20) Ringer, A. I.; Frankel, E. M. The Chemistry of Gluconeogenesis: IX. The Formation of Glucose in the Diabetic Organism. *J. Biol. Chem.* **1914**, *18*, 233–236.

(21) Macdermot, H. Dioxyacetone. *Can. Med. Assoc. J.* **1925**, *15*, 412.

(22) Rabinowitch, I. M. Blood Sugar Time Curves Following the Ingestion of Dihydroxyacetone. *J. Biol. Chem.* **1925**, *65*, 55–58.

(23) Rabinowitch, I. M. A Case of Diabetic Coma Treated with Dioxyacetone, with Recovery. *Can. Med. Assoc. J.* **1925**, *15*, 520–522.

(24) Goldman, L.; Barkoff, J.; Blaney, D.; Nakai, T.; Suskind, R. Investigative Studies with the Skin Coloring Agents Dihydroxyacetone and Glyoxal. *J. Invest. Dermatol.* **1960**, *35*, 161–164.

(25) Maillard, L. C. Action Des Acides Amines Sur Les Sucres: Formation Des Melanoidines Par Voie Methodique (English Translation: Action of Amino Acids on Sugars. Formation of Melanoidins in a Methodical Way). *Compt. Rend. Hebd. Seances Acad. Sci.* **1912**, *154*, 66–68.

(26) Hodge, J. E. Chemistry of Browning Reactions in Model Systems. *J. Agric. Food Chem.* **1953**, *1*, 928–943.

(27) Wittgenstein, E.; Berry, H. K. Staining of Skin with Dihydroxyacetone. *Science.* **1960**, *132*, 894–895.

(28) Wittgenstein, E. V. A.; Berry, H. K. Reaction of Dihydroxyacetone (DHA) with Human Skin Callus and Amino Compounds. *J. Invest. Dermatol.* **1961**, *36*, 283–286.

(29) Fu, J. M.; Dusza, S. W.; Halpern, A. C. Sunless Tanning. *J. Am. Acad. Dermatol.* **2004**, *50*, 706–713.

(30) Petersen, A. B.; Wulf, H. C.; Gniadecki, R.; Gajkowska, B. Dihydroxyacetone, the Active Browning Ingredient in Sunless Tanning Lotions, Induces DNA Damage, Cell-Cycle Block and Apoptosis in Cultured HaCaT Keratinocytes. *Mutat. Res.* **2004**, *560*, 173–186.

(31) Jung, K.; Seifert, M.; Herrling, T.; Fuchs, J. UV-Generated Free Radicals (FR) in Skin: Their Prevention by Sunscreens and Their Induction by Self-Tanning Agents. *Spectrochim. Acta Part A Mol. Biomol. Spectrosc.* **2008**, *69*, 1423–1428.

(32) Pagoto, S. Sunless Tanning. In *Shedding Light on Indoor Tanning*; Heckman, C. J., Manne, S. L., Eds.; Springer: Dordrecht, Heidelberg, London, New York, 2012; pp 165–178.

(33) O'Leary, R. E.; Diehl, J.; Levins, P. C. Update on Tanning: More Risks, Fewer Benefits. *J. Am. Acad. Dermatol.* **2014**, *70*, 562–568.

(34) Sanner, T. Opinion on Dihydroxyacetone. Scientific Committee on Consumer Safety. **2010**, SCCS/1347/10; pp 1–35.

(35) Taylor, C.; Kwangsukstith, C.; Wimberly, J.; Kollias, N.; Anderson, R. R. Turbo-PUVA: Dihydroxyacetone-Enhanced Photochemotherapy for Psoriasis. *Arch. Dermatol.* **1999**, *135*, 540–544.

(36) Lentini, P. J. Compositions Useful in the Phototherapeutic Treatment of Proliferative Skin Disorders. US Patent WO 97/28784, 1999.

(37) Rajatanavin, N.; Suwanachote, S.; Kulkollakarn, S. Dihydroxyacetone: A Safe Camouflaging Option in Vitiligo. *Int. J. Dermatol.* **2008**, *47*, 402–406.

(38) Fesq, H.; Brockow, K.; Strom, K.; Mempel, M.; Ring, J.; Abeck, D. Dihydroxyacetone in a New Formulation - A Powerful Therapeutic Option in Vitiligo. *Dermatology* **2001**, *203*, 241–243.

(39) Quintana, R. P.; Garson, L. R.; Lasslo, A.; Sanders, S. I.; Buckner, J. H.; Gouck, H. K.; Gilbert, I. H.; Weidhaas, D. E.; Schreck, C. E. Mosquito-Repellent Dihydroxyacetone Monoesters. *J. Econ. Entomol.* **1970**, *63*, 1128–1131.

(40) Stanko, R. T.; Robertson, R. J.; Galbreath, R. W.; Reilly, J. J.; Greenawalt, K. D.; Goss, F. L. Enhanced Leg Exercise Endurance with a High-Carbohydrate Diet and Dihydroxyacetone and Pyruvate. *J. Appl. Physiol.* **1990**, *69*, 1651–1656.

(41) Niknahad, H.; Ghelichkhani, E. Antagonism of Cyanide Poisoning by Dihydroxyacetone. *Toxicol. Lett.* **2002**, *132*, 95–100.

(42) Turner, B. B.; Hulpieu, H. R. A Study of the Antidotal Action of Sodium Thiosulphate and Dihydroxyacetone in Cyanide Poisoning, and the Alleged Anti-Dotal Action of Glucose. *J. Pharmacol. Exp. Ther.* **1933**, *48*, 445–469.

(43) Erni, B.; Siebold, C.; Christen, S.; Srinivas, A.; Oberholzer, A.; Baumann, U. Small Substrate, Big Surprise: Fold, Function and Phylogeny of Dihydroxyacetone Kinases. *Cell. Mol. Life Sci.* **2006**, *63*, 890–900.

(44) Pratt, C.; Voet, D.; Voet, J. *Fundamentals of Biochemistry: Life at the Molecular Level*, Third Edit.; John Wiley & Sons: Hoboken, NJ, USA, 2008.

(45) Akar, A.; Talinli, N. Synthesis of a Polyspiroacetal. *Die Makromol. Chemie Rapid Commun.* **1989**, *10*, 127–130.

(46) Davis, L. The Structure of Dihydroxyacetone in Solution. *Bioorg. Chem.* **1973**, *2*, 197–201.

(47) Slepokura, K.; Lis, T. Crystal Structures of Dihydroxyacetone and Its Derivatives. *Carbohydr. Res.* **2004**, *339*, 1995–2007.

(48) Reynolds, S. J.; Yates, D. W.; Pogson, C. I. Dihydroxyacetone Phosphate. Its Structure and Reactivity with Alpha-Glycerophosphate Dehydrogenase, Aldolase and Triose Phosphate Isomerase and Some Possible Metabolic Implications. *Biochem. J.* **1971**, *122*, 285–297.

(49) Zelikin, A. N.; Zawaneh, P. N.; Putnam, D. A Functionalizable Biomaterial Based on Dihydroxyacetone, an Intermediate of Glucose Metabolism. *Biomacromolecules* **2006**, *7*, 3239–3244.

(50) Grazi, E.; Rowley, P. T.; Cheng, T.; Tchola, O.; Horecker, B. L. The Mechanism of Action of Aldolases III. Schiff Base Formation with Lysine. *Biochem. Biophys. Rsearch Commun.* **1962**, *9*, 38–43.

(51) Jia, J.; Schorken, U.; Lindqvist, Y.; Sprenger, G. A.; Schneider, G. Crystal Structure of the Reduced Schiff-Base Intermediate Complex of Transaldolase B from Escherichia Coli: Mechanistic Implications for Class I Aldolases. *Protein Sci.* **1997**, *6*, 119–124.

(52) Carnali, J. O.; Madison, S. A.; Shah, P.; Qiu, Q. Structure/Property Relationship for Ethylenediamine Derivatives as Aids in Sunless Tanning. *Ind. Eng. Chem. Res.* **2012**, *51*, 15573–15581.

(53) Jia, Y.; Li, J. Molecular Assembly of Schiff Base Interactions: Construction and Application. *Chem. Rev.* **2015**, *115*, 1597–1621.

(54) Nguyen, B.-C.; Kochevar, I. E. Influence of Hydration on Dihydroxyacetone-Induced Pigmentation of Stratum Corneum. *J. Invest. Dermatol.* **2003**, *120*, 655–661.

(55) Johnson, J. A.; Fusaro, R. M. Alteration of Skin Surface Protein with Dihydroxyacetone: A Useful Application of the Maillard Browning Reaction. In *Maillard Reactions in Chemistry, Food, and Health*; Labuza, T. P., Reineccius, G. A., Monnier, V. M., O'Brien, J., Baynes, J. W., Eds.; The Royal Society of Chemistry: Cambridge, 1994; pp 114–119.

(56) Boekel, M. A. J. S. Van. Kinetic Aspects of the Maillard Reaction : A Critical Review. *Nahrung/Food* **2001**, *45*, 150–159.

(57) Martins, S. I. F. S.; Jongen, W. M. F.; Boekel, M. A. J. S. Van. A Review of Maillard Reaction in Food and Implications to Kinetic Modelling. *Trends Food Sci. Technol.* **2001**, *11*, 364–373.

(58) Nuyken, O.; Pask, S. Ring-Opening Polymerization—An Introductory Review. *Polymers (Basel).* **2013**, *5*, 361–403.

(59) Lee, A. L. Z.; Ng, V. W. L.; Gao, S.; Hedrick, J. L.; Yang, Y. Y. Injectable Hydrogels from Triblock Copolymers of Vitamin E-Functionalized Polycarbonate and Poly(ethylene Glycol) for Subcutaneous Delivery of Antibodies for Cancer Therapy. *Adv. Funct. Mater.* **2014**, *24*, 1538–1550.

(60) Stevens, D. M.; Rahalkar, A.; Spears, B.; Gilmore, K.; Douglas, E.; Muthukumar, M.; Harth, E. Semibranched Polyglycidols as "fillers" in Polycarbonate Hydrogels to Tune Hydrophobic Drug Release. *Polym. Chem.* **2015**, *6*, 1096–1102.

(61) Lee, A. L. Z.; Ng, V. W. L.; Gao, S.; Hedrick, J. L.; Yang, Y. Y. Injectable Biodegradable Hydrogels from Vitamin D-Functionalized Polycarbonates for the Delivery of Avastin with Enhanced Therapeutic Efficiency against Metastatic Colorectal Cancer. *Biomacromolecules* **2015**, *16*, 465–475.

(62) Jiang, T.; Li, Y. M.; Lv, Y.; Cheng, Y. J.; He, F.; Zhuo, R.-X. Amphiphilic Polycarbonate Conjugates of Doxorubicin with pH-Sensitive Hydrazone Linker for Controlled Release. *Colloids Surfaces B Biointerfaces* **2013**, *111*, 542–548.

(63) Ke, X.; Coady, D. J.; Yang, C.; Engler, A. C.; Hedrick, J. L.; Yang, Y. Y. pH-Sensitive Polycarbonate Micelles for Enhanced Intracellular Release of Anticancer Drugs: A Strategy to Circumvent Multidrug Resistance. *Polym. Chem.* **2014**, *5*, 2621–2628.

(64) Magno, M. H. R.; Kim, J.; Srinivasan, A.; McBride, S.; Bolikal, D.; Darr, A.; Hollinger, J. O.; Kohn, J. Synthesis, Degradation and Biocompatibility of Tyrosine-Derived Polycarbonate Scaffolds. *J. Mater. Chem.* **2010**, *20*, 8885–8893.

(65) Kim, J.; Magno, M. H. R.; Waters, H.; Doll, B. A.; McBride, S.; Alvarez, P.; Darr, A.; Vasanji, A.; Kohn, J.; Hollinger, J. O. Bone Regeneration in a Rabbit Critical-Sized Calvarial Model Using Tyrosine-Derived Polycarbonate Scaffolds. *Tissue Eng. Part A* **2012**, *18*, 1132–1139.

(66) Xu, J.; Filion, T. M.; Prifti, F.; Song, J. Cytocompatible Poly(ethylene Glycol)-Co-Polycarbonate Hydrogels Crosslinked by Copper-Free, Strain-Promoted "Click" Chemistry. *Chem. - An Asian J.* **2011**, *6*, 2730–2737.

(67) Xu, J.; Feng, E.; Song, J. Renaissance of Aliphatic Polycarbonates: New Techniques and Biomedical Applications. *J. Appl. Polym. Sci.* **2014**, *131*, 39822.

(68) Feng, J.; Zhuo, R.-X.; Zhang, X.-Z. Construction of Functional Aliphatic Polycarbonates for Biomedical Applications. *Prog. Polym. Sci.* **2012**, *37*, 211–236.

(69) Wang, L. S.; Jiang, X. S.; Wang, H.; Cheng, S. X.; Zhuo, R. X. Preparation and Cytotoxicity of Novel Aliphatic Polycarbonate Synthesized from Dihydroxyacetone. *Chinese Chem. Lett.* **2005**, *16*, 572–574.

(70) Wang, L.-S.; Cheng, S.-X.; Zhuo, R.-X. Novel Biodegradable Aliphatic Polycarbonate Based on Ketal Protected Dihydroxyacetone. *Macromol. Rapid Commun.* **2004**, *25*, 959–963.

(71) Cesarotti, E.; Antognazza, P.; Pallavicini, M.; Villa, L. Synthesis and Ruthenium-Catalyzed Enantioselective Hydrogenation of 3-O-Substituted 1,3-Dihydroxypropan-2-Ones. *Helv. Chim. Acta* **1993**, *76*, 2344–2349.

(72) Ferroni, E. L.; DiTella, V.; Ghanayem, N.; Jeske, R.; Jodlowski, C.; O'Connell, M.; Styrsky, J.; Svoboda, R.; Venkataraman, A.; Winkler, B. M. A Three-Step Preparation of Dihydroxyacetone Phosphate Dimethyl Acetal. *J. Org. Chem.* **1999**, *64*, 4943–4945.

(73) Wang, L.-S.; Cheng, S.-X.; Zhuo, R.-X. Synthesis and Hydrolytic Degradation of Aliphatic Polycarbonate Based on Dihydroxyacetone. *Polym. Sci. Ser. B* **2013**, *55*, 604–610.

(74) Pearson, D. M.; Conley, N. R.; Waymouth, R. M. Palladium-Catalyzed Carbonylation of Diols to Cyclic Carbonates. *Adv. Synth. Catal.* **2011**, *353*, 3007–3013.

(75) Simon, J.; Olsson, J. V.; Kim, H.; Tenney, I. F.; Waymouth, R. M. Semicrystalline Dihydroxyacetone Copolymers Derived from Glycerol. *Macromolecules* **2012**, *45*, 9275–9281.

(76) Helou, M.; Brusson, J.-M.; Carpentier, J.-F.; Guillaume, S. M. Functionalized Polycarbonates from Dihydroxyacetone: Insights into the Immortal Ring-Opening Polymerization of 2,2-Dimethoxytrimethylene Carbonate. *Polym. Chem.* **2011**, *2*, 2789–2795.

(77) Helou, M.; Miserque, O.; Brusson, J.-M.; Carpentier, J.-F.; Guillaume, S. M. Organocatalysts for the Controlled "Immortal" Ring-Opening Polymerization of Six-Membered-Ring Cyclic Carbonates: A Metal-Free, Green Process. *Chem. - A Eur. J.* **2010**, *16*, 13805–13813.

(78) Zawaneh, P. N.; Doody, A. M.; Zelikin, A. N.; Putnam, D. Diblock Copolymers Based on Dihydroxyacetone and Ethylene Glycol: Synthesis, Characterization, and Nanoparticle Formulation. *Biomacromolecules* **2006**, *7*, 3245–3251.

(79) Weiser, J. R.; Zawaneh, P. N.; Putnam, D. Poly(carbonate-Ester)s of Dihydroxyacetone and Lactic Acid as Potential Biomaterials. *Biomacromolecules* **2011**, *12*, 977–986.

(80) Guerin, W.; Helou, M.; Slawinski, M.; Brusson, J.-M.; Carpentier, J.-F.; Guillaume, S. M. Macromolecular Engineering via Ring-Opening Polymerization (3): Trimethylene Carbonate Block Copolymers Derived from Glycerol. *Polym. Chem.* **2014**, *5*, 1229–1240.

(81) Wang, L.; Cheng, S.; Zhuo, R. Syntheses and Properties of Novel Copolymers of Polylactide and Aliphatic Polycarbonate Based on Ketal-Protected Dihydroxyacetone. *Polym. Plast. Technol. Eng.* **2013**, *52*, 1063–1067.

(82) Wang, L.; Cheng, S.; Zhuo, R. Syntheses and Properties of Novel Copolymers of Polycaprolactone and Aliphatic Polycarbonate Based on Ketal-Protected Dihydroxyacetone. *Polym. Bull.* **2014**, *71*, 47–56.

(83) Wang, L.; Cheng, S.; Zhuo, R. Syntheses and Properties of Novel Copolymers of Poly (1,4-Dioxane-2-One) and Aliphatic Polycarbonate Based on Ketal-Protected Dihydroxyacetone. *Macromol. Chem. Phys.* **2013**, *214*, 458–463.

(84) Sun, J.; Dong, Y.; Cao, L.; Wang, X.; Wang, S.; Hu, Y. Highly Efficient Chemoselective Deprotection of O,O-Acetals and O,O-Ketals Catalyzed by Molecular Iodine in Acetone. *J. Org. Chem.* **2004**, *69*, 8932–8934.

(85) Garson, L. R.; Quintana, R. P.; Lasslo, A. Monomer and Dimer Formation in Esters of Dihydroxyacetone. *Can. J. Chem.* **1969**, *47*, 1249–1251.

(86) Quintana, R. P.; Garson, L. R.; Lasslo, A. Monomolecular Films of Compounds with Potential Dermophilic and Prophylactic Properties. Esters of Dihydroxyacetone. *Can. J. Chem.* **1969**, *47*, 853–856.

(87) Putnam, D.; Yazdi, S. Biodegradable Compositions and Materials. U.S. Patent WO2008101173, 2008.

(88) Strain, H. H.; Dore, W. H. Polymerization of Dihydroxyacetone. *J. Am. Chem. Soc.* **1934**, *56*, 2649–2650.

(89) Alder, R. W.; Reddy, B. S. R. Attempted Equilibration of an Insoluble Spiran Polymer with Monomers and Oligomers through Reversible Chemical Reactions: Transketalization Route to Spiropolymers from 1,4-Cyclohexanedione and Pentaerythritol. *Polymer (Guildf).* **1994**, *35*, 5765–5772.

(90) Zelikin, A. N.; Putnam, D. Poly (carbonate-Acetal)s from the Dimer Form of Dihydroxyacetone. *Macromolecules* **2005**, *38*, 5532–5537.

(91) Putnam, D.; Zelikin, A. Dihydroxyacetone-Based Polymers. U.S. Patent US7659420, 2010.

(92) Jung, S.-H.; Jeong, J.-H.; Miller, P.; Wong, C.-H. An Efficient Multigram-Scale Preparation of Dihydroxyacetone Phosphate. *J. Org. Chem.* **1994**, *59*, 7182–7184.

(93) Linde, F.; Hvid, I.; Madsen, F. The Effect of Specimen Geometry on the Mechanical Behaviour of Trabecular Bone Specimens. *J. Biomech.* **1992**, *25*, 359–368.

(94) Goldstein, S. A. The Mechanical Properties of Trabecular Bone: Dependence on Anatomic Location and Function. *J. Biomech.* **1987**, *20*, 1055–1061.

(95) Arima, Y.; Iwata, H. Effects of Surface Functional Groups on Protein Adsorption and Subsequent Cell Adhesion Using Self-Assembled Monolayers. *J. Mater. Chem.* **2007**, *17*, 4079–4087.

(96) McCoy, C. P.; Morrow, R. J.; Edwards, C. R.; Jones, D. S.; Gorman, S. P. Neighboring Group-Controlled Hydrolysis: Towards "Designer" Drug Release Biomaterials. *Bioconjug. Chem.* **2007**, *18*, 209–215.

(97) Vaisocherová, H.; Yang, W.; Zhang, Z.; Cao, Z.; Cheng, G.; Piliarik, M.; Homola, J.; Jiang, S. Ultralow Fouling and Functionalizable Surface Chemistry Based on a Zwitterionic Polymer Enabling Sensitive and Specific Protein Detection in Undiluted Blood Plasma. *Anal. Chem.* **2008**, *80*, 7894–7901.

(98) Zhang, X.-Q.; Xu, X.; Lam, R.; Giljohann, D.; Ho, D.; Mirkin, C. A. A Strategy for Increasing Drug Solubility and Efficacy through Covalent Attachment to Polyvalent DNA-Nanoparticle Conjugates. *ACS Nano* **2011**, *5*, 6962–6970.

(99) Saito, H.; Hoffman, A. S.; Ogawa, H. I. Delivery of Doxorubicin from Biodegradable PEG Hydrogels Having Schiff Base Linkages. *J. Bioact. Compat. Polym.* **2007**, *22*, 589–601.

(100) Cui, W.; Cui, Y.; Zhu, P.; Zhao, J.; Su, Y.; Yang, Y.; Li, J. An Anticoagulant Activity System Using Nanoengineered Autofluorescent Heparin Nanotubes. *Chem. - An Asian J.* **2012**, *7*, 127–132.

(101) Ren, K.; Ji, J.; Shen, J. Tunable DNA Release from Cross-Linked Ultrathin DNA/PLL Multilayered Films. *Bioconjug. Chem.* **2006**, *17*, 77–83.

(102) Wu, X.; Yu, G.; Luo, C.; Maeda, A.; Zhang, N.; Sun, D.; Zhou, Z.; Puntel, A.; Palczewski, K.; Zheng-Rong, L. Synthesis and Evaluation of a Nanoglobular Dendrimer 5- Aminosalicylic Acid Conjugate with a Hydrolyzable Schiff Base Spacer for Treating Retinal Degeneration. *ACS Nano* **2014**, *8*, 153–161.

(103) Girelli, A. M.; Mattei, E.; Messina, A. Immobilized Tyrosinase Reactor for on-Line HPLC Application. Development and Characterization. *Sensors Actuators, B Chem.* **2007**, *121*, 515–521.

(104) Bao, H.; Liu, S.; Zhang, L.; Chen, G. Efficient Sample Proteolysis Based on a Microchip Containing a Glass Fiber Core with Immobilized Trypsin. *Microchim. Acta* **2012**, *179*, 291–297.

(105) Marques, M. E.; Mansur, A. A. P.; Mansur, H. S. Chemical Functionalization of Surfaces for Building Three-Dimensional Engineered Biosensors. *Appl. Surf. Sci.* **2013**, *275*, 347–360.

(106) Macbeath, G.; Schreiber, S. L. Printing Proteins as Microarrays for High-Throughput Function Determination. *Science (80-.).* **2000**, *289*, 1760–1763.

(107) Avseenko, N. V.; Morozova, T. Y.; Ataullakhanov, F. I.; Morozov, V. N. Immobilization of Proteins in Immunochemical Microarrays Fabricated by Electrospray Deposition. *Anal. Chem.* **2001**, *73*, 6047–6052.

(108) Tian, Y.; He, Q.; Chui, Y.; Li, J. Fabrication of Protein Nanotubes Based on Layer-by-Layer Assembly. *Biomacromolecules* **2006**, *7*, 2539–2542.

(109) Duan, L.; He, Q.; Yan, X.; Cui, Y.; Wang, K.; Li, J. Hemoglobin Protein Hollow Shells Fabricated through Covalent Layer-by-Layer Technique. *Biochem. Biophys. Res. Commun.* **2007**, *354*, 357–362.

(110) Langowska, K.; Kowal, J.; Palivan, C. G.; Meier, W. A General Strategy for Creating Self-Defending Surfaces for Controlled Drug Production for Long Periods of Time. *J. Mater. Chem. B* **2014**, *2*, 4684–4693.

(111) Jia, Y.; Fei, J.; Cui, Y.; Yang, Y.; Gao, L.; Li, J. pH-Responsive Polysaccharide Microcapsules through Covalent Bonding Assembly. *Chem. Commun.* **2011**, *47*, 1175–1177.

(112) Brandl, F.; Sommer, F.; Goepferich, A. Rational Design of Hydrogels for Tissue Engineering: Impact of Physical Factors on Cell Behavior. *Biomaterials* **2007**, *28*, 134–146.

(113) Nicodemus, G. D.; Bryant, S. J. Cell Encapsulation in Biodegradable Hydrogels for Tissue Engineering Applications. *Tissue Eng. Part B. Rev.* **2008**, *14*, 149–165.

(114) Billiet, T.; Vandenhaute, M.; Schelfhout, J.; Van Vlierberghe, S.; Dubruel, P. A Review of Trends and Limitations in Hydrogel-Rapid Prototyping for Tissue Engineering. *Biomaterials* **2012**, *33*, 6020–6041.

(115) Lee, K. Y.; Mooney, D. J. Alginate: Properties and Biomedical Applications. *Prog. Polym. Sci.* **2012**, *37*, 106–126.

(116) Kokabi, M.; Sirousazar, M.; Hassan, Z. M. PVA-Clay Nanocomposite Hydrogels for Wound Dressing. *Eur. Polym. J.* **2007**, *43*, 773–781.

(117) Kirker, K. R.; Luo, Y.; Nielson, J. H.; Shelby, J.; Prestwich, G. D. Glycosaminoglycan Hydrogel Films as Bio-Interactive Dressings for Wound Healing. *Biomaterials* **2002**, *23*, 3661–3671.

(118) Ghobril, C.; Grinstaff, M. W. The Chemistry and Engineering of Polymeric Hydrogel Adhesives for Wound Closure: A Tutorial. *Chem. Soc. Rev.* **2015**, *44*, 1820–1835.

(119) Oelker, A. M.; Grinstaff, M. W. Ophthalmic Adhesives: A Materials Chemistry Perspective. *J. Mater. Chem.* **2008**, *18*, 2521–2536.

(120) Schweizer, D.; Schönhammer, K.; Jahn, M.; Göpferich, A. Protein-Polyanion Interactions for the Controlled Release of Monoclonal Antibodies. *Biomacromolecules* **2013**, *14*, 75–83.

(121) Teles, H.; Vermonden, T.; Eggink, G.; Hennink, W. E.; de Wolf, F. A. Hydrogels of Collagen-Inspired Telechelic Triblock Copolymers for the Sustained Release of Proteins. *J. Control. Release* **2010**, *147*, 298–303.

(122) Oh, E. J.; Park, K.; Kim, K. S.; Kim, J.; Yang, J.-A.; Kong, J.-H.; Lee, M. Y.; Hoffman, A. S.; Hahn, S. K. Target Specific and Long-Acting Delivery of Protein, Peptide, and Nucleotide Therapeutics Using Hyaluronic Acid Derivatives. *J. Control. release* **2010**, *141*, 2–12.

(123) Chen, L. G.; Liu, Z.-L.; Zhuo, R.-X. Synthesis and Properties of Degradable Hydrogels of Konjac Glucomannan Grafted Acrylic Acid for Colon-Specific Drug Delivery. *Polymer (Guildf).* **2005**, *46*, 6274–6281.

(124) Chang, C.; Zhang, L. Cellulose-Based Hydrogels: Present Status and Application Prospects. *Carbohydr. Polym.* **2011**, *84*, 40–53.

(125) Burdick, J. A.; Prestwich, G. D. Hyaluronic Acid Hydrogels for Biomedical Applications. *Adv. Mater.* **2011**, *23*, 41–56.

(126) Augst, A. D.; Kong, H. J.; Mooney, D. J. Alginate Hydrogels as Biomaterials. *Macromol. Biosci.* **2006**, *6*, 623–633.

(127) Baker, M. I.; Walsh, S. P.; Schwartz, Z.; Boyan, B. D. A Review of Polyvinyl Alcohol and Its Uses in Cartilage and Orthopedic Applications. *J. Biomed. Mater. Res. - Part B Appl. Biomater.* **2012**, *100*, 1451–1457.

(128) Krsko, P.; Libera, M. Biointeractive Hydrogels. *Mater. Today* **2005**, *8*, 36–44.

(129) Zhu, J. Bioactive Modification of Poly(ethylene Glycol) Hydrogels for Tissue Engineering. *Biomaterials* **2010**, *31*, 4639–4656.

(130) Lu, S.; Anseth, K. S. Photopolymerization of Multilaminated poly(HEMA) Hydrogels for Controlled Release. *J. Control. Release* **1999**, *57*, 291–300.

(131) Sun, L.; Li, D.; Hemraz, U. D.; Fenniri, H.; Webster, T. J. Self-Assembled Rosette Nanotubes and poly(2-Hydroxyethyl Methacrylate) Hydrogels Promote Skin Cell Functions. *J. Biomed. Mater. Res. - Part A* **2014**, *102A*, 3446–3451.

(132) Lao, U. L.; Sun, M.; Matsumoto, M.; Mulchandani, A.; Chen, W. Genetic Engineering of Self-Assembled Protein Hydrogel Based on Elastin-like Sequences with Metal Binding Functionality. *Biomacromolecules* **2007**, *8*, 3736–3739.

(133) Xu, C.; Breedveld, V.; Kopeček, J. Reversible Hydrogels from Self-Assembling Genetically Engineered Protein Block Copolymers. *Biomacromolecules* **2005**, *6*, 1739–1749.

(134) Dandu, R.; Cresce, A. Von; Briber, R.; Dowell, P.; Cappello, J.; Ghandehari, H. Silk–elastinlike Protein Polymer Hydrogels: Influence of Monomer Sequence on Physicochemical Properties. *Polymer (Guildf).* **2009**, *50*, 366–374.

(135) Zawaneh, P. N.; Singh, S. P.; Padera, R. F.; Henderson, P. W.; Spector, J. A.; Putnam, D. Design of an Injectable Synthetic and Biodegradable Surgical Biomaterial. *Proc. Natl. Acad. Sci. U. S. A.* **2010**, *107*, 11014–11019.

(136) Henderson, P. W.; Kadouch, D. J. M.; Singh, S. P.; Zawaneh, P. N.; Weiser, J.; Yazdi, S.; Weinstein, A.; Krotscheck, U.; Wechsler, B.; Putnam, D.; Spector, J. a. A Rapidly Resorbable Hemostatic Biomaterial Based on Dihydroxyacetone. *J. Biomed. Mater. Res. A* **2010**, *93*, 776–782.

(137) Uhrich, K. E.; Cannizzaro, S. M.; Langer, R. S.; Shakesheff, K. M. Polymeric Systems for Controlled Drug Release. *Chem. Rev.* **1999**, *99*, 3181–3198.

(138) Bajpai, A. K.; Shukla, S. K.; Bhanu, S.; Kankane, S. Responsive Polymers in Controlled Drug Delivery. *Prog. Polym. Sci.* **2008**, *33*, 1088–1118.

(139) Kumar, M. N. V. R.; Kumar, N. Polymeric Controlled Drug-Delivery Systems: Perspective Issues and Opportunities. *Drug Dev. Ind. Pharm.* **2001**, *27*, 1–30.

(140) James, H. P.; John, R.; Alex, A.; Anoop, K. R. Smart Polymers for the Controlled Delivery of Drugs – a Concise Overview. *Acta Pharm. Sin. B* **2014**, *4*, 120–127.

(141) Kost, J.; Langer, R. Responsive Polymeric Delivery Systems. *Adv. Drug Deliv. Rev.* **1991**, *6*, 19–50.

(142) Weiser, J. R.; Yueh, A.; Putnam, D. Protein Release from Dihydroxyacetone-Based Poly(carbonate Ester) Matrices. *Acta Biomater.* **2013**, *9*, 8245–8253.

(143) Weiser, J. R.; Ricapito, N. G.; Yueh, A.; Weiser, E. L.; Putnam, D. A Mechanistic Analysis of the Quantitation of A-Hydroxy Ketones by the Bicinchoninic Acid Assay. *Anal. Biochem.* **2012**, *430*, 116–122.

(144) Dorgan, J. R.; Lehermeier, H. J.; Palade, L.-I.; Cicero, J. Polylactides: Properties and Prospects of an Environmentally Benign Plastic from Renewable Resources. *Macromol. Symp.* **2001**, *175*, 55–66.

(145) Kumar, R.; Choudhary, V.; Mishra, S.; Varma, I. K.; Mattiason, B. Adhesive and Plastics Based on Soy Protein Products. *Ind. Crops Prod.* **2002**, *16*, 155–172.

(146) Mülhaupt, R. Green Polymer Chemistry and Bio-Based Plastics: Dreams and Reality. *Macromol. Chem. Phys.* **2013**, *214*, 159–174.

(147) Mohanty, A. K.; Misra, M.; Drzal, L. T. Sustainable Bio-Composites from Renewable Resources: Opportunities and Challenges in the Green Materials World. *J. Polym. Environ.* **2002**, *10*, 19–26.

(148) Painter, R. M.; Pearson, D. M.; Waymouth, R. M. Selective Catalytic Oxidation of Glycerol to Dihydroxyacetone. *Angew. Chem. Int. Ed. Engl.* **2010**, *49*, 9456–9459.

(149) Kwon, Y.; Birdja, Y.; Spanos, I.; Rodriguez, P.; Koper, M. T. M. Highly Selective Electro-Oxidation of Glycerol to Dihydroxyacetone on Platinum in the Presence of Bismuth. *ACS Catal.* **2012**, *2*, 759–764.

CHAPTER 2

INSIGHT INTO THE UNEXPECTEDLY RAPID DEGRADATION OF DIHYDROXYACETONE-BASED HYDROGELS

(Contributors: Jonathan Mares and Daniel Petralia)

2.1. Abstract

Biodegradable hydrogels are an important class of biomaterials with a diverse range of applications. In some cases, a rapid hydrogel degradation rate is advantageous, for example, in wound healing dressings or chemoembolization technologies. Polycarbonate hydrogels based on dihydroxyacetone (DHA), a natural metabolite, have been reported to undergo surprisingly fast hydrolytic degradation. In the present work, insight into the key features of DHA that contribute to the observed degradation rates is gained. In vitro degradation (mass loss) of three different chemically cross-linked polycarbonate hydrogels is investigated to shed light on the role of the ketone functional group, as well as the carbon-chain length between the ketone and carbonate bonds. The ketone is found to be the main cause for rapid degradation. Hydrogels containing DHA degrade 96.3±3.4% in less than 4 hours, under physiological conditions, whereas similar non-ketone containing hydrogels only degrade 27.7±6.1% over 14 days. A one-unit increase in carbon-chain length decreases the degradation rate, with full degradation in 22.5 hours. DHA-hydrogel mass loss is accelerated by increased temperature and pH, offering insight into potential tuning parameters and storage conditions. The results show that DHA is a promising monomeric unit for the design of rapidly degrading, biocompatible, and functional biomaterials.

---

*Chapter 2 is reprinted with permission from Ricapito, N. G.; Mares, J.; Petralia, D.; Putnam, D. Insight into the Unexpectedly Rapid Degradation of Dihydroxyacetone-Based Hydrogels. *Macromol. Chem. Phys.* **2016.** DOI: 10.1002/macp.201600170. Copyright (2016) Wiley-VCH Verlag GmbH & Co. KGaA, Weinheim.

2.2. Introduction

Hydrogels are highly versatile polymeric systems used in the development of tissue engineering scaffolds,[1–3] drug delivery devices,[4–7] embolic agents,[8–10] and various additional biomedical materials.[11–13] In some applications, the presence of hydrogel is desirable for only short time periods. For example, degradable starch microparticles are used clinically for chemoembolization in the localized treatment of cancers.[14,15] Other examples of rapidly degradable hydrogel applications include template structures to fabricate specialized tissue architectures,[16] and to facilitate insertion of cortical neural probes into the brain by providing short-lived structural integrity to the otherwise flexible probes.[17,18]

Different mechanisms have been used to modulate the rate of hydrogel degradation. For example, starch microparticles are used for temporary vessel embolization owing to their rapid hydrolysis by α-amylase in blood.[19] Polymers bearing pendant nucleophilic groups can undergo intramolecular reactions with the polymer backbone leading to chain cleavage.[20] Adjustment of cross-linking density, as well as the size and quantity of hydrophilic units relative to hydrophobic units, can lead to differences in water uptake and offer valuable control parameters for hydrolytic degradation.[21] Additionally, titration of hydrolytically unstable monomers is also used to fine tune the rate of polymer degradation.[22]

Our group has worked with the synthesis of biomaterials using the biomolecule dihydroxyacetone (DHA, Figure 2.1).[23–25] DHA is an attractive molecule for use in biodegradable biomaterials as it is a natural product in human metabolism and therefore offers reduced probability of toxicity and inflammation upon polymer degradation in the body.[26] One intriguing characteristic of these materials is their unexpectedly rapid degradation rate under aqueous conditions.[27–29] Zawaneh et al. reported 100% degradation of monomethoxy

poly(ethylene glycol)-poly(DHA) diblock copolymers within 24 hours, in vitro.[27] Weiser et al. found that the degradation rate of random copolymers of lactic acid and DHA increased with increasing DHA content.[28]

In this work, we explore the direct synthesis of hydrogel-forming polycarbonate networks, chemically cross-linked with DHA, and probe the mechanism through which these materials degrade in water. Three polycarbonate networks were synthesized using glycerol ethoxylate (GE, I, Figure 2.2), a tri(ethylene glycol) bis(chloroformate) (TEGBC, II, Figure 2.2) cross-linker, and one of three diols: (i) DHA (ii) 1,5 dihydroxy-pentan-3-one (15DH), a molecule similar in structure to DHA but contains two additional carbon atoms, and (iii) tri(ethylene glycol) (TEG), a small hydrophilic compound devoid of a ketone group (Figure 2.1). The results indicate that both the presence of the ketone on DHA, and the carbon chain length between the ketone and carbonate bonds, are contributing factors to the observed degradation rates of DHA-based hydrogels. The effect of DHA on the rapid breakdown of hydrogel in aqueous solution was further confirmed via ^{1}H and diffusion-ordered nuclear magnetic resonance spectroscopy of polymer degradation products. Furthermore, degradation rates were found to increase with increasing pH and temperature, providing insight into potential degradation tuning parameters, polymer processing, sample preparation, and storage conditions for DHA-based materials.

To date, the fast resorption rates of DHA-based hydrogels have proven useful in the prevention of post-operative seromas and also in the development of hemostatic agents.[27,30] The current results illuminate the potential for DHA as a tool in the design of rapidly degrading biomaterials for a broader range of applications. In combination with the amine-reactive functionality of the ketone group, DHA is a promising building block for the development of functional biomaterials.

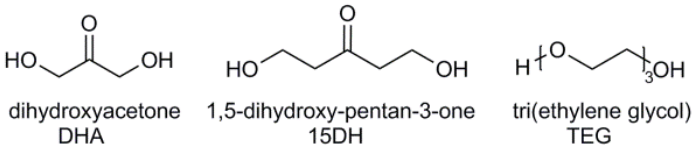

Figure 2.1 Three diols selected for the synthesis of chemically cross-linked hydrogels.

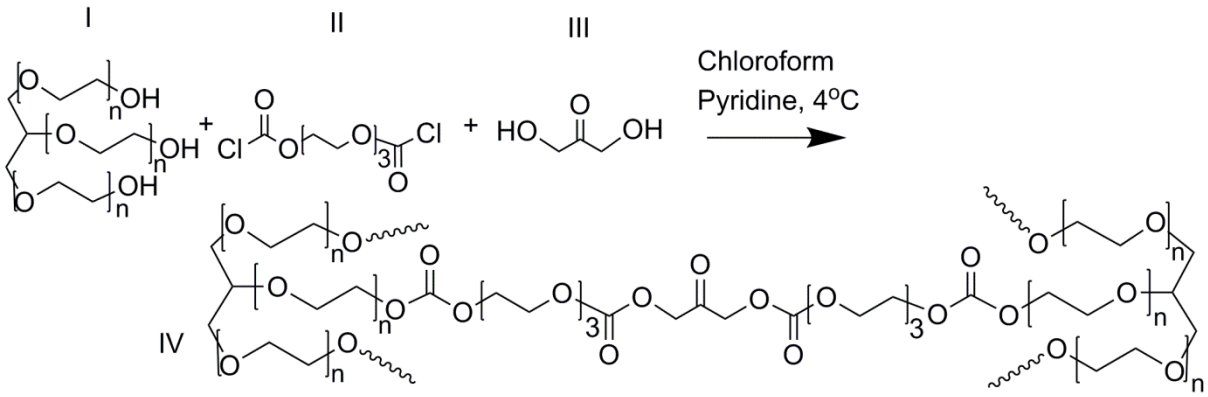

Figure 2.2 CC-DHA polycarbonate network synthesis. (I) glycerol ethoxylate, (II) tri(ethylene glycol) bis(chloroformate), (III) DHA, (IV) CC-DHA polymer network. (~): The symbol serves to indicate continuous cross-linking of the polymer matrix.

2.3. Materials and Methods

2.3.1. Materials

DHA dimer, tri(ethylene glycol) bis(chloroformate), glycerol ethoxylate (M_n ~1,000, n=6-7), anhydrous pyridine, and anhydrous chloroform were purchased from Sigma Aldrich. Chloroform (BDH Chemicals) was purchased from VWR international and 2-propanol (J.T. Baker) was purchased from Avantor Performance Materials (Center Valley, PA). Triethylene glycol was purchased from Alfa Aesar and used as received. 1,5-dihydroxypentan-3-one was purchased from Chem-Impex International, Inc (Wood Dale, IL). Dulbecco's phosphate buffered saline (PBS, 1X, pH 7.4, without calcium or magnesium, Corning Cellgro) and disc filters (0.45µm, Pall Corporation) were purchased from VWR international. Deuterium oxide and dimethyl sulfoxide-d_6 (DMSO-d_6) are produced by Cambridge Isotope Laboratories, Inc. (Andover, MA). Elemental analysis was performed by Intertek Pharmaceutical Services (Whitehouse, NJ) and Midwest Microlab, Inc. (Indianapolis, IN).

Solid state NMR spectra were acquired on a Varian INOVA spectrometer operating at 100.53 MHz for ^{13}C observation with a Varian 7 mm MAS probehead. The samples were packed in silicon nitride rotors and spun at approximately 6000 Hz. Single pulse, direct polarization experiments were performed with a 90 degree excitation pulse of 5 µs duration. Continuous wave ^{1}H decoupling was used with 78 kHz γ B_1. DOSY experiments were acquired at 600 MHz using the convection compensated, double bipolar-pulse stimulated echo sequence (Dbppste_cc) provided in VnmrJ. Diffusion gradients were 3.0 ms long and their strength was varied between 1.9 and 46.8 G-cm^{-1} in 64 increments. Diffusion delay was 150 ms. For each gradient value, 8 scans were acquired with a 1.7 s acquisition time. NMR datasets were processed using MestReNova software. Infrared spectroscopy was performed on a Bruker Tensor 27 FTIR spectrometer using a pike MIRacle ATR with ZnSe crystal.

2.3.2. Preparation of DHA Monomer

DHA dimer was converted to the monomeric form by recrystallization from 2-propanol. 2-Propanol (400 mL) was added to DHA dimer (4 g) and stirred, while partially submerged in a 60^{o}C oil bath, for 40min to ensure complete dissolution. The resulting solution was filtered and approximately 225-275 mL of 2-propanol was removed by rotoevaporation at 50-55^{o}C over a period of 95 minutes or less. The remaining solution was placed at -20^{o}C overnight, after which the crystallized DHA was filtered and dried at room temperature to yield 1.46±0.26 g (36.5±6.5%, n=21). The initial concentration can be increased for greater efficiency: DHA dimer (12 g) is suspended in 2-propanol (400 mL), stirred at 60^{o}C for 1.17hr, followed by filtration and removal of approximately 100 mL of 2-propanol by rotoevaporation, to yield 5.46g (45.5%). ^{1}H NMR spectra were recorded with a 25 s relaxation delay and 90^{o} pulse angle. ^{1}H NMR (400 MHz, DMSO-d_6, δ): 5.02 (t, 2H, OH), 4.16 (d, 4H, CH_2). ^{13}C NMR (100 MHz, DMSO-d_6, δ): 211.46 (C=O), 65.65 (CH_2). Anal. calcd for $C_3H_6O_3$: C 40.00, H 6.71; found (n=22): C 39.93±0.62, H 6.72±0.12. Due to the hygroscopic nature of DHA, elemental analysis was sometimes performed after a period of drying at 80^{o}C.

2.3.3. Polymer Network Synthesis

Chemically cross-linked polycarbonates containing dihydroxyacetone (CC-DHA, Figure 2.3a) were synthesized as follows: tri(ethylene glycol) bis(chloroformate) (TEGBC, 1.8 mL, 0.0088 mol) was added dropwise over 6 min to a stirring mixture of dihydroxyacetone monomer (0.394 g, .00438 mol) and glycerol ethoxylate (GE, 2.919 g, 0.00292 mol) in 6 mL anhydrous chloroform, under N_2, on ice. Next, pyridine (1.62 mL, 0.02 mol) was added over 5.4 min to the bottom of the stirring solution using two 6-inch syringe needles, consecutively. The reaction

begins to form a gel during the final stages of pyridine addition and, with adequate mixing, will fully form a gel in less than 10 minutes of reaction time (Figure A.1). The reaction was completed in a 50mL round-bottom flask with a 15 mm x 6 mm egg-shaped, Teflon-coated, stir bar. Stirring is assisted by movement of the reaction flask across the stir plate during pyridine addition, such that the stir bar can access multiple points of the mixture. The gel was held at 4^{o}C for 3 hours and then cut into 3-4 pieces using a standard weighing spatula. Purification was performed by extraction through gel placement into 400 mL chloroform which was removed and replaced with fresh chloroform six times over a 4 day period. The gel was further purified through 10 minute incubation steps in 25:75, 50:50, and 75:25 volume-to-volume solutions of diethyl ether and chloroform, respectively, followed by 20 minutes in 100% diethyl ether. Lastly, the gel was dried over two nights in vacuo, briefly washed with MilliQ water, lyophilized, and stored under N_2 at 4^{o}C. Yield: 3.720g ± 0.234g, n=4

CC-Control gels (Figure 2.3b, yield: 4.183 g) and CC-15Dihydroxy gel (Figure 2.3c, yield: 2.918 g) were synthesized using the same protocol; however, triethylene glycol (0.584 mL, .00438 mol) and 1,5-dihydroxypentan-3-one (0.432 mL, 0.00417 mol), were used, respectively, in place of dihydroxyacetone. Chemical structures and solid state ^{13}C NMR spectra for all three polymer networks are shown in Figure 2.3.

2.3.4. In Vitro Degradation

The degradation rate of CC-DHA, CC-15Dihydroxy, and CC-Control gels were tested under physiologically relevant conditions. Known weights of each gel (19.9-20.5 mg) were cut using a standard razor blade, placed in PBS (1.0 mL, pH=7.4), and rotated at 37 ^{o}C. At specified time points, each sample was removed, poured over a pre-weighed 0.45µm membrane disc filter,

and washed with DI water. The filter and hydrogel were lyophilized and re-weighed to determine the remaining mass of hydrogel.

The degradation behavior dependence of CC-DHA gels on pH and temperature was evaluated using the same methodology. For temperature dependence, samples were incubated at 4^{o}C, room temperature, and 37^{o}C in PBS, pH=7.4. To study the effect of pH, samples were incubated at 37^{o}C in 0.1 M sodium phosphate buffer adjusted to pH=6, pH=7, and pH=8.

To study the degradation products of CC-DHA hydrogels, 20 mg samples were rotated for 7 hours in a D_2O/PBS solution (1.0 mL each) at 37^{o}C. D_2O/PBS was prepared by lyophilization of 1x PBS (5mL, pH=7.4) followed by resuspension in D_2O (5mL). The final solution was evaluated by ^{1}H NMR, diffusion-ordered ^{1}H NMR, and ^{1}H-^{13}C heteronuclear multiple-bond correlation (HMBC) NMR spectroscopy.

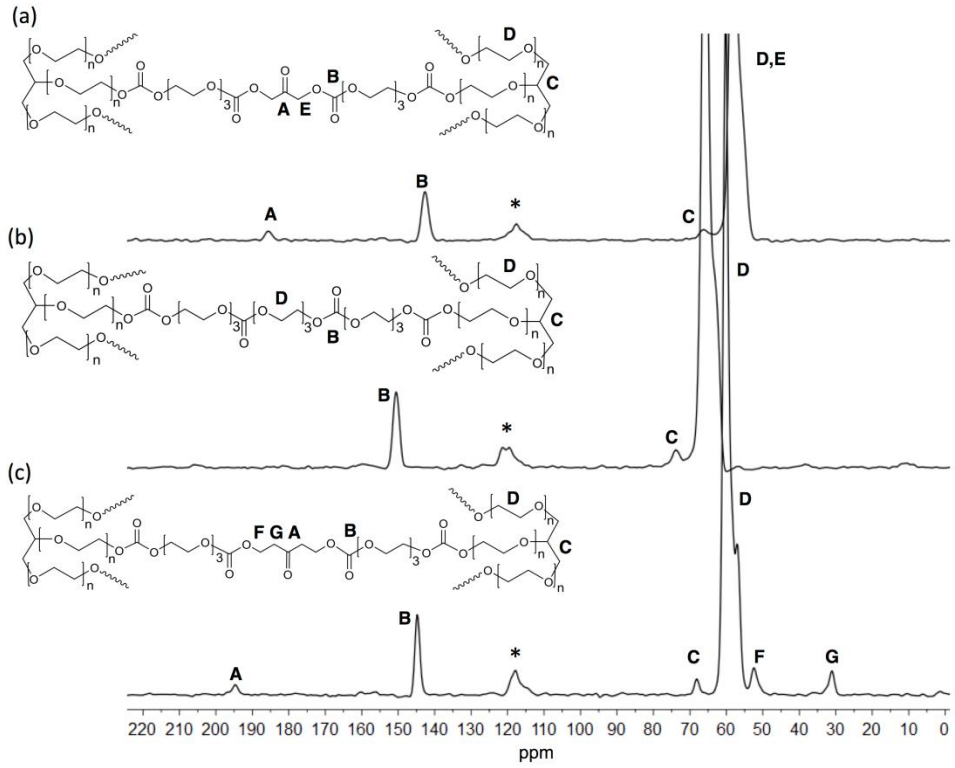

Figure 2.3 Chemical structures and solid state ^{13}C NMR spectra of (a) CC-DHA, (b) CC-Control and (c) CC-15Dihydroxy polycarbonate networks. *Spinning side band.

2.3.5. Hydrogel Swelling Analysis

Three samples (19.9-20 mg) of each hydrogel were cut using a razor blade and then rotated in 1.0 mL of PBS at 37 ^{o}C. At 10 minute intervals, the gels were removed, drained of excess liquid, gently dried with filter paper, and weighed. Once weighed, the gels were placed in 1.0 mL of fresh PBS (pre-warmed to 37 ^{o}C) and placed back under rotation at 37^{o}C. Percent swelling was calculated according to Equation 2.1.

$$\%\, Swelling = \frac{Wet\ mass\ (mg)}{Initial\ dry\ mass\ (mg)} x100 \qquad (Eq.\ 2.1)$$

2.4. Results and Discussion

2.4.1. Preparation of DHA Monomer

The monomeric form of dihydroxyacetone (Figure 2.1) is obtained by stirring a heated mixture of DHA dimer and 2-propanol, followed by partial solvent removal and recrystallization. The results were confirmed via NMR spectroscopy and elemental analysis. ^{1}H NMR performed in DMSO-d_6 shows coupling between the α-hydroxy hydrogen atoms and -CH_2- protons, as reported previously by Davis using a separate lyophilization-based protocol to achieve the solid monomer.[31] In many cases, additional very low intensity peaks arise in both the carbon and hydrogen NMR spectra, which may be due to small quantities of equilibrium structures.[32] To further support the formation of monomeric DHA, FT-IR spectroscopy was performed on the solid product to confirm the presence of ketone groups, which are not present in dimeric DHA (Figure A.2). Yields for the monomer formation were low (36.5±6.5%, n=21), which is possibly a result of prolonged exposure to 50-60^{o}C temperatures as DHA has reduced stability when heated.[33,34]

2.4.2. Network Synthesis and Characterization

Dihydroxyacetone-based polycarbonate networks were synthesized utilizing the synthetic scheme shown in Figure 2.2. Glycerol ethoxylate (I, GE, Figure 2.2) is the key contributor to gel hydrophilicity and tri(ethylene glycol) bis(chloroformate) (II, TEGBC, Figure 2.2) offers a facile synthetic method to create DHA cross-links in the polymer matrix. Chloroformate-containing compounds, such as TEGBC, react readily with primary alcohols like those in DHA, in the presence of a base, without interfering with the ketone functional group.[23,35]

Since the chloroformate groups of TEGBC are reactive with the primary alcohol groups on GE as well as DHA, the exact polymerization and crosslinking pattern is not predictable, which is characteristic of networks formed in this way. To maximize the likelihood of creating the desired polymers (Figure 2.3a) and to preserve consistency between batches, a molar ratio of GE (1): TEGBC (3): DHA (1.5) was employed. With adequate mixing, all reaction components appear as a gel in less than 10 minutes of reaction time.

To investigate the effect of the ketone functional group on the rapid degradation of DHA-based hydrogels, two similar hydrogels were synthesized, and their degradation rates were determined for comparison. In one case, DHA is replaced by TEG (Figure 2.1), a small non-ketone containing crosslinker. Hydrogels made with TEG are referred to as CC-Control gels (Figure 2.3b). In the other case, DHA is replaced by 15DH (Figure 2.1), a crosslinker similar to DHA, but with an additional carbon between the ketone and hydroxyl groups. Hydrogels containing 15DH are referred to as CC-15Dihydroxy gels (Figure 2.3c).

Solid state ^{13}C NMR was used to verify the successful synthesis of each polymer network. It is important to note that precise shift values (and expected values) differ slightly between each spectrum due to the absence of an internal reference. The spectra show that all three polymers

contain carbonate bonds (~143-151ppm) and glycerol ethoxylate peaks (~55-70ppm), while only CC-DHA and CC-15Dihydroxy gels contain ketone peaks (186ppm and 195ppm, respectively). The ketone group in DHA-based polycarbonates has been shown to appear at 199ppm and 205ppm in previously reported DHA carbonates.[23] Therefore, a downfield correction of 10-15ppm, which is reasonable due to the carbonate peak appearance at 143ppm,[36] yields an expected ketone shift for a DHA-based polycarbonate. Lastly, the carbon chain between the ketone and carbonate bonds of CC-15Dihydroxy gels is evident through the peaks appearing at 31ppm and 52ppm in Figure 2.3c.

2.4.3. Hydrogel Degradation and Swelling

To study hydrogel degradation, samples of each gel were incubated in PBS (pH=7.4) at 37^{o}C and evaluated for mass loss at pre-determined incubation times. The results are shown in Figure 2.4. It was found that CC-DHA gels are 96.3±3.4% degraded in 3.8 hours, whereas CC-Control gels are only 27.7±6.1% degraded after 14 days of incubation. It is evident that DHA drastically increases the rate of degradation compared to TEG. CC-15Dihydroxy gels were found to degrade more slowly than CC-DHA gels, but on a similar timescale, with full degradation occurring in approximately one day of incubation. The CC-15Dihydroxy results further suggest that the ketone group plays a primary role in the observed rapid degradation, and also indicates that the ketone's neighboring carbon chain length plays an important role in the measured rates.

All gels were swollen to at least twice their original mass within 20 minutes of incubation (Figure 2.5). Due to the random nature of the reaction, CC-DHA gels were tested for batch-to-batch variance (Figure 2.5a). Swelling variance is observed between batches, however, all gels show the same trend; a rapid decline in mass within the early stages of incubation due to the

competing rate of degradation over the observed timeframe. Despite the variance in swelling, all DHA-based gels degrade on a similarly rapid timescale, as expected. The four CC-DHA batches are included in the CC-DHA degradation curve shown in Figure 2.4, and are displayed individually in Appendix A (Figure A.3).

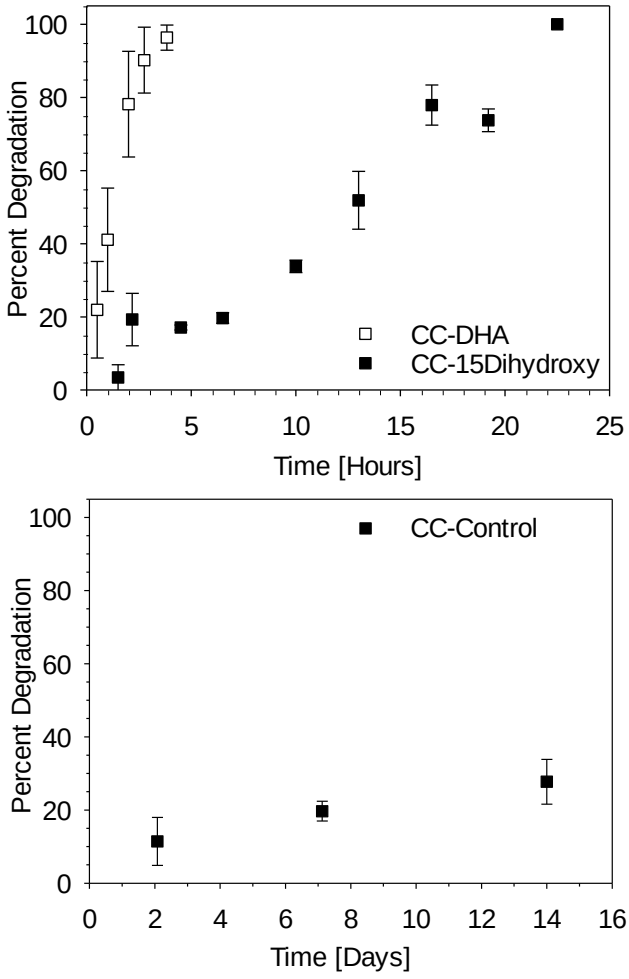

Figure 2.4. Degradation profiles of 20 mg samples of CC-DHA (n=12 per time point, 4 batches), CC-15Dihydroxy (n=3 per time point, 1 batch), and CC-Control gels (n=3 per time point, 1 batch) in PBS at 37^{o}C.

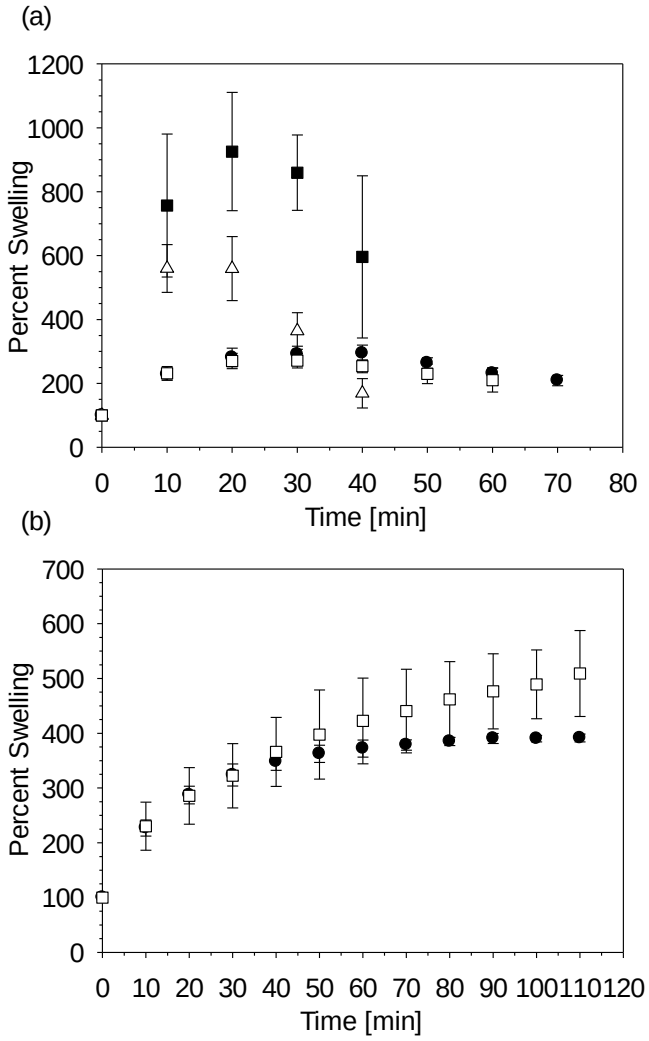

Figure 2.5. Percent swelling vs. time in PBS, pH=7.4, at 37°C. (a) Four batches of CC-DHA hydrogels where n=3 for each batch. (■) Batch 1, (△) Batch 2, (●) Batch 3, and (□) Batch 4 (b) Percent swelling of (●) CC-Control (n=3, 1 batch), and (□) CC-15Dihydroxy (n=3, 1 batch) hydrogels.

The data shown in Figure 2.4 provide evidence that both the presence of the ketone on DHA, as well as the short carbon chain length between the ketone and neighboring carbonate bonds, contribute to the rapid rate of degradation of DHA-based materials. To provide further mechanistic insight into the breakdown of CC-DHA gels, the water-soluble polymer degradation products after 7 hours of incubation in D_2O/PBS, at 37°C, were studied. The CC-DHA hydrogels

contain two types of carbonate linkages, each with unique neighboring groups; those that connect GE and TEGBC, and those that connect DHA and TEGBC (Figure 2.6). The degradation profiles reported in Figure 2.4 show the percent of hydrogel mass that is breaking down into soluble components, but do not indicate which carbonate bonds were cleaved. Since both types of carbonate bonds contribute to cross-linking, cleavage of either, or both types, could yield the observed degradation of the gel. NMR analysis of the degradation products reveals that carbonate bonds linking GE and TEGBC remain intact after the 7 hour incubation period, whereas the bonds between DHA and the polymer backbone are cleaved (Figure 2.7a). A ^{1}H-^{13}C HMBC NMR spectrum is included in Appendix A (Figure A.4).

Diffusion-ordered NMR (DOSY) was used to show that DHA is not bound to the large molecular weight polymer backbone after the allotted degradation time. DOSY is used to distinguish peaks that belong to slow-moving, large molecules from those that belong to fast-moving, small molecules.[37,38] A normalized signal attenuation plot (based on peak integration) provides strong evidence that DHA is not covalently bound to the GE backbone (Figure 2.7b). The methylene proton peaks of DHA attenuate more rapidly than the protons of GE, with increasing gradient, which corresponds to faster diffusion in solution, indicating that the respective compounds are not attached.

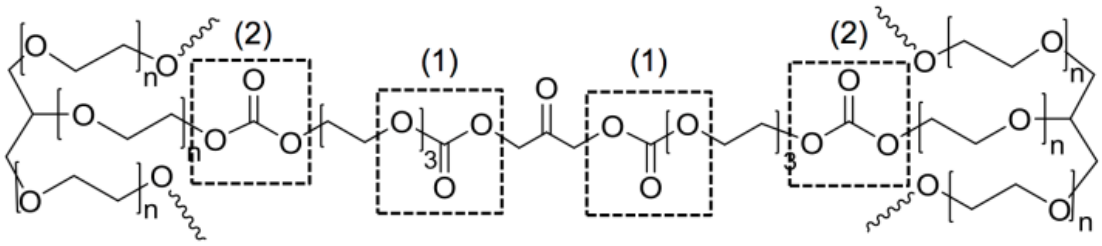

Figure 2.6. Sample structure of CC-DHA polymer networks containing (1) carbonate bonds formed by DHA and TEGBC, and (2) carbonate bonds formed between GE and TEGBC.

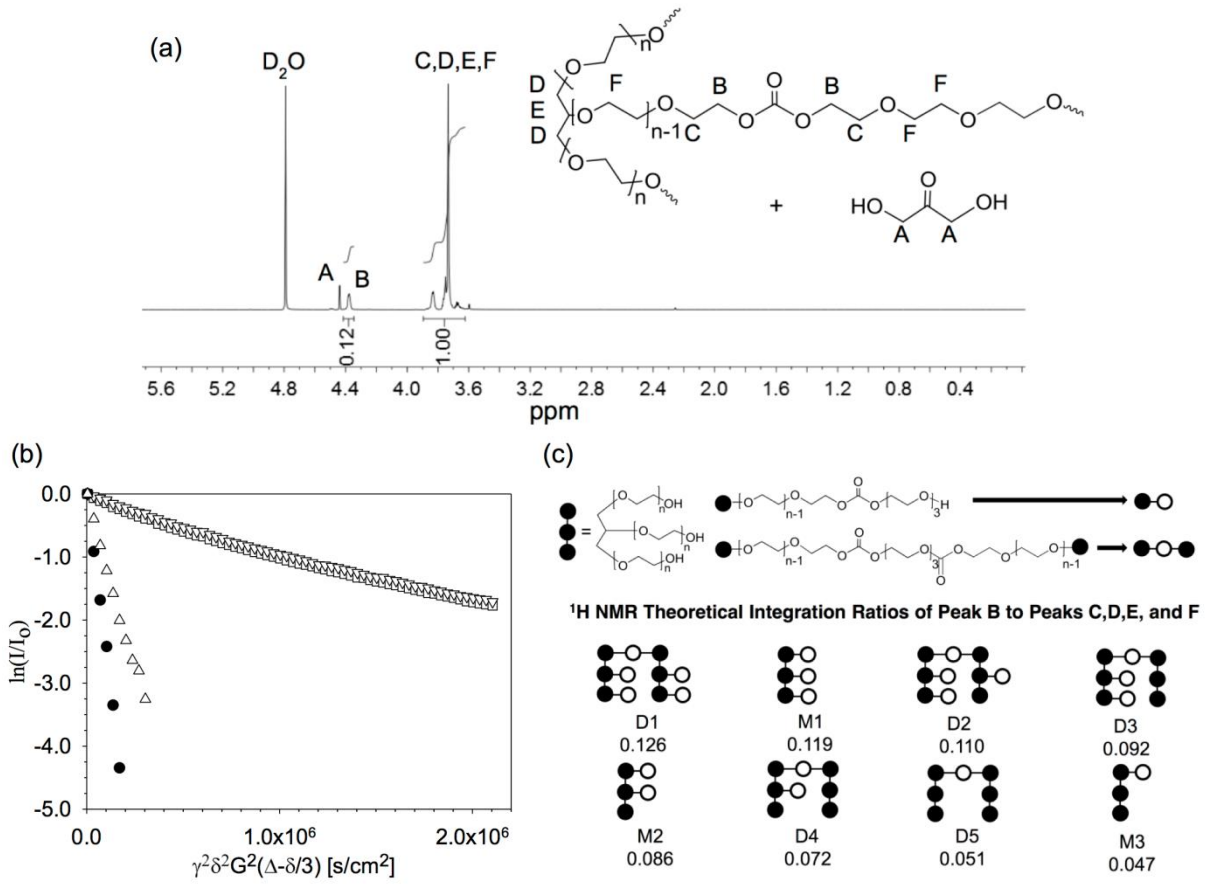

Figure 2.7. Analysis of CC-DHA degradation products following incubation in D_2O/PBS at 37°C, for 7 hours. (a) ^{1}H NMR spectrum. The (~) symbol serves to represent different extension possibilities, for example, a terminating hydroxyl group, or a carbonate bond followed by further polymerization with TEGBC. (b) Normalized signal attenuation data collected via diffusion-ordered ^{1}H NMR. [□] peaks C,D,E, and F, [▽] Peak B, [△] Peak A, [●] D_2O (c) Possible hydrogel degradation products include, but are not limited to, the structures shown. For each structure, the theoretical integration ratio of peak B to the combined integration of peaks C,D,E, and F, is calculated For these values, the repeat unit of GE is n=6. The ratio decreases with decreasing carbonate linkages between GE and TEG. Species D1, M1, and D2 are nearest the measured ratio of 0.12 (Figure 2.7a). Since the measured ratio is comparable to species of GE that are highly conjugated to TEG, it is concluded that minimal hydrolysis, if any, of GE-TEG carbonate linkages occurs in the 7 hour incubation time.

The integration ratio of peak B (Figure 2.7a) to all other polymer backbone peaks (peaks C,D,E, and F, Figure 2.7a) was studied to gain insight into the proportion of GE-TEGBC carbonate bonds (2, Figure 2.6) that were cleaved in the 7 hour incubation time. The integration

ratio was found to be 0.12 to 1.00 (n=3), respectively, as shown in Figure 2.7a. Due to the random nature of the reaction, there exists a mixture of GE-TEGBC combinations in the final products. A few example possibilities of remaining monomeric and dimeric GE species are illustrated in Figure 2.7c. Note that of the pictured structures, the theoretical integration ratio is nearest the measured value of 0.12 for compounds with high, or maximal, conjugation of TEGBC (D1,M1,D2, Figure 2.7c). Overall, while the precise makeup of final structures is challenging to characterize, it is clear that minimal hydrolysis, if any, occurred between GE and TEGBC in the first 7 hours of incubation. It can be concluded that the broken bonds, causing a once insoluble hydrogel to break apart and dissolve into solution, were the carbonate bonds formed between TEGBC and DHA.

The results indicate that the rapid degradation rates of DHA-based materials observed by Zawaneh et al.,[27] Weiser et al.,[28] and Wang et al.[29] are not limited to the specific systems studied. In hydrophilic environments, there appears to be an underlying mechanism for the observed rapid degradation rates in all systems.

Wang et al. studied the degradation of dimethoxy ketone-protected DHA homopolymers versus that of 42% deprotected (i.e. ketone-containing) DHA homopolymers.[29] Ketone-containing films were found to degrade much faster; 100% degradation was observed in 5 days, whereas the non-ketone containing films degraded less than 5% in 10 days. The difference in degradation rates was attributed to the increased hydrophilicity of the ketone-containing polymers. It is true that hydrophilicity of hydrolytically degradable polymer backbones plays a significant role in hydrolysis rates owing to increased water access to susceptible bonds. However, in the present study, CC-DHA gels were compared against similar hydrophilic materials, indicating that hydrophilicity does not fully account for the observed trends.

Neighboring group participation of carbonyl groups is known to significantly increase hydrolysis rates in several compounds.[39,40] One possible degradation mechanism in DHA-based systems that involves the ketone is an initial hydration step to form a gem-diol, followed by an intramolecular nucleophilic attack on neighboring carbonate bonds.[41–44] DHA is known to hydrate in aqueous solution and has an equilibrium ketone to hydrate ratio of 4:1, respectively, in D_2O at room temperature.[31] Other investigators have demonstrated that nearby hydroxyl groups can facilitate polycarbonate degradation. For example, Zhang and Grinstaff synthesized poly(1,2-glycerol carbonate)s, which contain pendant primary hydroxyl groups that react with neighboring carbonate bonds and promote polymer degradation. The polymers were shown to have a half-life of 2-3 days in DMF at 37^{o}C.[45] Acemoglu et al. also observed polycarbonate cleavage via intramolecular attack from pendant hydroxyl groups in poly(hydroxyalkylene carbonate)s.[46]

2.4.4. pH and Temperature Dependence

CC-DHA hydrogels were further studied for temperature and pH dependence. Degradation in sodium phosphate buffer was measured at pH 6, 7, and 8 for physiological relevance (Figure 2.8). The gels showed a clear trend for increasing degradation rate with increasing pH. While the underlying mechanism remains unknown, the fractional dry mass remaining over time can be fit to pseudo-first order kinetics for comparison of rates. Details on fitting are included in Appendix A (Figure A.5) and observed rate constants (min^{-1}) are k_{obs}=0.0014 ± 0.0002, k_{obs}= 0.023 ± 0.002, and k_{obs} = 0.028 ± 0.002, for pH=6, pH=7, and pH=8, respectively. The results suggest that pH is a potential tuning parameter for use in biomedical applications. Another interesting characteristic is hydrogel swelling at neutral pH. Similarly to

the aforementioned PBS trials (Figure 2.5a), swelling data show an increase in mass, followed by a rapid decline. One particular application where such behavior may be useful is chemoembolization, where temporary vascular embolization is used to locally target chemotherapeutics to specific organ locales (ex: reperfusion 26-39min).[14]

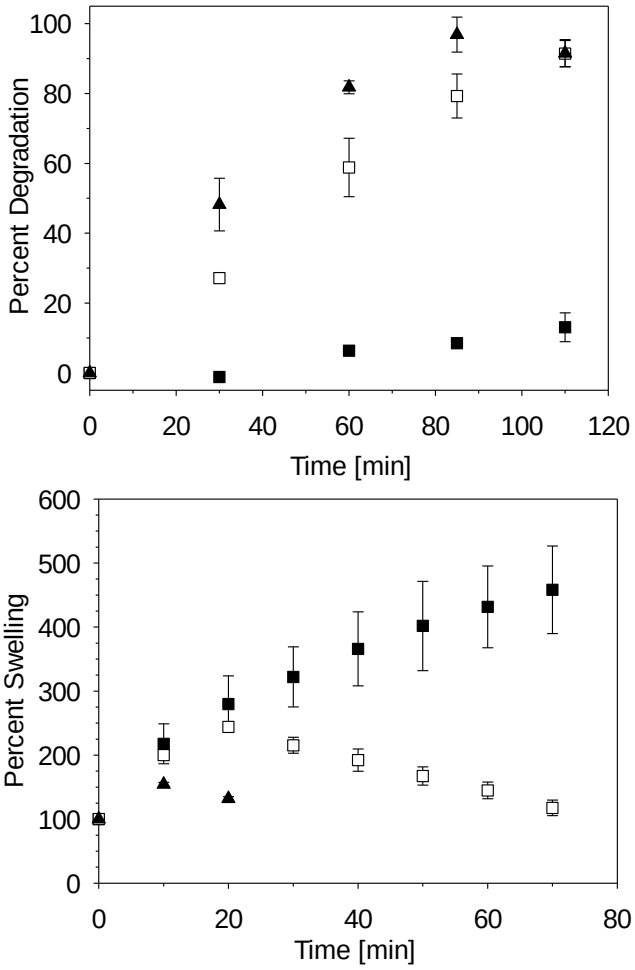

Figure 2.8. Degradation (n=3 per time point, at each pH) and swelling rates (n=3 for each pH) of 20 mg samples of CC-DHA in sodium phosphate buffer at (▲) pH=8, (□) pH=7, and (■) pH=6.

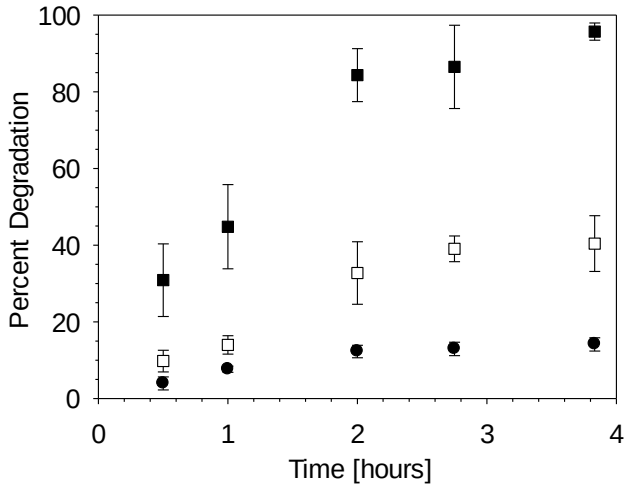

Figure 2.9. Degradation rate of CC-DHA (20 mg, n=3 per time point, at each temperature) in PBS at (●) 4°C (□) room temperature and (■) 37°C.

Rapidly degrading hydrogels have significant use in various biomedical applications; therefore, polymer stability is desired during material preparation and storage. Consequently, we studied the effect of temperature on hydrogel stability (Figure 2.9). It was found that CC-DHA hydrogels are significantly more stable at 4°C than 37°C, suggesting that DHA-based polymers could be sufficiently stable when handled and stored in cold and dehumidified environments. A pseudo-first order fit (Figure A.6) of fractional dry mass remaining over time yields observed rate constants (hr^{-1}) of $k_{obs} = 0.039 \pm 0.004$ (at 4°C), $k_{obs} = 0.15 \pm 0.02$ (at 23°C), and $k_{obs} = 0.87 \pm 0.08$ (at 37°C), with associated pseudo-first order calculated half-lives of 18 ± 2.0 hr, 4.6 ± 0.5 hr, and 0.80 ± 0.07 hr, for temperatures at 4°C, room temperature, and 37°C, respectively.

2.5. Conclusions

Dihydroxyacetone-based materials have been shown to degrade rapidly under aqueous conditions. The precise degradation mechanism remains unknown; however, insight into the key

contributing factors has been gained from the investigation of the hydrogels reported herein. The present study confirms that the ketone present on DHA is a principle factor leading to the observed trends. Degradation rates also appear to be affected by the one-carbon chain length between ketone and carbonate bonds. Extension to two carbon units leads to retardation of hydrogel degradation rate. Additionally, CC-DHA hydrogels showed a trend for increasing degradation with increasing pH and temperature, which are potential tuning parameters for the application of DHA-based materials. Overall, DHA is a promising candidate for the synthesis of rapidly degrading hydrophilic biomaterials.

2.6. Acknowledgments

We would like to thank Dr. Ivan Keresztes for his expertise and assistance with solid state, diffusion-ordered, and HMBC NMR spectroscopy. This work was made possible by the Cornell Chemistry NMR facility. This work also made use of the Cornell Center for Materials Research shared facilities which are supported through the NSF MRSEC program (DMR-1120296).

2.7. References

(1) Drury, J. L.; Mooney, D. J. Hydrogels for Tissue Engineering: Scaffold Design Variables and Applications. *Biomaterials* **2003**, *24*, 4337–4351.

(2) Bryant, S. J.; Anseth, K. S. The Effects of Scaffold Thickness on Tissue Engineered Cartilage in Photocrosslinked Poly(ethylene Oxide) Hydrogels. *Biomaterials* **2001**, *22*, 619–626.

(3) Elisseeff, J.; Puleo, C.; Yang, F.; Sharma, B. Advances in Skeletal Tissue Engineering with Hydrogels. *Orthod. Craniofacial Res.* **2005**, *8*, 150–161.

(4) Zhang, S.; Ermann, J.; Succi, M. D.; Zhou, A.; Hamilton, M. J.; Cao, B.; Korzenik, J. R.; Glickman, J. N.; Vemula, P. K.; Glimcher, L. H.; Traverso, G.; Langer, R.; Karp, J. M. An Inflammation-Targeting Hydrogel for Local Drug Delivery in Inflammatory Bowel Disease. *Sci. Transl. Med.* **2015**, *7*, 300RA128.

(5) Sharpe, L. A.; Daily, A. M.; Horava, S. D.; Peppas, N. A. Therapeutic Applications of Hydrogels in Oral Drug Delivery. *Expert Opin. Drug Deliv.* **2014**, *11*, 901–915.

(6) Qiu, B.; Stefanos, S.; Ma, J.; Lalloo, A.; Perry, B. A.; Leibowitz, M. J.; Sinko, P. J.; Stein, S. A Hydrogel Prepared by in Situ Cross-Linking of a Thiol-Containing Poly(ethylene Glycol)-Based Copolymer: A New Biomaterial for Protein Drug Delivery. *Biomaterials* **2003**, *24*, 11–18.

(7) Vashist, A.; Vashist, A.; Gupta, Y. K.; Ahmad, S. Recent Advances in Hydrogel Based Drug Delivery Systems for the Human Body. *J. Mater. Chem. B* **2014**, *2*, 147–166.

(8) Su, X.; Bu, L.; Dong, H.; Fu, S.; Zhuo, R.; Zhong, Z. An Injectable PEG-Based Hydrogel Synthesized by Strain-Promoted Alkyne–azide Cycloaddition for Use as an Embolic Agent. *RSC Adv.* **2016**, *6*, 2904–2909.

(9) Gobin, Y. P.; Viñuela, F.; Vinters, H. V.; Ji, C.; Chow, K. Embolization with Radiopaque Microbeads of Polyacrylonitrile Hydrogel: Evaluation in Swine. *Radiology* **2000**, *214*, 113–119.

(10) Weng, L.; Rostambeigi, N.; Zantek, N. D.; Rostamzadeh, P.; Bravo, M.; Carey, J.; Golzarian, J. An in Situ Forming Biodegradable Hydrogel-Based Embolic Agent for Interventional Therapies. *Acta Biomater.* **2013**, *9*, 8182–8191.

(11) Grinstaff, M. W. Designing Hydrogel Adhesives for Corneal Wound Repair. *Biomaterials* **2007**, *28*, 5205–5214.

(12) Quinn, C. A. P.; Connor, R. E.; Heller, A. Biocompatible, Glucose-Permeable Hydrogel for in Situ Coating of Implantable Biosensors. *Biomaterials* **1997**, *18*, 1665–1670.

(13) Zhou, C.; Li, P.; Qi, X.; Sharif, A. R. M.; Poon, Y. F.; Cao, Y.; Chang, M. W.; Leong, S. S. J.; Chan-Park, M. B. A Photopolymerized Antimicrobial Hydrogel Coating Derived from Epsilon-Poly-L-Lysine. *Biomaterials* **2011**, *32*, 2704–2712.

(14) Pieper, C. C.; Meyer, C.; Vollmar, B.; Hauenstein, K.; Schild, H. H.; Wilhelm, K. E. Temporary Arterial Embolization of Liver Parenchyma with Degradable Starch Microspheres (EmboCept(R)S) in a Swine Model. *Cardiovasc. Intervent. Radiol.* **2015**, *38*, 435–441.

(15) Hakansson, L.; Hakansson, A.; Morales, O.; Thorelius, L.; Warfving, T. Spherex (Degradable Starch Microspheres) Chemo-Occlusion - Enhancement of Tumor Drug Concentration and Therapeutic Efficacy: An Overview. *Semin. Oncol.* **1997**, *24*, S6–S100 – S6–S109.

(16) Sakai, S.; Inagaki, H.; Liu, Y.; Matsuyama, T.; Kihara, T.; Miyake, J.; Kawakami, K.; Taya, M. Rapidly Serum-Degradable Hydrogel Templating Fabrication of Spherical Tissues and Curved Tubular Structures. *Biotechnol. Bioeng.* **2012**, *109*, 2911–2919.

(17) Lo, M.; Wang, S.; Singh, S.; Damodaran, V. B.; Kaplan, H. M.; Kohn, J.; Shreiber, D. I.; Zahn, J. D. Coating Flexible Probes With An Ultra Fast Degrading Polymer to Aid in Tissue Insertion. *Biomed. Microdevices* **2015**, *17*, 34.

(18) Lewitus, D.; Smith, K. L.; Shain, W.; Kohn, J. Ultrafast Resorbing Polymers for Use as Carriers for Cortical Neural Probes. *Acta Biomater.* **2011**, *7*, 2483–2491.

(19) Hamdi, G.; Ponchel, G. Enzymatic Degradation of Epichlorohydrin Crosslinked Starch Microspheres by Alpha-Amylase. *Pharm. Res.* **1999**, *16*, 867–875.

(20) Deshmukh, M.; Singh, Y.; Gunaseelan, S.; Gao, D.; Stein, S.; Sinko, P. J. Biodegradable Poly(ethylene Glycol) Hydrogels Based on a Self-Elimination Degradation Mechanism. *Biomaterials* **2010**, *31*, 6675–6684.

(21) Truong, V.; Blakey, I.; Whittaker, A. K. Hydrophilic and Amphiphilic Polyethylene Glycol-Based Hydrogels with Tunable Degradability Prepared by "Click" Chemistry. *Biomacromolecules* **2012**, *13*, 4012–4021.

(22) Dijk-Wolthuis, W. N. E. van; Hoogeboom, J. A. M.; Steenbergen, M. J. van; Tsang, S. K. Y.; Hennink, W. E. Degradation and Release Behavior of Dextran-Based Hydrogels. *Macromolecules* **1997**, *30*, 4639–4645.

(23) Zelikin, A. N.; Zawaneh, P. N.; Putnam, D. A Functionalizable Biomaterial Based on Dihydroxyacetone, an Intermediate of Glucose Metabolism. *Biomacromolecules* **2006**, *7*, 3239–3244.

(24) Zawaneh, P. N.; Doody, A. M.; Zelikin, A. N.; Putnam, D. Diblock Copolymers Based on Dihydroxyacetone and Ethylene Glycol: Synthesis, Characterization, and Nanoparticle Formulation. *Biomacromolecules* **2006**, *7*, 3245–3251.

(25) Weiser, J. R.; Yueh, A.; Putnam, D. Protein Release from Dihydroxyacetone-Based Poly(carbonate Ester) Matrices. *Acta Biomater.* **2013**, *9*, 8245–8253.

(26) Ricapito, N. G.; Ghobril, C.; Zhang, H.; Grinstaff, M. W.; Putnam, D. Synthetic Biomaterials from Metabolically Derived Synthons. *Chem. Rev.* **2016**, *116*, 2664–2704.

(27) Zawaneh, P. N.; Singh, S. P.; Padera, R. F.; Henderson, P. W.; Spector, J. A.; Putnam, D. Design of an Injectable Synthetic and Biodegradable Surgical Biomaterial. *Proc. Natl. Acad. Sci. U. S. A.* **2010**, *107*, 11014–11019.

(28) Weiser, J. R.; Zawaneh, P. N.; Putnam, D. Poly(carbonate-Ester)s of Dihydroxyacetone and Lactic Acid as Potential Biomaterials. *Biomacromolecules* **2011**, *12*, 977–986.

(29) Wang, L.-S.; Cheng, S.-X.; Zhuo, R.-X. Synthesis and Hydrolytic Degradation of Aliphatic Polycarbonate Based on Dihydroxyacetone. *Polym. Sci. Ser. B* **2013**, *55*, 604–610.

(30) Henderson, P. W.; Kadouch, D. J. M.; Singh, S. P.; Zawaneh, P. N.; Weiser, J.; Yazdi, S.; Weinstein, A.; Krotscheck, U.; Wechsler, B.; Putnam, D.; Spector, J. a. A Rapidly Resorbable Hemostatic Biomaterial Based on Dihydroxyacetone. *J. Biomed. Mater. Res. A* **2010**, *93*, 776–782.

(31) Davis, L. The Structure of Dihydroxyacetone in Solution. *Bioorg. Chem.* **1973**, *2*, 197–201.

(32) Kobayashi, Y.; Takahashi, H. Conformational Studies of Glycolaldehyde and 1,3-Dihydroxyacetone in Solution by 1H-NMR. *Spectrochim. Acta Part A Mol. Biomol. Spectrosc.* **1979**, *35*, 307–314.

(33) Zhu, Y.; Youssef, D.; Porte, C.; Rannou, A.; Delplancke-Ogletree, M. P.; Lung-Somarriba, B. L. M. Study of the Solubility and the Metastable Zone of 1,3-Dihydroxyacetone for the Drowning-out Process. *J. Cryst. Growth* **2003**, *257*, 370–377.

(34) Hettwer, J.; Oldenburg, H.; Flaschel, E. Enzymic Routes to Dihydroxyacetone Phosphate or Immediate Precursors. *J. Mol. Catal. B Enzym.* **2002**, *19-20*, 215–222.

(35) J. N. Korley, S. Yazdi, K. McHugh, J. Kirk, J. Anderson, D. Putnam. One-step synthesis, biodegradation and biocompatibility of polyesters based on the metabolic synton, dihydroxyacetone. *Biomaterials* **2016**, *98*, 41.

(36) Copeland, C.; Conway, R. J.; Patroni, J. J.; Stick, R. V. The Use of 13C N.M.R. Spectroscopy for the Characterization of Carbonates, Thiocarbonates, Dithiocarbonates and Trithiocarbonates. *Aust. J. Chem.* **1981**, *34*, 555–557.

(37) Crawford, L.; Putnam, D. Synthesis and Characterization of Macromolecular Rhodamine Tethers and Their Interactions with P-Glycoprotein. *Bioconjug. Chem.* **2014**, *25*, 1462–1469.

(38) Momot, K. I.; Kuchel, P. W. Pulsed Field Gradient Nuclear Magnetic Resonance as a Tool for Studying Drug Delivery Systems. *Concepts Magn. Reson. Part A* **2003**, *19A*, 51–64.

(39) Bowden, K. Intramolecular Catalysis: Carbonyl Groups in Ester Hydrolysis. *Chem. Soc. Rev.* **1995**, *24*, 431–435.

(40) Bowden, K. Neighbouring Group Participation by Carbonyl Groups in Ester Hydrolysis. In *Advances in Physical Organic Chemistry*; Bethell, D., Ed.; Elsevier, Inc., 1993; Vol. 28, pp 171–206.

(41) Bender, M. L.; Silver, M. S. The Hydrolysis of Methyl O-Formylbenzoate. Participation of the Neighboring Aldehyde Group in the Hydroxide Ion and Morpholine-Catalyzed Reactions. *J. Am. Chem. Soc.* **1962**, *84*, 4589–4590.

(42) Newman, M. S.; Hishida, S. Alkaline Hydrolysis of Normal and Pseudo Methyl Esters of O-Benzoylbenzoates and of Hindered Alkyl Acetates. *J. Am. Chem. Soc.* **1962**, *84*, 3582–3584.

(43) Shalitin, Y.; Bernhard, S. A. Neighboring Group Effects on Ester Hydrolysis. II. Neighboring Carbonyl Groups. *J. Am. Chem. Soc.* **1964**, *86*, 2292.

(44) Walder, J. A.; Johnson, R. S.; Klotz, I. M. Neighboring-Group Participation of Aldehydes and Ketones in Ester Hydrolysis. Mechanism of Hydrolysis of O-Acetylsalicylaldehyde. *J. Am. Chem. Soc.* **1978**, *100*, 5156–5159.

(45) Zhang, H.; Grinstaff, M. W. Synthesis of Atactic and Isotactic Poly(1,2-Glycerol Carbonate)s: Degradable Polymers for Biomedical and Pharmaceutical Applications. *J. Am. Chem. Soc.* **2013**, *135*, 6806–6809.

(46) Acemoglu, M.; Bantle, S.; Mindt, T.; Nimmerfall, F. Novel Bioerodible Poly(hydroxyalkylene Carbonates)s: A Versatile Class of Polymers for Medical and Pharmaceutical Applications. *Macromolecules* **1995**, *28*, 3030–3037.

CHAPTER 3

A BIODEGRADABLE INTRAPERITONEAL SHIELD WITH SHORT RESIDENCE TIME TO FACILITATE ABDOMINAL CLOSURE AFTER LAPAROTOMY

The research presented in this chapter was performed in collaboration with Dr. Jason A. Spector and his research team at the Laboratory for Bioregenerative Medicine and Surgery, in the Department of Surgery, Division of Plastic Surgery, at Weill Cornell Medical College, New York, NY. Contributors: Kerry A. Morrison and Dr. Omer Kaymakcalan, See Acknowledgements for additional detail.

3.1. Abstract

After abdominal surgery, the suturing of incised fascia within the abdominal wall must be performed in a careful and controlled manner to avoid injury to the bowel such as accidental needle puncture. The primary method to protect the bowel involves coverage by a firm shield that is removed prior to placement of the final sutures. In the present work, a rapidly biodegradable intraperitoneal shield is developed and studied in a mouse model. A firm yet rapidly hydrolyzable device would enable greater bowel protection during the complete closure of the abdominal wall and also remove the potential risk of a retained surgical instrument. Chemically crosslinked polycarbonate hydrogels (CC-DHA) containing the biomolecule dihydroxyacetone were previously shown to undergo rapid degradation in vitro. The results presented herein show that CC-DHA hydrogels also undergo rapid degradation in vivo and can be fabricated into thin disks or sheets that demonstrate resistance to inadvertent needle puncture. Twelve hours after implantation, sheets with approximate dimensions of 5mm x 5mm x 1.5-2mm were found to have a mass (swollen with natural abdominal fluid) that is only 1.5 ± 2.6% of the

originally implanted dry mass. Disks of 20mm and 8mm diameter, each of approximately 2mm thickness, were completely degraded in 9 hours and 3 hours, respectively. Mortality occurred with the use of 20-mm disks which may be due to disk size or dehydration. In the case of 8mm disks, mice received intra and post operatory saline and appeared healthy 8 days post implantation. Overall, CC-DHA hydrogels are promising biomaterials for the prevention of bowel injuries during abdominal closure after a laparotomy.

3.2. Introduction

A laparotomy is a widely used medical procedure in which an abdominal incision is made to provide access to the peritoneal cavity for abdominal surgery.[1] Post-operatory closure requires suturing of the incised fascia (fibrous connective tissue) located within the abdominal wall. Failure to appropriately secure the fascia can lead to incisional hernia;[2–4] the protrusion of an organ (such as the bowel) or tissue through the weakened wound region. Suturing, however, poses a risk of bowel injury due to inadvertent needle puncture or entanglement within a stitch loop as it is tightened. A common technique to avoid bowel impairment is to use a removable firm object as a barrier between the abdominal organs and incised fascia.[5–7]

Figure 3.1. FISH® Glassman Visceral Retainer: a removable device for use as a protective barrier to prevent bowel injury during abdominal closure

The object distances the bowel from the wound site and prevents stitching from causing accidental damage. Once a significant portion of the fascia is sutured, the device is removed, and the procedure is completed with minimal visualization of the internal abdomen. Such devices are beneficial for the initial suturing process, however, they leave the intestines susceptible to puncture or suture entanglement during the final stages of completion.

One such device is a thin metal sheet known as a malleable retractor. To enable facile removal, the metal retractor contains a small width, particularly in comparison to the bowel, which offers limited protection during closure. Another popular object used for bowel displacement and coverage is the FISH® Glassman Visceral Retainer (Figure 3.1) which is made of a flexible material and is available in a variety of sizes. Similarly, the FISH® must be removed from the wound site prior to completion, limiting the effective coverage that is possible while still remaining removable, and also providing no protection during the final stitches. A major drawback of both devices is their potential risk as retained surgical instruments. Although avoidable in principle, retained instruments continue to be a problem in the medical community and can lead to significant postoperative morbidities as well as severe legal consequences.[8–13] Precise incident rates are unknown; however, an estimation of 1 retained foreign body in every 1000-1500 intraabdominal operations is commonly cited.[10,11,13,14] Incidents of retained metal malleable retractors or "fish" type viscera retainers have been reported by Gayer et al., Alexandrov et al., and Ariz et al.[15–17]

A potential solution to the risk of retained instruments as well as incomplete protection throughout a full abdominal closure is the development of a shield that is degradable within the peritoneal cavity. Previously, a rapidly degrading chemically cross-linked hydrogel (CC-DHA, Figure 3.2) based on dihydroxyacetone (DHA), a natural metabolite, and glycerol ethoxylate, a

3-arm poly(ethylene glycol) polymer, was described (Chapter 2). In the present work, CC-DHA was fabricated into disks and sheets of varying size and tested for its potential as a biodegradable intraperitoneal shield to facilitate post-laparotomy closure with reduced risk of bowel injury. In vivo degradation was studied in a mouse model. Hydrogels degraded on a rapid timescale (approximately 12 hours or less), however, large disks (20 mm diameter and approximately 2mm thickness) were found to cause mortality. It is possible that the large hydrogel sample mass combined with hydrophilic nature of the material led to severe dehydration. Follow up experiments with reduced-diameter disks (8-mm diameter, approximately 2mm thickness) combined with intra and post-operative hydration led to rapid hydrogel degradation, absence of visible inflammation in the abdominal cavity, and mice that appeared in good health eight days post-implantation.

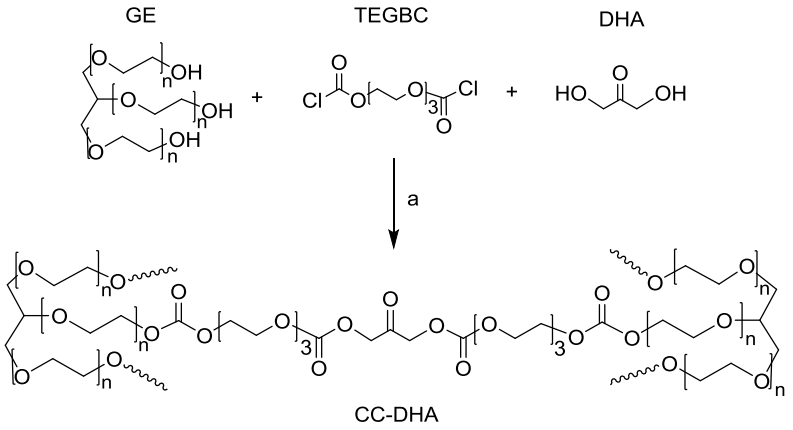

Figure 3.2. Synthetic scheme to CC-DHA hydrogels. (a) chloroform, pyridine, on ice, 1 hour. Nomenclature: GE: glycerol ethoxylate, TEGBC: tri(ethylene glycol) bis(chloroformate), DHA: dihydroxyacetone, CC-DHA: chemically crosslinked dihydroxyacetone-based hydrogel

3.3. Materials and Methods

3.3.1. Materials

The CC-DHA reaction flask (Appendix Figure B.1) was custom made from the Cornell Chemistry Glass Shop. Biopsy punches (20mm) were custom made from the Cornell Machine Shop. The Progressive Prep Solutions Multi Slicer was purchased from Walmart (Appendix Figure B.1). DHA dimer was purchased from Sigma Aldrich and 2-propanol (J.T. Baker) was purchased from Avantor Performance Materials (Center Valley, PA). C57BL/6N mice were purchased from Charles River Laboratories.

3.3.2. Preparation of DHA Monomer

DHA dimer was converted to the monomeric form according to a protocol previously described in Chapter 2. 2-Propanol (400 mL) was combined with DHA dimer (12 g) and stirred, while partially immersed in a 60^{o}C oil bath for 1 hour and 10 minutes. The resulting solution was filtered and rotoevaporation at 50-55^{o}C was performed, over a period of 95 minutes or less, to remove approximately 100 mL of 2-propanol. The remaining solution was held at -20^{o}C overnight, after which the crystallized DHA was recovered by filtration and dried at room temperature to yield 6.15 ± 0.62 g (51.2 ± 5.18%, n=3). Characterization and discussion are provided in Chapter 2.

3.3.3. CC-DHA Hydrogel synthesis

Square CC-DHA hydrogel samples measuring approximately 5mm x 5mm, with ~1.5-2mm thickness (Figure 3.3a), were prepared from CC-DHA hydrogels that were synthesized according to the previously described protocol in Chapter 2. Samples were cut using a standard razor blade and stored in a dry environment, under N_2 at -20^{o}C.

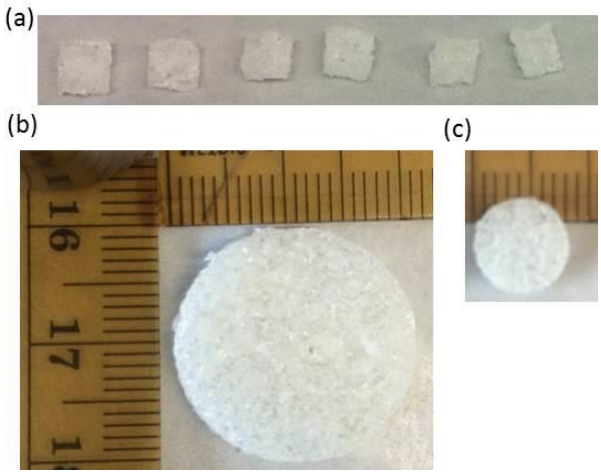

Figure 3.3. Examples of CC-DHA hydrogel samples of the following sizes: (a) approximately 5mm x 5mm with 1.5-2mm thickness; (b) and (c) 20mm and 8mm in diameter, respectively, with approximately 2mm thickness.

To create cylindrical disks (Figure 3.3b and 3.3c), the previously reported CC-DHA hydrogel synthesis protocol was modified. A custom-made cylindrical flask (OD: 41mm, ID: 36.7mm, height: 90mm, Figure B.1) and a 15 mm x 6 mm egg-shaped, Teflon-coated, stir bar were flame-dried and then cooled under a nitrogen gas stream. Next, a solution of glycerol ethoxylate (GE, 2.919 g, 0.00292 mol) and anhydrous chloroform (6 mL) were added. Solid DHA monomer (0.394 g, .00438 mol) was carefully poured into the GE/chloroform solution, resulting in a suspension due to the insolubility of DHA in chloroform. Next, the flask was lowered into an ice bath and stirred magnetically. Tri(ethylene glycol) bis(chloroformate) (TEGBC, 1.8 mL, 0.0088 mol) was added dropwise over 6 min, followed by addition of pyridine (1.62 mL, 0.02 mol) over approximately 5.4 min. Pyridine was added to the bottom and sides of the reaction mixture, in an alternating fashion, using a 6 inch syringe needle. A gel began to form during the final stages of pyridine addition and, with sufficient mixing, a fully formed gel was obtained in 10 minutes. To avoid "plugging" of the needles, pyridine was added using two

separate 1 mL syringes, each containing half of the total quantity to be added. Movement of the reaction flask across the stir plate during pyridine addition enables the stir bar to access multiple points of the mixture and provides enhanced mixing of reagents. The final gel was held for 1 hour, on ice, and then approximately 30 mL of diethyl ether was poured into the reaction flask. In ~30 min, once the top layer of the gel appeared white due to the insolubility of GE chains, the gel was slowly peeled from the glass edges using a weighing spatula, and then allowed to sit within the diethyl ether overnight at room temperature.

Next, the gel was sliced and purified. Diethyl ether was decanted from the reaction flask and the gel was removed. If the top, non-rounded, portion of the gel was highly uneven, a razor was used to create a level surface. To further flatten the top of the gel, a light "sanding" procedure was performed by applying pressure in a circular motion on a mildly rough surface. Once the top layer was appropriately flat, the gel was sliced using a Progressive Prep Solutions Multi Slicer with the "thin slices" insert. The stir bar was removed when accessible, and slicing continued until gel thickness was no longer sufficient for cutting. All slices from each batch were placed into 400 mL of chloroform for purification by extraction. Impurities were extracted by repeated removal and replacement of fresh chloroform which occurs six times over a minimum of 4 days. The gel was further purified through incubation in 25:75, 50:50, and 75:25 volume-to-volume solutions of diethyl ether and chloroform, respectively, for 10 minutes each, followed by 20 minutes in diethyl ether. Lastly, the gel was dried in vacuo for two nights, washed briefly with MilliQ water, and lyophilized. 8-mm and 20-mm diameter cylindrical slices were prepared using 8-mm and 20 mm biopsy punches. Gels were stored in a dry environment, under N_2 at -20^{o}C.

3.3.4. In vivo Degradation

The in vivo degradation of rectangular CC-DHA samples and 20mm cylindrical disks (Figure 3.3a and 3.3b) was tested in 8 week old wild type C57BL/6N mice. An abdominal incision was made and a CC-DHA polymer sample was inserted onto the bowel. A taper cutting needle was used to tag polymer samples with long-tail 6-0 polypropylene sutures to facilitate identification and removal of remaining hydrogel at specified time points. Peritoneum and fascia were closed using a running stitch with polypropylene suture. Tegaderm dressing was placed over the incision area with mastisol adhesive. Animals were sacrificed and re-opened at specified time points. The final mass and size of polymer samples were recorded as received after removal (i.e. without washing and drying).

Due to the fluid uptake of the hydrogel, the *in vivo* degradation kinetics of CC-DHA were also studied with the use of intra and post-operatory saline injection. 8-mm diameter disks of approximately 2mm thickness were tested in 9 week old C57BL/6N mice. The procedure was performed as follows: Mice received a 200μL intraperitoneal injection of a Ketamine/Xylazine solution followed by a 1mL subcutaneous injection of pre-warmed saline through the dorsal skin. Abdominal hair was removed using a razor and Nair product, after which the skin was prepped with Betadine and 70% ethanol. A 2.5 cm midline incision was made and the 8-mm CC-DHA disk was sewn to the inner right abdominal wall using a 7-0 polypropylene suture. CC-DHA polymer disks were bound to the abdominal wall through a single stitch. Peritoneum and abdominal musculature were closed by a running stitch of 7-0 polypropylene suture followed by skin closure with a 5-0 nylon suture. The wound was covered with a Tegaderm dressing after which animals were placed under a heat lamp and temporarily removed to receive 20mg Atipamezole followed by 1mL warmed saline injected subcutaneously. Incision, implantation,

and suturing took place over 12 minutes. A total of 17 mice were utilized. At 3, 6, and 9 hours after implantation (n=4 per time point), mice were sacrificed and re-opened to examine the remaining CC-DHA hydrogel and abdominal fluid levels. At 24 hours post implantation (n=4), mice were anesthetized, examined, sutured, and retained for 1 week post operation in group housing. Additionally, a separate, single mouse was examined at 8 days following the procedure and also kept in group housing.

3.4. Results and Discussion

3.4.1. CC-DHA Hydrogel Synthesis

Hydrogels have profound use in biomedical engineering with various applications such as tissue engineering,[18] drug delivery,[19] and wound healing.[20] Biodegradable hydrogels, in particular, are advantageous owing to their ability to serve a distinct function and subsequently be eliminated from the body without requiring surgical removal. Hydrolyzable bonds such as polycarbonates are frequently used in the development of biodegradable materials.[21,22] Dihydroxyacetone (DHA), a three carbon sugar, was recently found to induce rapid degradation of neighboring carbonate bonds in aqueous solutions (Chapter 2). Degradation of DHA-based polymers releases free DHA monomer which can be safely eliminated from the body via natural metabolic pathways, making DHA a promising molecule for biocompatible biomaterials.[23] Zawaneh et al. showed that diblock copolymers of DHA and monomethoxy poly(ethylene glycol) (MPEG-pDHA) create rapidly degradable and injectable hydrogels that have use in post-operative seroma prevention.[24] Recent studies show that the mechanism of rapid degradation in DHA-based materials involves the ketone present on DHA (Chapter 2). Therefore, more advanced DHA-based hydrogels can be synthesized that exhibit unique mechanical properties

while retaining the characteristic of rapid degradation rates under physiological conditions. CC-DHA is a flexible and non-injectable chemically cross-linked polycarbonate hydrogel consisting of DHA and glycerol ethoxylate (GE).

CC-DHA is synthesized according to the scheme shown in Figure 3.2. Polymer samples were prepared in three different sizes for in vivo testing in a C57BL/6N mouse model (Figure 3.3). Rectangular samples (Figure 3.3a) were prepared from CC-DHA hydrogels that were synthesized in an anhydrous environment, as previously described in Chapter 2. Due to the water sensitivity of the reaction (i.e. the chloroformate groups of TEGBC are susceptible to reaction with atmospheric water molecules, which decreases the degree of polymerization with DHA), an anhydrous environment is preferred. Therefore, the reaction is conducted in a round-bottom flask equipped with an enclosable 24/40 joint neck. At the end of the reaction, the hydrogel exists as a single mass. A drawback of the reaction vessel is the requirement to slice the hydrogel such that it can be removed through the narrow neck.

To retain the large diameter of the gel that occurs during synthesis, CC-DHA hydrogel disks (Figure 3.3b and 3.3c) were synthesized using a modified procedure; a test-tube shaped flask containing a wide open neck was utilized such that the gel could be removed without impairment (Appendix Figure B.1). CC-DHA hydrogels are subject to variability in degradation and swelling rates due to the random nature of the reaction, as discussed in Chapter 2. The non-anhydrous nature of the modified reaction will increase structural and performance variability, however, all samples were found to degrade in vivo on the desired rapid timescale, as will be discussed in the following sections. The presumed major cause of variance is the manual addition of pyridine and non-uniform mixing rates during synthesis. For commercialization, an air-tight reactor with controlled reagent flow rates and stirring would be ideal to enhance the

uniformity of CC-DHA polymer disks.

For increased efficiency of purification, hydrogel disks are purified in sliced form, cut using a Progressive Prep Solutions Multi Slicer (PPSMS, Appendix Figure B.1). Ultimately, the PPSMS yields samples that are approximately 2 mm thick, with minor differences due to the applied pressure during slicing. It is important to note that the hydrogel swells during purification. When fully swollen with chloroform, the gel is sensitive to fractures and tears, and therefore should be handled with care.

Following purification and drying, polymer samples were found to have sufficient flexibility for facile handling and implantation. In addition, the hydrogel showed resistance to inadvertent needle puncture (Figure 3.4a), indicating its potential as a barrier for accidental bowel injury during fascial closure.

3.4.2. In Vivo Degradation

Previously, CC-DHA polymers were shown to undergo rapid in vitro degradation under physiological conditions. Samples (20mg) submerged in phosphate buffered saline (pH=7.4) and rotated at 37^{o}C were found to degrade 96.3±3.4% in less than 4 hours (Chapter 2). In the present study, the in vivo degradation of CC-DHA was determined in a mouse model. Rectangular CC-DHA samples (Figure 3.3a) were implanted into the intraperitoneal cavity of C57BL/6N mice and tested for percent degradation at 3, 6, and 12 hours. Separate mice were analyzed for each time point and animals were sacrificed immediately before examination. Hydrogels were tagged with a suture for facile explantation. Results are shown in Table 3.1a.

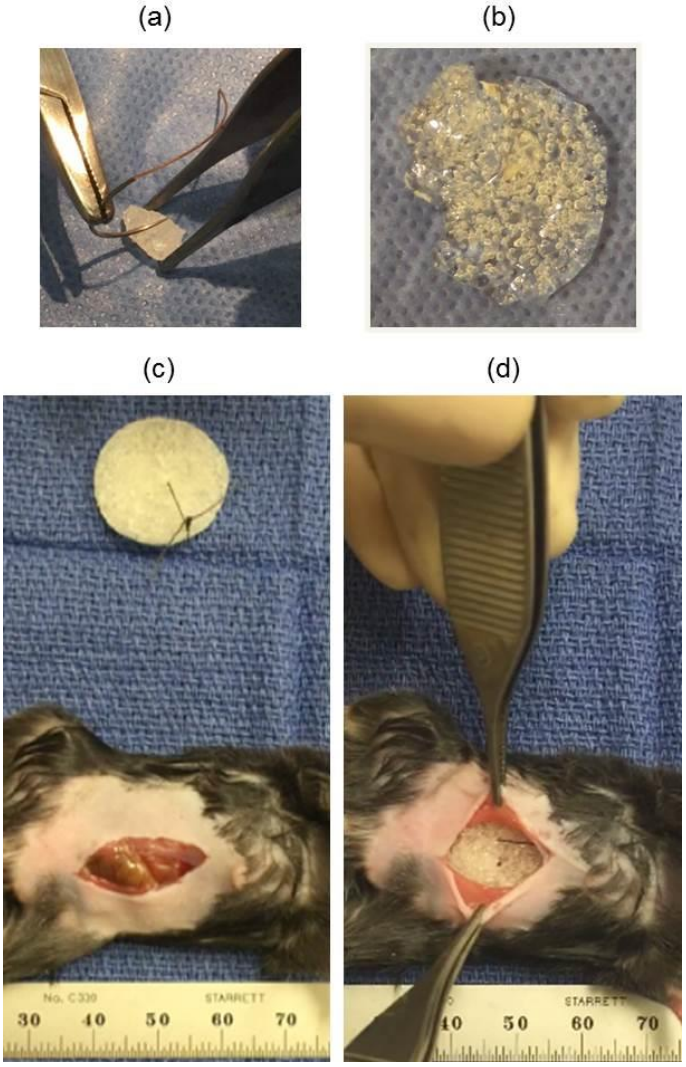

Figure 3.4. (a) A rectangular CC-DHA hydrogel sample demonstrates resistance to inadvertent needle puncture. (b) CC-DHA hydrogel disk that was removed following 6 hours of implantation into the mouse abdomen and contains a mass that is 177.8% of its original size due to swelling. At initial implantation, the disk was cylindrical with a 20 mm diameter; the non-circular shape of the explanted hydrogel is due to degradation of the CC-DHA polymer network. (c) 20 mm CC-DHA hydrogel disks before and (d) after implantation into the intraperitoneal cavity.

Table 3.1. Analysis of CC-DHA hydrogels at specified time points before and after implantation in a mouse model. Final mass consists of non-degraded CC-DHA polymer as well as liquid absorbed into the gel from the abdominal cavity. Absorbed fluid is the cause for >100% CC-DHA mass at extraction. (a) Approximate dimensions of the initial dry implanted hydrogel were 5mm x 5mm x 1.5-2mm. (b) Initial dry implanted hydrogels were cylindrical disks of 20 mm diameter and approximately 2mm thickness.

(a)

Evaluation Time (hr)	Mouse (g)	CC-DHA Initial mass (mg)	CC-DHA Mass at Extraction (mg)	% CC-DHA Mass at Extraction	CC-DHA Width at Extraction (mm)	CC-DHA Height at Extraction (mm)
3	29	48.4	38.4	79.3	6	2.5
	34	46.9	102.7	219	8	4
	25.5	49.5	12.2	24.6	4	1.5
6	35.5	*102.7	0.3	0.3	1	0.4
	35.5	48.1	0	0	0	0
	**28	50.0	0	0	0	0
	28.5	45.4	0.3	0.7	1.6	0.35
12	24	41.8	0	0	0	0
	20.5	42.7	1.9	4.4	0.07	0.15
	20.1	47.4	0	0	0	0

*Test sample, unknown dimensions **Intraabdominal bleeding encountered

(b)

Evaluation Time (hr)	CC-DHA Initial mass (mg)	CC-DHA Mass at Extraction (mg)	% CC-DHA Mass at Extraction
6	559.2	0	0
	601.0	26.9	4.5
	621.3	1104.7	177.8
9	569.8	0	0
	602.6	0	0
	634.8	0	0
	593.3	0	0
	603.3	0	0
	639.7	0	0

"% CC-DHA Mass at Extraction" (Table 3.1) was calculated according to Equation 3.1, where "CC-DHA Mass at Extraction" includes fluid that has been absorbed into the hydrogel from the abdominal cavity.

$$\left[\frac{CC-DHA\ Mass\ at\ Extraction}{CC-DHA\ Initial\ Mass}\right] x100 \qquad (eq.3.1)$$

Three hours after implantation, the CC-DHA hydrogels were still present in all mice with varying degrees of degradation. Two samples show a decrease in mass between implantation and extraction (79.3% and 24.6% mass at extraction), while one sample shows a large increase (219% mass at extraction). The increase is mass is due to fluid absorption into the hydrogel. CC-DHA hydrogels contain highly hydrophilic poly(ethylene glycol) chains within the polymer network that promote the uptake of water into the polymer matrix (Chapter 2). It is important to note that swelling and degradation occur simultaneously, and therefore the observed mass increase is not an indication of a non-degraded hydrogel disk. At both the 6 and 12 hour time points, CC-DHA hydrogels are significantly degraded and have an average mass percent at extraction of 0.2 ± 0.3% and 1.5 ± 2.6%, respectively. Therefore, despite the random nature of the polymer matrix, all CC-DHA hydrogels degrade on a rapid timescale in vivo as expected.

Similar results occur in the testing of large cylindrical disks of 20-mm diameter (Table 3.1b). Due to the increased size of the hydrogel sample, degradation occurs over a longer timescale than for the small rectangular disks. Six hours after implantation, high variance in the % CC-DHA mass at extraction is observed. Two samples are substantially degraded with 100% degradation in one sample and 4.5% mass at extraction for the second. The third trial measuring degradation 6 hours post-implantation was found to have 177.8% mass at extraction, however,

clear signs of degradation are present (Figure 3.4b). At 9 hours, all 20-mm disks are 100% degraded. As previously mentioned, CC-DHA hydrogels experience variability in swelling and degradation rates due to the random nature of reaction and manual control of reagent addition and stirring. It is expected that appropriate reactor design would significantly reduce the observed variability.

The hydrophilic nature of the polymer network contributes to the rapid degradation of the hydrogel, however, can also lead to patient dehydration due to absorption of bodily fluid into the disk. Larger CC-DHA disks will absorb more fluid from the abdominal cavity and increase the potential risk for dehydration. Unlike the small rectangular CC-DHA samples, 20 mm diameter disks were found to cause mortality in all mice observed 9 hours after implantation. It is believed that the quantity of hydrogel used in these studies exceeded the limits of the mouse model. A 20-mm disk sufficiently covers the mouse abdominal organs as desired (Figure 3.4c and 3.4d). In translation to a human, however, only the diameter of the CC-DHA disks would need to be increased proportionally to patient size. Hydrogel thickness is a function of needle shape and force, rather than abdominal cavity depth. It is not expected that the mass ratio of hydrogel:mouse used in the 20 mm disk study would be analogous to the hydrogel:human mass ratio for an equal abdominal surface coverage. An additional important factor to consider is the maximal tolerable level of degradation products per patient size. Degradation products include DHA, various GE-tri(ethylene glycol) combinations as previously discussed in detail in Chapter 2, and presumably CO_2 due to the breakdown of polycarbonate bonds.[25,26] DHA is a natural metabolite, which reduces risk of toxicity, and GE is a type of 3-arm poly(ethylene glycol) polymer; Poly(ethylene glycol)s are known biocompatible polymers and are commonly utilized in both linear and branched forms in biomedical applications.[27] Overall, the current study

highlights the rapid degradation of CC-DHA hydrogel disks, while also suggesting that patient hydration may be necessary to prevent discomfort or morbidity. Future work involves the determination of size constraints for various species and their translation to the human abdomen.

In a subsequent study, smaller cylindrical disks (Figure 3.3c) were tested for in vivo degradation with the use of intra and post implantation hydration in a mouse model. In practice, fluid administration and monitoring is normal for patients undergoing abdominal surgery.[28] Therefore, it's possible that the hydrophilic nature of CC-DHA would not require substantial additional consideration with regard to intraoperative hydration. Mice received a 1 mL injection of warm saline subcutaneously both at the beginning and after hydrogel disk implantation and were found to be ambulating 15-60 min from completion of the procedure. In this study, CC-DHA disks were tagged to the inner right abdominal wall using a single stitch (Figure 3.5). Three hours after insertion, the hydrogel disks appeared completely dissolved. Accordingly, mice tested at 6, 9, and 24 hours also showed full degradation of the 8 mm-diameter CC-DHA disks.

Figure 3.5. Example of cylindrical CC-DHA hydrogel disk of 8mm diameter bound to the inner right abdominal wall of a mouse.

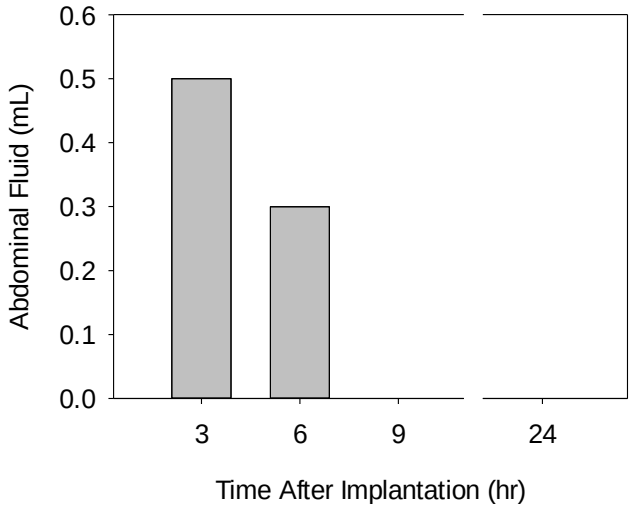

Figure 3.6. Abdominal fluid measured at specified time points following implantation of CC-DHA hydrogel disks of 8-mm diameter, and approximately 2 mm thickness, into a mouse model. For each time point, n=4 mice.

The mass of the hydrogel disks used in this study were an average of 81.4 ± 13.9 mg. The large standard deviation in hydrogel mass is partially due to minor variations in hydrogel thickness, however, can be largely attributed to the random nature of the synthesis as previously mentioned. Despite the deviation in hydrogel mass, all disks degraded on a rapid timescale and abdominal fluid demonstrated low variability at each time point. Figure 3.6 shows the volume of fluid within the abdomen for each mouse at each time point. Fluid is retained at 3 and 6 hours post implantation, however, all excess fluids appear to be absorbed within 9 hours. Excess abdominal fluid can lead to complications such as increased intraabdominal pressure,[29] however, the observed rapid resorption rates suggests minimal risk for excess fluid related morbidities. Raw data for each mouse is included in Appendix B (Table B.1).

At time points of 3, 6, and 9 hours, mice were sacrificed prior to abdominal examination; however, mice evaluated at 24 hours post-implantation were anesthetized, examined, and

retained for an additional week. All mice were ambulating, grooming, drinking, and eating normally as well as passing regular stools. One additional mouse was not evaluated until 8 days post implantation and also appeared to be in good health. Furthermore, no signs of inflammation, adhesion formation, or fibrosis were observed by visual inspection of any mouse upon evaluation at each time point.

3.5. Conclusions

The results indicate that CC-DHA hydrogels are flexible, capable of resisting inadvertent needle puncture and rapidly degrade in vivo. High variance in swelling and degradation at early time points pose a clinical issue. Therefore, future work should be performed to develop more uniform polymer disks. Due to the hydrophilic nature of CC-DHA, patient hydration should be taken into consideration for large samples with high abdominal coverage. Overall, the hydrogels show promising biocompatibility and are potential biodegradable intraperitoneal shields for the facilitation of post-laparotomy closure.

3.6. Acknowledgements

This work was made possible by Dr. Jason A. Spector and his surgical team at the Weill Cornell Medical College in New York, NY; thank you to Kerry A. Morrison and Dr. Omer Kaymakcalan for their contributions to the results presented in this chapter. Data represented by Table 3.1 and Figure 3.4 were provided by Kerry A. Morrison. Data represented by Figures 3.5 and 3.6 as well as Appendix B Table B.1 were provided by Dr. Omer Kaymakcalan. Additionally, this work made use of the Cornell Chemistry Glass Shop, Cornell Machine Shop, and Cornell Chemistry NMR Facility.

3.7. References

(1) Burger, J. W. A.; Van 't Riet, M.; Jeekel, J. Abdominal Incisions: Techniques and Postoperative Complications. *Scand. J. Surg.* **2002**, *91*, 315–321.

(2) Fink, C.; Baumann, P.; Wente, M. N.; Knebel, P.; Bruckner, T.; Ulrich, A.; Werner, J.; Büchler, M. W.; Diener, M. K. Incisional Hernia Rate 3 Years After Midline Laparotomy. *Br. J. Surg.* **2014**, *101*, 51–54.

(3) Hodgson, N. C. F.; Malthaner, R. A.; Ostbye, T. The Search for an Ideal Method of Abdominal Fascial Closure: A Meta-Analysis. *Ann. Surg.* **2000**, *231*, 436–442.

(4) O'Dwyer, P. J.; Courtney, C. A. Factors Involved in Abdominal Wall Closure and Subsequent Incisional Hernia. *Surg. J. R. Coll. Surg. Edinburgh Irel.* **2003**, *1*, 17–22.

(5) Stockwell, D. K. Method and Apparatus for Assisting in Would Closure. US Patent Pub. No. US 2014/0345629, 2014.

(6) Medwid, A. Visceral Retractor. US Patent No. 4,747,393, 1988.

(7) Freedman, D. L. Surgical Aid. US Patent No. 6,736,141, 2004.

(8) Stawicki, S. P.; Evans, D. C.; Cipolla, J.; Seamon, M. J.; Lukaszczyk, J. J.; Prosciak, M. P.; Torigian, D. A.; Doraiswamy, V. A.; Yazzie, N. P.; Gunter, O. L.; Steinberg, S. M. Retained Surgical Foreign Bodies: A Comprehensive Review of Risks and Preventive Strategies. *Scand. J. Surg.* **2009**, *98*, 8–17.

(9) Gayer, G.; Petrovitch, I.; Jeffrey, R. B. Foreign Objects Encountered in the Abdominal Cavity at CT. *Radiographics* **2011**, *31*, 409–428.

(10) Cima, R. R.; Kollengode, A.; Storsveen, A. S.; Weisbrod, C. A.; Deschamps, C.; Koch, M. B.; Moore, D.; Pool, S. R. A Multidisciplinary Team Approach to Retained Foreign Objects. *Jt. Comm. J. Qual. Patient Saf.* **2009**, *35*, 123–132.

(11) Gawande, A. A.; Studdert, D. M.; Orav, E. J.; Brennan, T. A.; Zinner, M. J. Risk Factors for Retained Instruments and Sponges After Surgery. *N. Engl. J. Med.* **2003**, *348*, 229–235.

(12) Murdock, D. B. Trauma : When There's No Time to Count. *AORN J.* **2008**, *87*, 329–330.

(13) Lincourt, A. E.; Harrell, A.; Cristiano, J.; Sechrist, C.; Kercher, K.; Heniford, B. T. Retained Foreign Bodies After Surgery. *J. Surg. Res.* **2007**, *138*, 170–174.

(14) Hyslop, J. W.; Maull, K. I. Natural History of the Retained Surgical Sponge. *South. Med. J.* **1982**, *75*, 657–660.

(15) Gayer, G.; Karni, T.; Vasserman, M. Case Report: CT Appearance of a Retained “Fish” in the Abdomen. *Am. J. Roentgenol.* **2005**, *184*, S75–S77.

(16) Alexandrov, A.; Jelev, L.; Nikolov, D.; Malinova, L.; Hristov, S. Large Metal Retractor Left in the Abdominal Cavity for 27 Years after Colorectal Surgery. *Int. J. Case Reports Images* **2013**, *4*, 228–231.

(17) Ariz, C.; Horton, K. M.; Fishman, E. K. 3D CT Evaluation of Retained Foreign Bodies. *Emerg. Radiol.* **2004**, *11*, 95–99.

(18) Vo, T. N.; Shah, S. R.; Lu, S.; Tatara, a. M.; Lee, E. J.; Roh, T. T.; Tabata, Y.; Mikos, a. G. Injectable Dual-Gelling Cell-Laden Composite Hydrogels for Bone Tissue Engineering. *Biomaterials* **2016**, *83*, 1–11.

(19) Jensen, B. E. B.; Dávila, I.; Zelikin, A. N. Poly(vinyl Alcohol) Physical Hydrogels: Matrix-Mediated Drug Delivery Using Spontaneously Eroding Substrate. *J. Phys. Chem. B* **2016**, *120*, 5916-5926.

(20) Goh, M.; Hwang, Y.; Tae, G. Epidermal Growth Factor Loaded Heparin-Based Hydrogel Sheet For Skin Wound Healing. *Carbohydr. Polym.* **2016**, *147*, 251–260.

(21) Xu, J.; Feng, E.; Song, J. Renaissance of Aliphatic Polycarbonates: New Techniques and Biomedical Applications. *J. Appl. Polym. Sci.* **2014**, *131*, 39822.

(22) Feng, J.; Zhuo, R.-X.; Zhang, X.-Z. Construction of Functional Aliphatic Polycarbonates for Biomedical Applications. *Prog. Polym. Sci.* **2012**, *37*, 211–236.

(23) Ricapito, N. G.; Ghobril, C.; Zhang, H.; Grinstaff, M. W.; Putnam, D. Synthetic Biomaterials from Metabolically Derived Synthons. *Chem. Rev.* **2016**, *116*, 2664–2704.

(24) Zawaneh, P. N.; Singh, S. P.; Padera, R. F.; Henderson, P. W.; Spector, J. A.; Putnam, D. Design of an Injectable Synthetic and Biodegradable Surgical Biomaterial. *Proc. Natl. Acad. Sci. U. S. A.* **2010**, *107*, 11014–11019.

(25) Zhu, K. J.; Hendren, R. W.; Jensen, K.; Pitt, C. G. Synthesis, Properties, and Biodegradation of Poly (1,3-Trimethylene Carbonate). *Macromolecules* **1991**, *24*, 1736–1740.

(26) Østergaard, J.; Larsen, C. Bioreversible Derivatives of Phenol. 2. Reactivity of Carbonate Esters with Fatty Acid-like Structures towards Hydrolysis in Aqueous Solutions. *Molecules* **2007**, *12*, 2396–2412.

(27) Zhu, J. Bioactive Modification of Poly(ethylene Glycol) Hydrogels for Tissue Engineering. *Biomaterials* **2010**, *31*, 4639–4656.

(28) Futier, E.; Biais, M.; Godet, T.; Bernard, L.; Rolhion, C.; Bourdier, J.; Morand, D.; Pereira, B.; Jaber, S. Fluid Loading in Abdominal Surgery - Saline versus Hydroxyethyl Starch (FLASH Trial): Study Protocol for a Randomized Controlled Trial. *Trials* **2015**, *16*, 582.

(29) Holte, K.; Sharrock, N. E.; Kehlet, H. Pathophysiology and Clinical Implications of Perioperative Fluid Excess. *Br. J. Anaesth.* **2002**, *89*, 622–632.

CHAPTER 4

KINETIC ANALYSIS OF THE REACTION BETWEEN DIHYDROXYACETONE AND ETHANOLAMINE

4.1. Abstract

The ability to control chemistries at the surface of macromolecular structures has enabled the development of a wide range of valuable technologies (ex: protein immobilization platforms, scavenger resins, drug delivery vehicles, etc.). Amine reactive surfaces, in particular, are of high interest owing to the vast population of natural and synthetic compounds bearing amine functional groups. Dihydroxyacetone is well known to react with primary and secondary amines and can be formulated into a variety of macromolecular structures. To predict the binding capability of DHA-based polymers with various proteins or synthetic chemicals, a model reaction of free DHA and ethanolamine was studied. Reactions were performed in aqueous solutions, over a temperature range of 4^{o}C to 55^{o}C, using real-time infrared spectroscopy. The method of initial rates was employed to minimize the effect of downstream Maillard reaction products. Reaction progress was measured by the decrease in carbonyl absorption (1714-1755 cm^{-1}) during the initial 3-5 minutes of reaction and kinetic parameters were calculated according to a bimolecular kinetic model. The work presented herein is the first step in a broad goal to explore the feasibility of DHA-based materials in amine reactive surface applications.

4.2. Introduction

Surface-based chemistries play a role in several fields including drug delivery[1], proteomics,[2] bioreactor design,[3] and polymer-assisted solution phase synthesis.[4] Surfaces that

covalently bind amine functional groups are of considerable interest in biomedical engineering due to the multitude of biomolecules and drugs that contain amine functional groups, as well as the range of macromolecular structures that can be formulated from functional materials. One strategy to develop an amine-reactive surface is to create a bulk material containing carbonyl groups. The reaction between an amine and a carbonyl group forms a Schiff base (-C=N-, a, Figure 4.1). Schiff base formation is a facile and pH sensitive reaction that is reversible, except in the presence of a reducing agent (b, Figure 4.1).

Schiff base chemistry has enabled the development of controlled release drug delivery devices,[5] platforms for high throughput protein activity assays,[6] scavenger resins for facile purification in chemical synthesis,[7] and other technologies.[8] For example, Langowska et al. demonstrated that aldehyde-coated polymersomes could be permanently attached to amine coated silicon surfaces via reductive amination of Schiff base linkages, and locally release antibiotics, to prevent infection over an extended period.[1] Hillebrenner et al. developed amine-functionalized silica nano-tubes that could be "corked" with aldehyde functionalized polystyrene nanoparticles via Schiff base bonds, and potentially be utilized as a drug carrier.[9] Saito et al. and Dai et al. showed that Schiff base chemistry can be used to develop pH-responsive delivery systems.[5,10] Pioneering work in the field of protein microarrays was performed by Macbeth and Schreiber who demonstrated that 10,800 proteins could be immobilized onto an aldehyde-coated slide through Schiff-base interactions.[6]

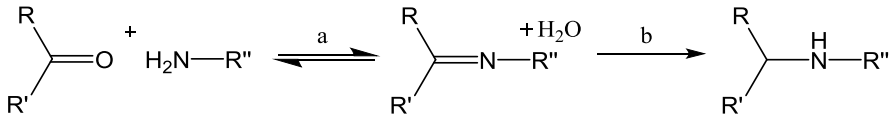

Figure 4.1. (a) Formation of a Schiff base. R"≠H. (b) Reducing agent, ex: $NaBH_4$

As previously mentioned in Chapter 1, dihydroxyacetone (DHA) contains a ketone group that is known to react with primary and secondary amines. Additionally, DHA can be polymerized into polyesters and polycarbonates with various morphologies such as microparticles or hydrogels. To date, however, the reactive functionality and utility of each DHA biomaterial has yet to be explored. As a first step in understanding the capabilities of amine-reactive DHA-based materials, this chapter examines a model reaction between free DHA and ethanolamine (EA) along with an analysis of several kinetic parameters. Knowledge of the reaction kinetics between DHA and primary amines will shed light on potential future applications of DHA polymers and can also assist in the mathematical modeling of some applications, such as drug release rates. The reaction of DHA and EA was monitored using real-time FT-IR spectroscopy; DHA concentration profiles in time were calculated by tracking the decrease in carbonyl absorbance (1714-1755 cm^{-1}) during the initial stages of reaction. The method of initial rates was employed to gather rate constants at various temperatures and to determine reaction orders, as well as the activation energy, according to a bimolecular kinetic model.

4.3. Materials and Methods

4.3.1. Materials

IR spectra were recorded on a ReactIR 4000 (Mettler Toledo) equipped with a 30-bounce, silicon tipped probe (tested for chemical compatibility, Table C.1). Phosphate buffered saline (pH=7.4, Corning Cellgro) was purchased from VWR international. Ethanolamine and dihydroxyacetone dimer were purchased from Sigma Aldrich. Curve fitting was performed using

SigmaPlot software. For temperature compensated pH acquisition, the pH meter was calibrated at 25°C. Manual compensation was performed by adjusting the pH meter to the appropriate temperature and testing the pH=10.01 (25°C) standard solution for appropriate transition (pH = 9.88 at 37°C). ^{1}H NMR spectra were recorded on a 600MHz Varian INOVA spectrometer.

4.3.2. Preparation of DHA Monomer for Kinetic Studies

Dihydroxyacetone dimer was converted to monomeric form using the protocol described in Chapter 2. In brief, DHA dimer (4 g) is combined with 2-propanol (400 mL) and stirred, while partially submerged in a 60°C oil bath, for 40min. The solution is then filtered and approximately 225-275 mL of 2-propanol are removed by rotoevaporation, over a period of 95 minutes or less, at 50-55°C. The resulting liquid is held at -20°C overnight, after which the white crystallized DHA is recovered and dried under vacuum at room temperature. Larger concentration crystallizations were also utilized: 2-propanol (400 mL) is added to DHA dimer (12 g), stirred at 60°C for 1.17hr, followed by filtration and removal of approximately 100 mL of 2-propanol by rotoevaporation. Yield, characterization, and discussion are reported in Chapter 2.

4.3.3. DHA Monomer Temperature Dependence

The ketone to hydrate ratio of DHA in aqueous solutions, at equilibrium, is temperature dependent. ^{1}H NMR was used to determine the concentration of the ketone-containing form at various temperatures. In this study, DHA monomer was prepared by stirring DHA dimer (2g) in DI water (200 mL) at room temperature for 24 hours. The sample was then lyophilized to obtain DHA monomer as a white powder. ^{1}H NMR (400 MHz, DMSO-d_6, 25°C, δ): 5.02 (t, 2H, OH), 4.16 (d, 4H, CH_2). ^{13}C NMR (100 MHz, DMSO-d_6, 25°C, δ): 211.49 (C=O), 65.68 (CH_2).

A 5 mg/mL solution of DHA monomer in D_2O was cooled to 4°C within the NMR chamber, allowed to stand for 10 minutes, and a ^1H NMR spectrum was recorded (25 s relaxation delay, 90 degree pulse). The chamber was heated to 15°C, 22°C, 37°C, 45°C, and 55°C, respectively, and allowed to stand for 10minutes at each temperature before a ^1H NMR spectrum was acquired. The solvent peak shifted with temperature (a normal observation for atoms capable of hydrogen bonding) and spectra were referenced according to Equation 4.1 by Gottlieb et al., where T is the temperature in Celsius, and δ is the chemical shift in ppm.[11] ^1H NMR (600 MHz, D_2O, δ): 4.40 (s, 4H, CH_2, ketone monomer), 3.56 (s, 4H, CH_2, hydrate).

$$\delta = 5.060 - 0.0122T + (2.11x10^{-5})T^2 \qquad (eq. 4.1)$$

4.3.4. Kinetic Analysis

Real-time infrared spectroscopy was used to determine kinetic parameters. The reaction between DHA monomer and ethanolamine was monitored using various initial concentrations of each reagent (Table 4.1). A sample reaction is described as follows: The probe was inserted into a cylindrical flask with stirring phosphate buffered saline (pH=7.4, 5.0mL). The flask was placed into a 37°C water bath, allowed 10 minutes to reach 37°C, and then a background spectrum was recorded. Next, the flask was charged with a concentrated solution of DHA monomer (200µL, Table C.2) in PBS using a 6 inch syringe needle. Details on DHA injection-sample preparation are included in Appendix C (Table C.2). Lastly, a concentrated solution of ethanolamine (150µL, Table C.3) in PBS was injected into solution. The carbonyl band (1714-1755 cm^{-1}) was monitored over 15 minutes, scans were recorded at 15 second intervals, and all reactions were measured in duplicate. Absorbance was found to be directly proportional to concentration (Figure C.1).

Table 4.1: Initial concentration of DHA (total; both ketone and hydrate forms) and EA in each reaction.

Reaction	Temp. (^{o}C)	Total DHA (mM)	EA (mM)
1	37	158	50
2	37	158	100
3	37	158	200
4	37	158	300
5	37	158	400
6	37	158	465
7	37	50	200
8	37	100	200
9	37	200	200
10	37	296	200
11	37	400	200
12	37	505	200
13	4	200	200
14	15	200	200
15	22	200	200
16	45	200	200
17	55	200	200

The temperature dependence of the reaction was studied using the same methodology. Reactions were monitored at 4^{o}C, 15^{o}C, 22^{o}C, 37^{o}C, 45^{o}C, and 55^{o}C using a 200mM initial concentration of total DHA monomer and a 200mM concentration of ethanolamine.

4.3.5. pH Determination

The initial pH of reaction was determined for reactions 1-12 (Table 4.1). The reaction procedure used for infrared spectroscopy studies was implemented; however, a slightly different platform was utilized. In brief, the pH probe was inserted into a 10 mL beaker with stirring phosphate buffered saline (5.0mL), in a 37^{o}C water bath. The system was allowed 10 minutes to reach the appropriate temperature and then DHA monomer (200µL, Table C.2) was injected.

Next, ethanolamine (150µL, Table C.3) was injected into solution and the resulting pH was recorded.

4.4. Results and Discussion

4.4.1. DHA Monomer Temperature Dependence

In aqueous solutions, DHA exists partially in a hydrated form (I, Figure 4.2). The percentage of DHA monomer in ketone and hydrate forms, in D_2O, was determined using ^1H NMR spectroscopy and the results are shown in Table 4.2. The percentage of ketone-containing DHA in aqueous solution was found to increase with increasing temperature. This trend was also observed by Reynolds et al. in the case of dihydroxyacetone phosphate.[12] The data is further supported by the measurement of a 4:1 ratio of ketone to hydrate at room temperature, which was previously reported by Davis using ^1H NMR spectroscopy at 25°C.[13]

Table 4.2. Percent of DHA monomer in ketone and hydrate forms in D_2O calculated using ^1H NMR peak integration ratios of each component. *Minor NMR tuning difficulties were encountered prior to recording the ^1H spectrum at 55°C; however, the signal was highly resolved.

Temp (°C)	Integration Ratio of DHA Methylene Units in Ketone Form (4.40 ppm) to Hydrate Form (3.56 ppm)	% DHA Monomer (Ketone Form)	% Hydrate
4	1:0.37	73	27
15	1:0.31	76	24
22	1:0.25	80	20
37	1:0.17	85	15
45	1:0.14	88	12
55*	1:0.11	90	10

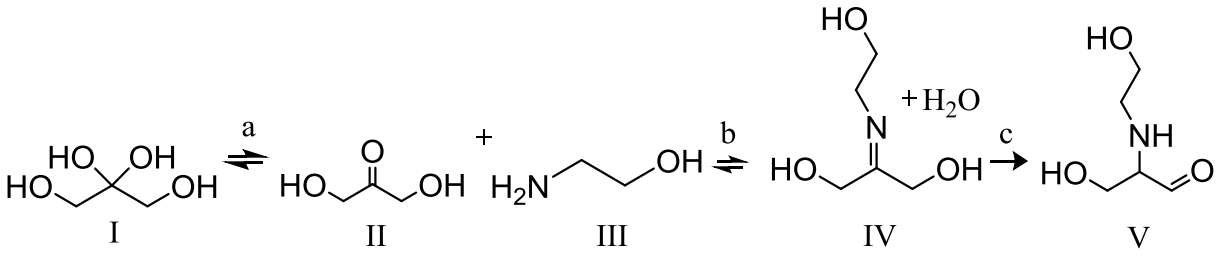

Figure 4.2. Generalized reaction scheme between DHA monomer and ethanolamine. (a) Equilibrium reaction between DHA monomer and DHA hydrate in aqueous solution (b) Schiff base formation (c) Heyns rearrangement. Nomenclature: (I) DHA hydrate (II) DHA monomer (DHA) (III) Ethanolamine (EA) (IV) Schiff base (V) Heyns rearrangement product (HRP).

4.4.2. Kinetic Analysis

The reaction between DHA and amine compounds results in the formation of melanoidins, or "browning", through a Maillard reaction type pathway.[14–16] The Maillard reaction occurs between reducing sugars and primary amines and is largely investigated for its relevance to the food industry as the reaction can lead to various flavor, color and aroma compounds in food products.[17–19] The mechanism is incredibly complex; the reaction is initiated by condensation of an amino group and a sugar, and then a series of rearrangements and further reactions occur that form a complicated network of processes resulting in many different products.[17,20] Kinetic analyses are therefore very difficult to perform and it is for this reason that Maillard kinetics are still not completely understood.[21,22]

The most traditionally accepted mechanistic outline of the Maillard reaction was developed by Hodge and describes the reaction as occurring in three stages: the initial stage, the intermediate stage, and the final stage.[20] The initial stage involves the condensation of sugar and amine compounds to form a Schiff base, followed by rearrangement into Amadori compounds (for aldoses) or Heyns products (for ketoses, such as DHA).[23] The goal of the current study was

to determine Schiff base reaction rate parameters and provide a basis of understanding for how DHA polymers might perform in amine-reactive surface applications. The model system chosen for analysis is the reaction between DHA monomer and ethanolamine (EA). EA was selected as the model amine for its structural simplicity and high water solubility. The reaction scheme is shown in Figure 4.2. In the case of DHA-based polymers, the hydroxyl groups on the C1 and C3 carbons of DHA are transformed into polyesters or polycarbonates. For the Heyns rearrangement to occur, as well as advanced Maillard reaction products, the reactive carbonyl group must possess a free α-hydroxy group.[17,24] Therefore, for the purpose of this study, we analyze only the initial stage of the reaction, using the method of initial rates, to gain information on Schiff base formation. It is important to note that Maillard reactions are highly dependent on parameters such as temperature, pH, amine/sugar starting reagents, and buffer. In the current study, the effect of temperature is evaluated as a starting point; a nonlinear Arrhenius plot may indicate different temperature sensitivities of underlying reactions and provide insight into the limitations of the current model in future studies.

A variety of models have been used to analyze Maillard kinetics ranging from simple to complex.[21,22] Complex approaches, such as multi-response modeling, are superior for gaining reaction mechanistic insight; however, a more simplistic model is employed herein as a first step in understanding the behavior of DHA and EA in solution. In a critical review of Maillard kinetic models, the approach of simplifying the initial stage of reaction to Equation 4.2 is discussed, where A represents unprotonated amino groups, S' is the reducing sugar in open chain form, and ARP is the Amadori rearrangement product.[22]

$$A + S' \xrightarrow{k_{obs}} ARP \quad (eq. 4.2)$$

In the case of measuring the decrease in concentration of reactants in the absence of interfering reactions, it is noted that k_{obs} would reflect the formation of the Schiff's base.[22] In the present work, the DHA and EA model system is simplified to Equation 4.3 where HRP is the Heyns rearrangement product.

$$\text{DHA Hydrate} \rightleftharpoons \text{DHA} + \text{EA} \xrightarrow{k_{obs}} \text{HRP} \qquad (eq.4.3)$$

Assuming a rapid equilibrium of DHA with DHA hydrate, a bimolecular kinetic model is utilized and shown in Equation 4.4, for t=0 seconds, where $v_{t=0}$ is the initial reaction rate and k_{obs} is the observed rate constant for Schiff base formation. The method of initial rates was used to determine reaction orders X and Y, k_{obs}, and an activation energy for the simplified reaction scheme.

$$v_{t=0} = -\left[\frac{d[DHA]}{dt}\right]_0 = k_{obs}[DHA]_0{}^X[EA]_0{}^Y \qquad (eq.4.4)$$

The decrease in DHA concentration during a series of reactions was monitored using various initial concentrations of DHA and EA as described in Table 4.1. The reaction was monitored by recording the decrease in carbonyl absorbance over time. In each curve, absorbance was converted to concentration by applying a directly proportional relationship using the known initial molarity of DHA in solution (average of five consecutive absorbance readings prior to the start of reaction). DHA concentration profiles for each reaction performed at 37^{o}C are shown in Figure 4.3. It is important to note that all reported initial DHA concentrations are 85% of the total DHA monomer administered into the reaction due to the 15% conversion to hydrate upon dissolution at 37^{o}C.

Figure 4.3. Concentration profiles of the ketone form of DHA during reaction with ethanolamine, at 37^{o}C, as determined by carbonyl absorbance readings using real-time infrared spectroscopy. (a) Initial ketone-containing DHA concentration in all trials is 135 mM (total DHA concentration: 158mM). (b) Initial EA concentration in all trials is 200mM. For all trials, n=2.

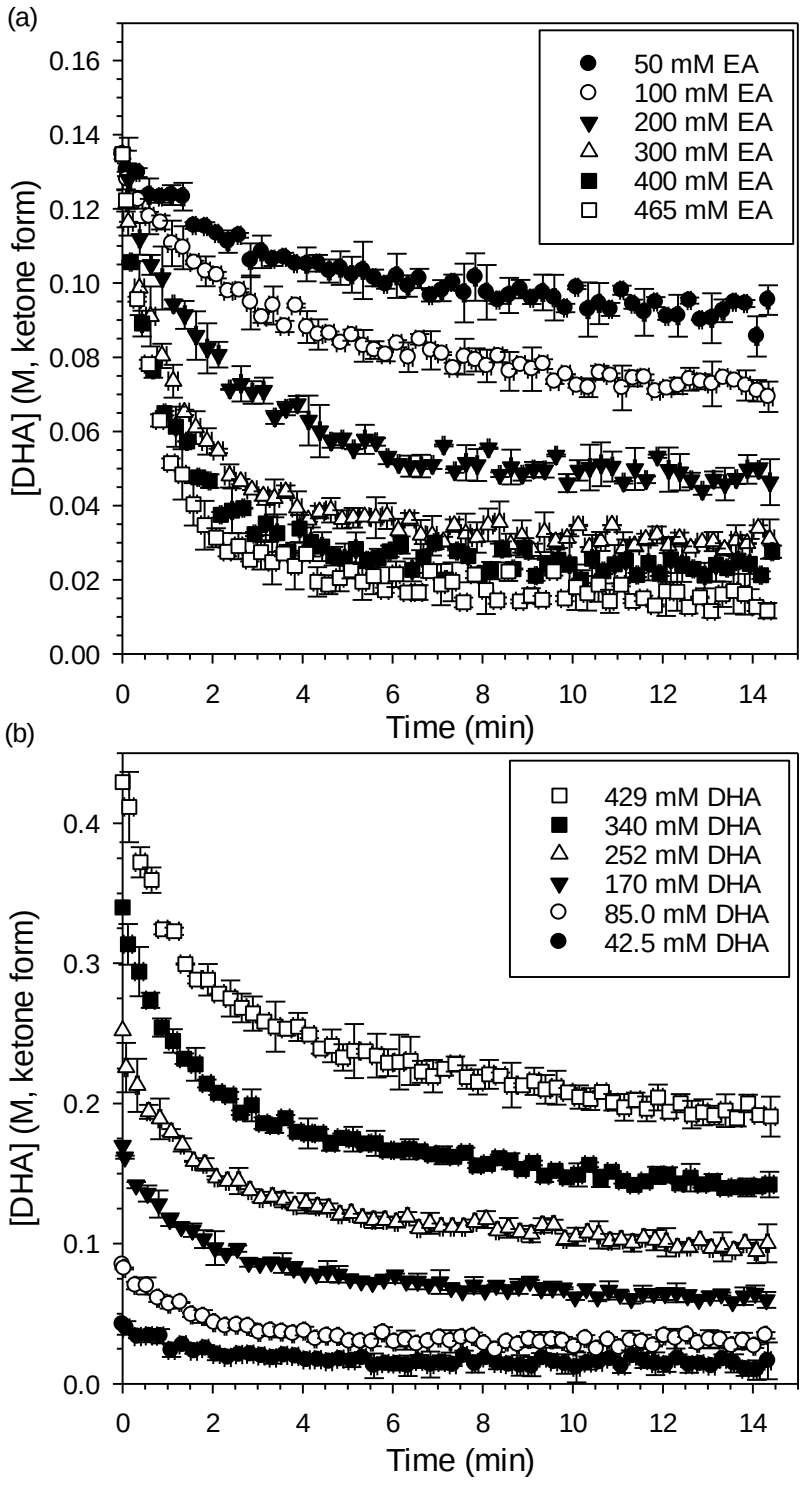
(a)
50 mM EA
100 mM EA
200 mM EA
300 mM EA
400 mM EA
465 mM EA
[DHA] (M, ketone form)
Time (min)
(b)
429 mM DHA
340 mM DHA
252 mM DHA
170 mM DHA
85.0 mM DHA
42.5 mM DHA
[DHA] (M, ketone form)
Time (min)

For each individual reaction, a second order polynomial was fit to the initial 3-5 minutes of the DHA reaction profile. The resulting Equation (4.5) shows DHA concentration as a function of time:

$$[DHA] = at^2 + bt + c \qquad (eq. 4.5)$$

The rate of reaction can be found by taking the derivative of Equation 4.5. The initial rate was determined by computing the derivative at t=0 seconds as described by Equations 4.6 and 4.7. Initial rate data for all trials are shown in Figure 4.4.

$$v = -\frac{d[DHA]}{dt} = -2at - b \quad (eq. 4.6)$$

$$v_{t=0} = -b \qquad (eq. 4.7)$$

Reaction order Y is determined by fitting a power function to the initial rate ($v_{t=0}$) vs. $[EA]_0$ graph in Figure 4.4a according to the following relationships:

$$v_{t=0} = k_{obs}[DHA]_0{}^X[EA]_0{}^Y$$

For $[DHA]_0 = 0.135$M, we define $k_{Yobs} = 0.135^X k_{obs}$

$$v_{t=0} = k_{Yobs}[EA]_0{}^Y$$

Similarly, reaction order X can be determined:

$$v_{t=0} = k_{Xobs}[DHA]_0{}^X$$

where, $k_{Xobs} = 0.2^Y k_{obs}$

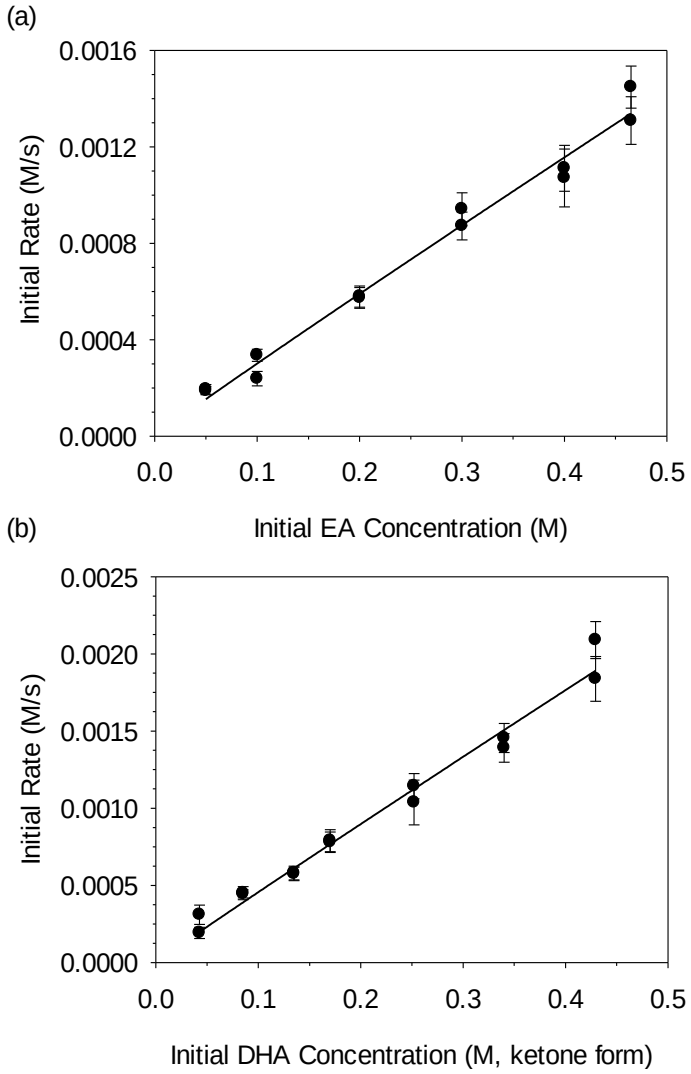

Figure 4.4. (a) Initial rate of reaction for 0.135M DHA (ketone form) reacted with various initial concentrations of EA, at 37°C. Power fit: $y=Ax^B$ where A = $2.81x10^{-3}$; standard error (A) = $1.73x10^{-4}$ and B=0.969; standard error (B) = 0.058. Standard error of estimate (SEE) = $5.91x10^{-5}$ (b) Initial rate of reaction for 0.2M EA reacted with various initial concentrations of DHA, at 37°C. Power fit: $y=A'x^{B'}$ where A' = $4.32x10^{-3}$; standard error (A') = $2.77x10^{-4}$ and B'=0.976; standard error (B') = 0.053. Standard error of estimate (SEE) = $8.57x10^{-5}$. Error bars indicate the standard error of the initial rate (i.e. of the "b" term in each polynomial fit) for each trial.

Table 4.3. Kinetic parameters for a bimolecular model of the initial reaction between DHA and EA at 37°C. Parameters were determined by the method of initial rates using infrared spectroscopy to monitor the DHA-ketone consumption in time.

$Rate=k_{obs}[DHA]^X[EA]^Y$	
k_{obs}	$20.2x10^{-3} \pm 2.4x10^{-3}$ 1/M-s
X	0.976 ± 0.053
Y	0.969 ± 0.058

Once X and Y are determined, k_{obs} can be extracted from k_{Xobs} and k_{Yobs}. A summary of kinetic parameters are shown in Table 4.3. Values of X and Y were close to one, indicating the reaction is likely first order in both reactants. A linear fit of initial rate vs. $[DHA]_0$ yields an R^2 value of 0.981 and a linear fit of initial rate vs. $[EA]_0$ yields R^2=0.985 indicating that the data fits well to a first order rate dependence on each reactant.

4.4.3. Temperature Effect on Reaction Rate

While physiological temperature is the most relevant condition to current applications of DHA polymers, a study of reactivity at various temperatures is of equal importance. For example, in drug delivery applications, protein loading and storage need not occur at physiological temperature. Also, in future applications such as protein immobilizing platforms, room temperature or lower may be of higher importance due to enhanced stability of both polymers and proteins at these temperatures. Therefore, the behavior of reaction in the range of 4°C-55°C was determined. The upper limit was determined based on the reduced stability of DHA monomer at high temperatures.[25]

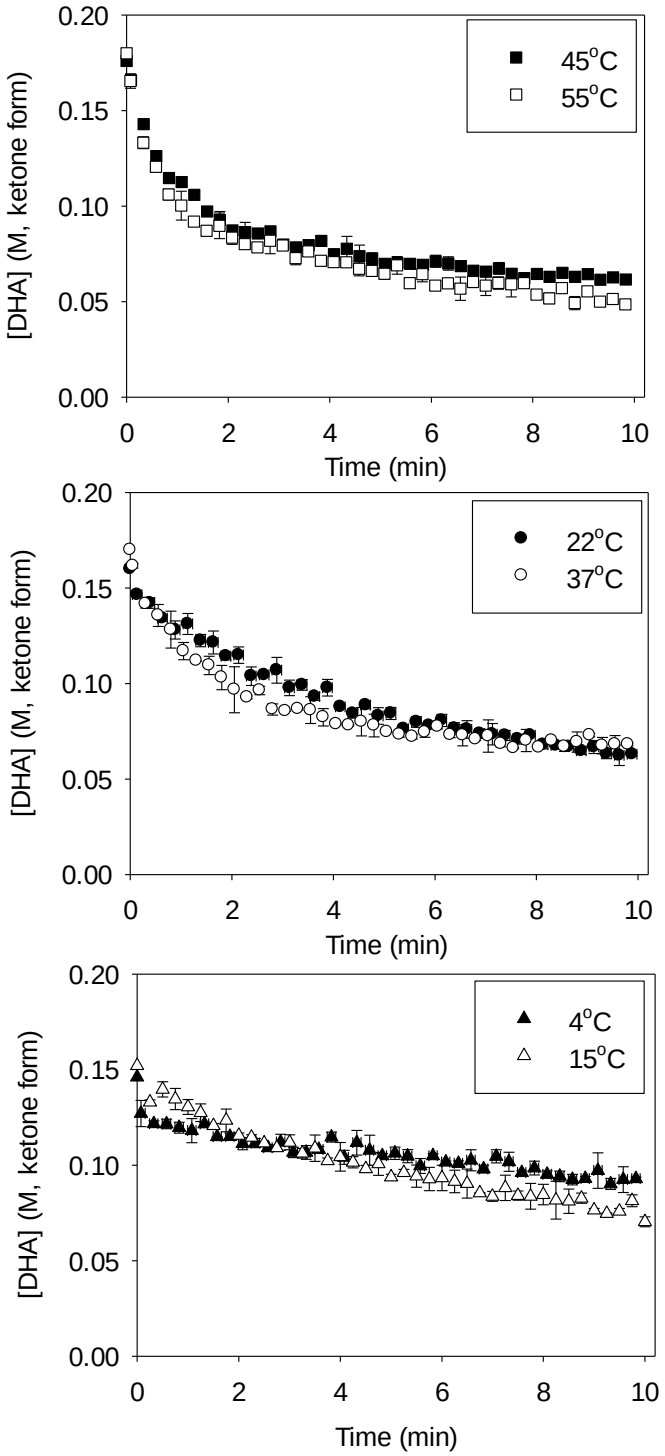

Figure 4.5. DHA reaction profiles with EA at various temperatures. For all trials, total initial DHA monomer (hydrate and ketone) concentration is 200mM and initial EA concentration is also 200mM. Reactions at each temperature were performed in duplicate.

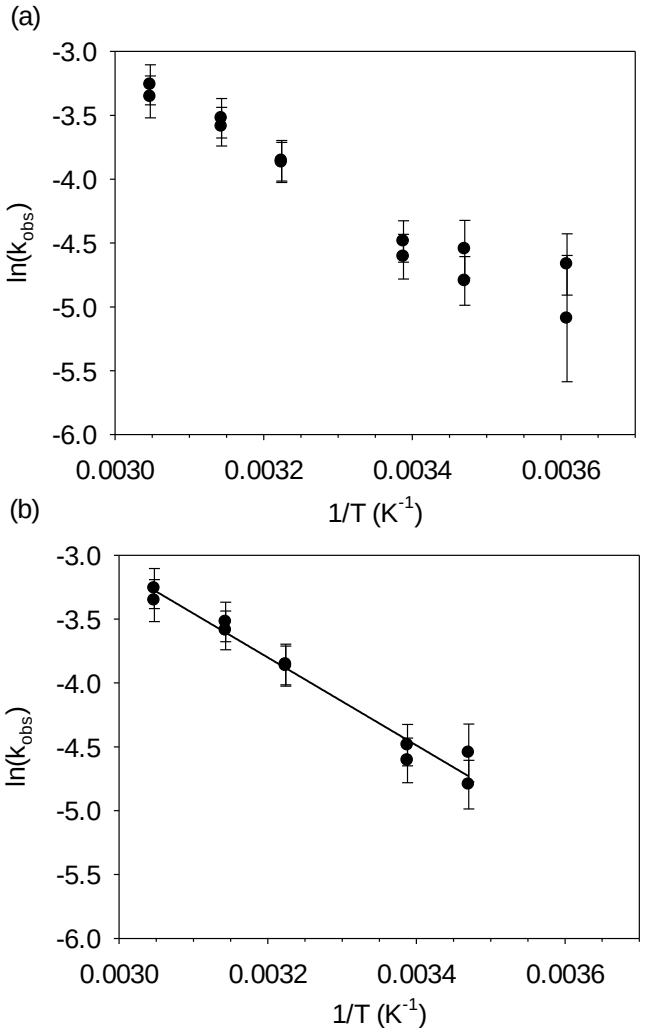

Figure 4.6. Arrhenius plot of rate constants obtained from the reaction of EA and DHA at various temperatures. (a) Two trials were performed at each temperature (4 ^{o}C, 15 ^{o}C, 22 ^{o}C, 37 ^{o}C, 45 ^{o}C, and 55 ^{o}C) and are plotted individually, each with their associated error. Error bars are generated from the propagated standard error of initial rate (i.e. of the "b" term in each polynomial fit) calculated from each trial. (b) Linear fit, excluding the 4^{o}C data point: y=mx+b. m=-3439.7, standard error (m): 202.5; b=7.21, standard error (b): 0.66. R^2 of fit: 0.973.

All experiments were performed with an initial 1:1 molar ratio of total dihydroxyacetone (200mM) and ethanolamine (200mM). Figure 4.5 shows the DHA concentration vs. time curves for each temperature tested. Due the varying percentage of ketone-containing DHA at each temperature, reaction rates are difficult to visually compare based on concentration profiles. Instead, rate constants were extracted and an Arrhenius plot is shown in Figure 4.6a. At 4^{o}C, a rapid initial drop in DHA concentration is observed followed by a slow progression of reaction. The results indicate a shift in the relative reaction rates of multiple underlying processes and therefore the point was excluded from the calculation of an overall E_a (Figure 4.6b). A linear trend is observed which yields an activation energy (E_a) of 28.6 ± 1.7 kJ/mol. The general trend for increasing rate of Schiff base formation with increasing temperature has been observed in different systems,[26–28] however, a direct comparison of kinetic information is challenging due to the dependence on specific sugar, amine, pH, temperature range, kinetic model, and solvent.

4.4.4. pH Determination

The initial pH of reaction for all 37^{o}C trials is shown in Figure 4.7. The concentration of ethanolamine in solution was found to exceed the buffering capacity of 1X PBS; therefore, reactions were performed under basic conditions. The initial pH range of each reaction is 10.43 to 11.03. The rate of Schiff base formation is affected by the concentration of unprotonated amine as well as protonated carbonyl group, which are favored in opposing pH conditions.[21] Investigations of the Maillard reaction often report increased rate of browning under basic conditions,[29–32] however, Namiki claims that the initial stage of reaction should reach a peak rate at weakly acidic pH.[33] Echevarría et al. showed that as pH increased, the overall rate constant for Schiff base formation between pyridoxal 5'-phosphate and L-tryptophan, at temperatures

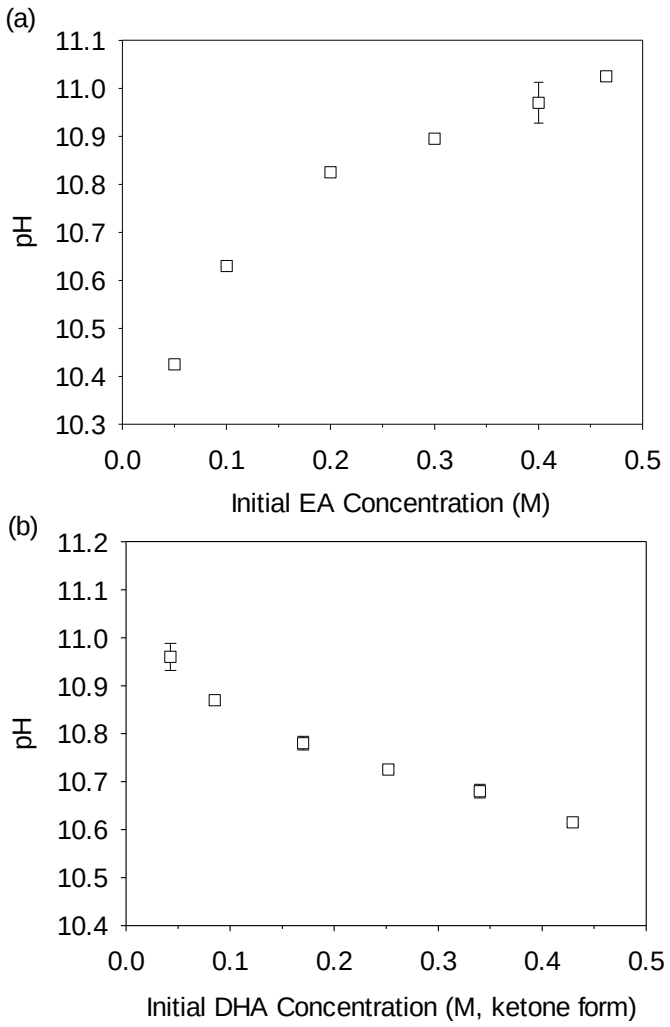

Figure 4.7. (a) Initial pH of reaction for 0.135M DHA (ketone form) reacted with various initial concentrations of EA, at 37^{o}C (b) Initial pH of reaction for 0.2M EA reacted with various initial concentrations of DHA, at 37^{o}C. For all trials, n=2.

between 10°C and 37°C, increased to a maximum and then decreased.[34] Further studies should be performed to measure the effect of pH on Schiff base formation in DHA systems as physiological conditions are most relevant to DHA-based biomaterials.

4.5. Model limitations

A factor to be considered is the possible structural change in DHA monomer due to the pH change at the start of reaction. The ketone to hydrate ratio was calculated based on a solution of DHA monomer in D_2O. Further information is needed to determine the equilibrium structures at the pH range tested in these studies to ensure that pH-based structural transformations do not affect the calculated kinetic parameters. Another important consideration is the assumption that the Heyns rearrangement product and further Maillard products are at low concentrations within the first few minutes of reaction, or convert rapidly to non-carbonyl containing compounds, such that the moiety does not significantly interfere with the ketone absorbance reading. Overall, the model mentioned herein is based on a simplified view of the initial stage of the Maillard reaction; a multiresponse model would be advantageous for gaining enhanced mechanistic information of the system.

4.6. Conclusions

The reaction between DHA monomer and ethanolamine (EA) is studied. The rate of DHA loss, as measured by the change in infrared carbonyl absorption in time, is taken to reflect the rate of Schiff base formation during the initial stages of reaction. Using a simple bimolecular kinetic model and the method of initial rates, the reaction was found to have a first order rate dependence on each reactant, which is reasonable as the concentration of both reactants were

shown to significantly contribute to the reaction rate. Observed rate constants for various temperatures are reported and an activation energy is tabulated based on the Arrhenius equation. The work provides a starting point for analyzing the potential of DHA based materials in amine-reactive surface applications. In the present study, reactions were performed under basic conditions and further work is needed to determine the effect of pH on reaction rate.

4.7. Acknowledgments

This work made use of the Cornell Chemistry NMR Facility; thank you to Dr. Ivan Keresztes for his NMR expertise. Also, thank you Dr. Jun Liang, Russel Algera, and Dr. David Collum for their assistance with real-time infrared spectroscopy and kinetic analysis.

4.8. References

(1) Langowska, K.; Kowal, J.; Palivan, C. G.; Meier, W. A General Strategy for Creating Self-Defending Surfaces for Controlled Drug Production for Long Periods of Time. *J. Mater. Chem. B* **2014**, *2*, 4684–4693.

(2) Zhu, H.; Bilgin, M.; Bangham, R.; Hall, D.; Casamayor, A.; Bertone, P.; Lan, N.; Jansen, R.; Bidlingmaier, S.; Houfek, T.; Mitchell, T.; Miller, P.; Dean, R. A.; Gerstein, M.; Snyder, M. Global Analysis of Protein Activities Using Proteome Chips. *Science.* **2001**, *293*, 2101–2105.

(3) Buck, M. E.; Lynn, D. M. Azlactone-Functionalized Polymers as Reactive Platforms for the Design of Advanced Materials: Progress in the Last Ten Years. *Polym. Chem.* **2012**, *3*, 66–80.

(4) Kirschning, A.; Monenschein, H.; Wittenberg, R. Functionalized Polymers - Emerging Versatile Tools for Solution-Phase Chemistry and Automated Parallel Synthesis. *Angew. Chemie Int. Ed.* **2001**, *40*, 650–679.

(5) Saito, H.; Hoffman, A. S.; Ogawa, H. I. Delivery of Doxorubicin from Biodegradable PEG Hydrogels Having Schiff Base Linkages. *J. Bioact. Compat. Polym.* **2007**, *22*, 589–601.

(6) Macbeath, G.; Schreiber, S. L. Printing Proteins as Microarrays for High-Throughput Function Determination. *Science.* **2000**, *289*, 1760–1763.

(7) Lin, C.; Zhang, Z.; Zheng, J.; Liu, M.; Zhu, X. X. Crosslinked Polyacrolein Microspheres with High Loading of Aldehyde Groups for Use as Scavenger Resins in Organic Synthesis. *Macromol. Rapid Commun.* **2004**, *25*, 1719–1723.

(8) Jia, Y.; Li, J. Molecular Assembly of Schiff Base Interactions: Construction and Application. *Chem. Rev.* **2015**, *115*, 1597–1621.

(9) Hillebrenner, H.; Buyukserin, F.; Kang, M.; Mota, M. O.; Stewart, J. D.; Martin, C. R. Corking Nano Test Tubes by Chemical Self-Assembly. *J. Am. Chem. Soc.* **2006**, *128*, 4236–4237.

(10) Dai, X.; Hong, C.; Pan, C. pH-Responsive Double-Hydrophilic Block Copolymers: Synthesis and Drug Delivery Application. *Macromol. Chem. Phys.* **2012**, *213*, 2192–2200.

(11) Gottlieb, H. E.; Kotlyar, V.; Nudelman, A. NMR Chemical Shifts of Common Laboratory Solvents as Trace Impurities. *J. Org. Chem.* **1997**, *62*, 7512–7515.

(12) Reynolds, S. J.; Yates, D. W.; Pogson, C. I. Dihydroxyacetone Phosphate. Its Structure and Reactivity with Alpha-Glycerophosphate Dehydrogenase, Aldolase and Triose

Phosphate Isomerase and Some Possible Metabolic Implications. *Biochem. J.* **1971**, *122*, 285–297.

(13) Davis, L. The Structure of Dihydroxyacetone in Solution. *Bioorg. Chem.* **1973**, *2*, 197–201.

(14) Shipar, A. H. Formation of the Heyns Rearrangement Products in Dihydroxyacetone and Glycine Maillard Reaction: A Computational Study. *Food Chem.* **2006**, *97*, 231–243.

(15) Blau, S.; Kanof, N.; Simonson, L. Dihydroxyacetone (DHA). A Keratin Coloring Agent. *Arch. Dermatol.* **1960**, *82*, 501–503.

(16) Meybeck, A. A Spectroscopic Study of the Reaction Products of Dihydroxyacetone with Amino Acids. *J. Soc. Cosmet. Chem.* **1977**, *28*, 25–35.

(17) Nursten, H. *The Maillard Reaction. Chemistry, Biochemistry, and Implication*; The Royal Society of Chemistry: Cambridge, 2005.

(18) Van Boekel, M. A. J. . Formation of Flavour Compounds in the Maillard Reaction. *Biotechnol. Adv.* **2006**, *24*, 230–233.

(19) Mottram, D. S. The Maillard Reaction: Source of Flavour in Thermally Processed Foods. In *Flavours and Fragrances: Chemistry, BioProcessing and Sustainability*; Berger, R. G., Ed.; Springer: Germany, 2007; pp 269–284.

(20) Hodge, J. E. Chemistry of Browning Reactions in Model Systems. *J. Agric. Food Chem.* **1953**, *1*, 928–943.

(21) Martins, S. I. F. S.; Jongen, W. M. F.; Boekel, M. A. J. S. Van. A Review of Maillard Reaction in Food and Implications to Kinetic Modelling. *Trends Food Sci. Technol.* **2001**, *11*, 364–373.

(22) Boekel, M. A. J. S. Van. Kinetic Aspects of the Maillard Reaction : A Critical Review. *Nahrung/Food* **2001**, *45*, 150–159.

(23) Dills Jr., W. L. Protein Fructosylation: Fructose and the Maillard Reaction. *Am. J. Clin. Nutr.* **1993**, *58*, 779S – 787S.

(24) Johnson, J. A.; Fusaro, R. M. Alteration of Skin Surface Protein with Dihydroxyacetone: A Useful Application of the Maillard Browning Reaction. In *Maillard Reactions in Chemistry, Food, and Health*; Labuza, T. P., Reineccius, G. A., Monnier, V. M., O'Brien, J., Baynes, J. W., Eds.; The Royal Society of Chemistry: Cambridge, 1994; pp 114–119.

(25) Hettwer, J.; Oldenburg, H.; Flaschel, E. Enzymic Routes to Dihydroxyacetone Phosphate or Immediate Precursors. *J. Mol. Catal. B Enzym.* **2002**, *19-20*, 215–222.

(26) Ge, S.-J.; Lee, T.-C. Kinetic Significance of the Schiff Base Reversion in the Early-Stage Maillard Reaction of a Phenylalanine - Glucose Aqueous Model System. *J. Agric. Food Chem.* **1997**, *45*, 1619–1623.

(27) Hedegaard, R. V.; Frandsen, H.; Skibsted, L. H. Kinetics of Formation of Acrylamide and Schiff Base Intermediates from Asparagine and Glucose. *Food Chem.* **2008**, *108*, 917–925.

(28) Wiesinger, H.; Hinz, H.-J. Kinetic and Thermodynamic Parameters for Schiff Base Formation of Vitamin B6 Derivatives with Amino Acids. *Arch. Biochem. Biophys.* **1984**, *235*, 34–40.

(29) Ashoor, S. H.; Zent, J. B. Maillard Browning of Common Amino Acids and Sugars. *J. Food Sci.* **1984**, *49*, 1206–1207.

(30) Kawashima, K.; Itoh, H.; Chibata, I. Nonenzymatic Browning Reactions of Dihydroxyacetone with Amino Acids or Their Esters. *Agric. Biol. Chem.* **1980**, *44*, 1595–1599.

(31) Renn, P. T.; Sathe, S. K. Effects of pH, Temperature, and Reactant Molar Ratio on L-Leucine and D-Glucose Maillard Browning Reaction in an Aqueous System. *J. Agric. Food Chem.* **1997**, *45*, 3782–3787.

(32) Lento, H. G.; Underwood, J. C.; Willits, C. O. Browning of Sugar Solutions. V. Effect of pH on the Browning of Trioses. *J. Food Sci.* **1960**, *25*, 757–763.

(33) Namiki, M. Chemistry of Maillard Reactions: Recent Studies on the Browning Reaction Mechanism and the Development of Antioxidants and Mutagens. *Adv. Food Res.* **1988**, *32*, 115–184.

(34) Echevarría, G. R.; Santos, J. G.; Basagoitia, A.; Blanco, F. G. Kinetic and Thermodynamic Study of the Reaction of Pyridoxal 5′-Phosphate with L-Tryptophan. *J. Phys. Org. Chem.* **2005**, *18*, 546–551.

CHAPTER 5

CONCLUSIONS AND FUTURE DIRECTIONS

5.1. Conclusions

Metabolic synthons are highly advantageous building blocks for the design of biodegradable and biocompatible materials. Dihydroxyacetone, a three carbon sugar, has been previously used in the synthesis of a variety of biomaterials including hydrogels, strong solids, tablets, and microparticles.[1–5] To date, DHA-based polymers have proven to be promising candidates for drug delivery devices, hemostatic agents, and seroma prevention tools.[2,4,6] Interestingly, previously reported hydrogels based on monomethoxy poly(ethylene glycol) and DHA (MPEG-pDHA) were shown to undergo rapid degradation in aqueous environments.[2] To gain mechanistic insight into the rapid hydrolysis rates, a chemically cross-linked polycarbonate hydrogel containing DHA was synthesized using a glycerol ethoxylate backbone and tri(ethylene glycol) bis(chloroformate) cross-linker. Degradation rates under physiological conditions were studied in comparison to similar hydrogels that differed only in the presence and location of a ketone functional group. It was found that the presence of the ketone on DHA is a major contributor to the observed rapid degradation rates and the short carbon chain length between the ketone and carbonate bonds also plays a significant role. The findings were additionally supported by analysis of degradation products using diffusion-ordered nuclear magnetic resonance spectroscopy. The spectra provided evidence that only carbonate bonds adjacent to the ketone group of DHA degrade on the observed rapid timescale. The results provide valuable insight into the future design of novel DHA-based polymers.

One example of how enhanced mechanistic understanding of degradation rates can shed

light on potential future applications is the current progress toward a biodegradable intraperitoneal shield to facilitate post laparotomy closure. Following abdominal surgery, incised fascia must be carefully sutured to avoid damage to the bowel. Solid objects such as malleable metal sheets or flexible visceral retainers are currently used to protect the bowel up until the final stages of suturing.[7–9] To complete the closure, the device must be removed and therefore leaves the bowel susceptible to accidental damage during the final stitches. Also, such devices increase the risk of a retained surgical instrument which can have severe consequences.[10–15] A biodegradable device would be advantageous in the prevention of such medical errors. The DHA-based hydrogels developed in this study (CC-DHA) are flexible, unlike the previously published DHA-based hydrogels (MPEG-pDHA) which are extrudable through a standard syringe needle.[2] The present work in a mouse model shows that rapid degradation rates of CC-DHA are observed in vivo, as expected, and the gels demonstrate promising biocompatibility and resistance to inadvertent needle puncture. Overall, the development of a biodegradable intraperitoneal shield for post laparotomy closure provides just one example of how mechanistic insight of DHA-based hydrogel degradation can lead to advanced materials for biomedical applications.

An additional advantageous feature of dihydroxyacetone that has yet to be fully exploited is the reactivity of the carbonyl group with amines to form Schiff bases.[16] Zelikin et al. showed that when the alpha hydroxy groups of DHA are used to form polycarbonates, the ketone remains reactive with primary amines.[3] The reactive functionality of DHA-based polymers offers possibilities for drug attachment, chemical cross-linking, and various surface modifications. To gain insight into the timescale of reaction, a model reaction between DHA and ethanolamine was studied using real-time infrared spectroscopy. A simple bimolecular model was evaluated and

progression of the reaction was monitored by measuring the decrease in absorbance of the carbonyl peak. To best avoid the influence of downstream Maillard reaction products, the method of initial rates was employed. Rate constants were determined at various temperatures under basic conditions. Future work should be performed to determine kinetics under physiological conditions.

5.2. Future Directions

5.2.1. DHA-Based Poly(urethane)s

A number of polymeric materials based on DHA have been reported in the literature.[1,3,17–19] Ring opening polymerization (ROP) is the main synthetic route employed, which has thus far enabled the synthesis of polycarbonates and poly(carbonate-ester)s of DHA and various compounds. Recently, polyesters were reported through the use of a Schötten-Baumann type reaction with acyl chloride compounds.[20] Poly(urethane)s, however, have yet to be extensively studied. Poly(urethane) materials haven proven useful in biomedical applications such as tissue engineering scaffolds, drug delivery devices, catheters, and various additional medical devices.[21–24] The extension of DHA-based materials to poly(urethane) linkages may lead to additional polymer properties, for example, a broader array of hydrolytic degradation rates, thereby expanding the potential applications of DHA-based macromolecular structures.

A proposed synthetic route to a urethane linkage between DHA and MPEG is shown in Figure 5.1. Dimethoxy-acetal protected DHA (MeO_2DHA, Figure 5.1) can be synthesized according to a previously established protocol as described in Chapter 1.[3] The resulting polymer is a DHA molecule end-capped with MPEG via urethane bonds. One possible method to gain information on hydrolytic degradation rate is through time course ^{1}H NMR experiments. Peak

integration ratios over time in buffered deuterium oxide solution (using the methoxy group of MPEG as a reference) can shed light on the rate at which DHA is removed from the polymer backbone. Additionally, degradation may be measured by gel permeation chromatography (GPC). Polymer degradation will result in a ~50% decrease in molecular weight. If the molecular weight of MPEG is sufficiently large, the growth of a shoulder or separate viewable peak may be visible in a GPC curve. Overall, the exploration of DHA-based urethanes may lead to interesting new findings for DHA-based polymers and increase the potential for future applications.

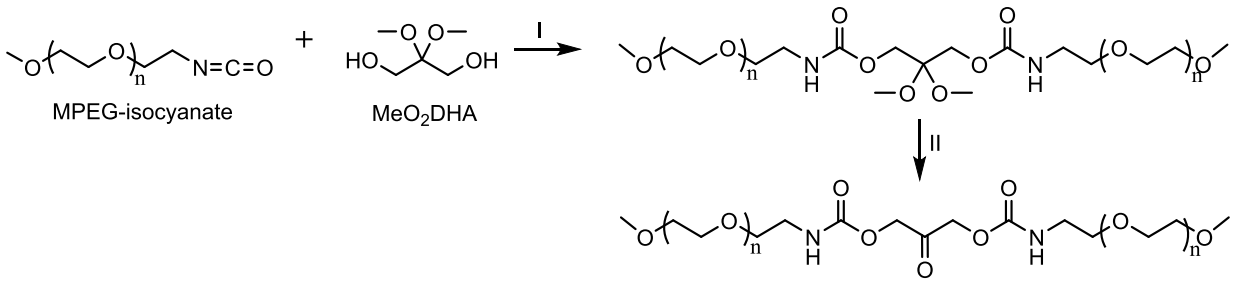

Figure 5.1. Proposed generalized synthetic scheme to urethane linkage between DHA and MPEG. I: organotin catalyst (ex: stannous octoate, dibutyltin dilaurate), 1,2-dichloroethane, elevated temperature range and reaction times should be explored.[25,26] II: triphenylcarbenium tetrafluoroborate, H_2O, DCM.[18]

5.2.2. Intraperitoneal Shield

Tissue adhesions are a common complication after abdominal surgery in which tissues that are not naturally connected become bound by fibrous bands, which can lead to chronic pain, bowel obstruction, and infertility.[27] A study conducted during the mid to late 1980s found that 93% of 210 patients that were undergoing a laparotomy had adhesions from one of their previous abdominal surgeries.[28] Prevention products such as Seprafilm®, a bioresorbable adhesion barrier, have shown success,[29,30] however, there remains a clinical unmet need to develop optimal

adhesion prevention methods. CC-DHA is currently under investigation for use in the prevention of post-operative tissue adhesions in addition to its use as a protective shield to prevent inadvertent bowel injury. A dual-purpose device would be highly advantageous for more efficient and effective abdominal closures.

The initial stages of evaluating CC-DHA as a rapidly degradable abdominal shield have shown promising results, however, several additional studies remain. First, mechanical testing would be important for the intended use of the device, particularly to provide a reader with an enhanced visualization of the material when it cannot be physically obtained. With regard to future development of CC-DHA hydrogels, elimination of the variability among early stage degradation rates, swelling, and sample densities is crucial as it would allow more facile clinical translation. Enhanced water-prevention measures may lead to improvements. A wide-neck flask with an enclosable lid that could be penetrated by a syringe needle would enable a more anhydrous environment while retaining simplistic gel removal post-polymerization. The use of an alternative solvent may also lead to improvements with regard to reagent mixing. The reaction is currently performed as a suspension due to the insolubility of DHA in chloroform. When choosing a solvent, however, it is important to verify that DHA remains in monomeric form when solubilized; synthesizing a linear version of the polymer in a new solvent system would be a recommended starting point for this task.

Lastly, alterations to the chemical composition of CC-DHA can be explored. A transition from the glycerol ethoxylate backbone to a branched PEG containing smaller molecular weight PEG chains can lead to decreased swelling capacity (and adversely, slower degradation rates). Decreased hydrogel swelling may reduce the risk for patient dehydration as well as undesired volume expansion of the device within the abdomen.

5.2.3. Reaction Kinetics

In the present work, a model reaction of DHA and ethanolamine was studied and the method of initial rates was employed to minimize the influence of downstream Maillard products. The present study provides interesting insight into reaction kinetics, but is only the beginning of a larger initiative to understand the potential for DHA-based materials in amine-reactive surface applications. The following experiments are recommended for future progress:

1. A ^{1}H and ^{13}C NMR analysis of the reaction between DHA and ethanolamine should be performed to determine which downstream Maillard reaction products can be observed during the initial stages of reaction. The study presented herein assumes that downstream reaction products are insignificant contributors to IR carbonyl peak changes during the first 3-5 minutes of reaction (Section 4.5). An NMR analysis may provide interesting insight into the assumption.
2. A study across a wider pH range would provide valuable information for the use of DHA-based materials in functional biomedical products. Also, as mentioned in model limitations (Section 4.5), a study should be performed (using NMR spectroscopy in buffered D_2O) to determine if DHA monomer undergoes a structural change at the pH range tested in the aforementioned analysis (pH = 10.43-11.03). It is important to have a thorough understanding of how each pH tested effects the starting structure of DHA (ex: ketone to hydrate ratio).
3. As previously mentioned in Chapter 1, aldehydes are more commonly utilized in Schiff base-forming technologies than ketones due to increased reactivity.[31] A comparison of the reaction rate of DHA with an amine, to that of an aldehyde-containing compound

with the amine, under the same conditions, would be a useful addition to the field. A similar rate constant would provide a compelling argument for use of DHA in amine-reactive surface applications. To avoid the complication of ketone and aldehyde hydration in aqueous solutions, a study performed in an organic solvent may provide a more facile comparison. For increased relevance to DHA-based polymeric materials, a small molecular weight analog of DHA-based polymers (reported by Zelikin et al.[3], discussed in Section 1.5.1.) would be an appropriate compound for analysis. Rapid-Inject NMR[32] is an interesting tool to explore, as opposed to real-time IR, for enhanced tracking of specific compounds as well as higher sensitivity (i.e. lower concentrations of reactants can be detected with high resolution).

4. In future work, it is recommended that the reaction between a polymerized version of DHA and various model amines be studied in aqueous solutions to reduce the concern for interfering structural rearrangements and Maillard reactions. A proposed water soluble linear ester of DHA is shown in Figure 5.2, whereby molecular weight can be adjusted based on PEG size. It is important to note that rapid degradation rates in aqueous environments may prevent the complete elimination of downstream Maillard products during kinetic analysis.

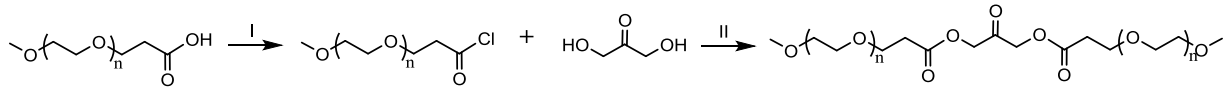

Figure 5.2. Proposed generalized synthetic scheme to ester linkage between DHA and MPEG. I. Thionyl chloride, heat[33,34] II. Chloroform, pyridine.[20]

5.3. References

(1) Zawaneh, P. N.; Doody, A. M.; Zelikin, A. N.; Putnam, D. Diblock Copolymers Based on Dihydroxyacetone and Ethylene Glycol: Synthesis, Characterization, and Nanoparticle Formulation. *Biomacromolecules* **2006**, *7*, 3245–3251.

(2) Zawaneh, P. N.; Singh, S. P.; Padera, R. F.; Henderson, P. W.; Spector, J. A.; Putnam, D. Design of an Injectable Synthetic and Biodegradable Surgical Biomaterial. *Proc. Natl. Acad. Sci. U. S. A.* **2010**, *107*, 11014–11019.

(3) Zelikin, A. N.; Zawaneh, P. N.; Putnam, D. A Functionalizable Biomaterial Based on Dihydroxyacetone, an Intermediate of Glucose Metabolism. *Biomacromolecules* **2006**, *7*, 3239–3244.

(4) Weiser, J. R.; Yueh, A.; Putnam, D. Protein Release from Dihydroxyacetone-Based Poly(carbonate Ester) Matrices. *Acta Biomater.* **2013**, *9*, 8245–8253.

(5) Putnam, D.; Yazdi, S. Biodegradable Compositions and Materials. U.S. Patent WO2008101173, 2008.

(6) Henderson, P. W.; Kadouch, D. J. M.; Singh, S. P.; Zawaneh, P. N.; Weiser, J.; Yazdi, S.; Weinstein, A.; Krotscheck, U.; Wechsler, B.; Putnam, D.; Spector, J. a. A Rapidly Resorbable Hemostatic Biomaterial Based on Dihydroxyacetone. *J. Biomed. Mater. Res. A* **2010**, *93*, 776–782.

(7) Stockwell, D. K. Method and Apparatus for Assisting in Would Closure. US Patent Pub. No. US 2014/0345629, 2014.

(8) Medwid, A. Visceral Retractor. US Patent No. 4,747,393, 1988.

(9) Freedman, D. L. Surgical Aid. US Patent No. 6,736,141, 2004.

(10) Stawicki, S. P.; Evans, D. C.; Cipolla, J.; Seamon, M. J.; Lukaszczyk, J. J.; Prosciak, M. P.; Torigian, D. A.; Doraiswamy, V. A.; Yazzie, N. P.; Gunter, O. L.; Steinberg, S. M. Retained Surgical Foreign Bodies: A Comprehensive Review of Risks and Preventive Strategies. *Scand. J. Surg.* **2009**, *98*, 8–17.

(11) Gayer, G.; Petrovitch, I.; Jeffrey, R. B. Foreign Objects Encountered in the Abdominal Cavity at CT. *Radiographics* **2011**, *31*, 409–428.

(12) Cima, R. R.; Kollengode, A.; Storsveen, A. S.; Weisbrod, C. A.; Deschamps, C.; Koch, M. B.; Moore, D.; Pool, S. R. A Multidisciplinary Team Approach to Retained Foreign Objects. *Jt. Comm. J. Qual. Patient Saf.* **2009**, *35*, 123–132.

(13) Gawande, A. A.; Studdert, D. M.; Orav, E. J.; Brennan, T. A.; Zinner, M. J. Risk Factors for Retained Instruments and Sponges After Surgery. *N. Engl. J. Med.* **2003**, *348*, 229–235.

(14) Murdock, D. B. Trauma : When There's No Time to Count. *AORN J.* **2008**, *87*, 329–330.

(15) Lincourt, A. E.; Harrell, A.; Cristiano, J.; Sechrist, C.; Kercher, K.; Heniford, B. T. Retained Foreign Bodies After Surgery. *J. Surg. Res.* **2007**, *138*, 170–174.

(16) Ricapito, N. G.; Ghobril, C.; Zhang, H.; Grinstaff, M. W.; Putnam, D. Synthetic Biomaterials from Metabolically Derived Synthons. *Chem. Rev.* **2016**, *116*, 2664–2704.

(17) Weiser, J. R.; Zawaneh, P. N.; Putnam, D. Poly(carbonate-Ester)s of Dihydroxyacetone and Lactic Acid as Potential Biomaterials. *Biomacromolecules* **2011**, *12*, 977–986.

(18) Simon, J.; Olsson, J. V.; Kim, H.; Tenney, I. F.; Waymouth, R. M. Semicrystalline Dihydroxyacetone Copolymers Derived from Glycerol. *Macromolecules* **2012**, *45*, 9275–9281.

(19) Guerin, W.; Helou, M.; Slawinski, M.; Brusson, J.-M.; Carpentier, J.-F.; Guillaume, S. M. Macromolecular Engineering via Ring-Opening Polymerization (3): Trimethylene Carbonate Block Copolymers Derived from Glycerol. *Polym. Chem.* **2014**, *5*, 1229–1240.

(20) Korley, J. N.; Yazdi, S.; McHugh, K.; Kirk, J.; Anderson, J.; Putnam, D. One-Step Synthesis, Biodegradation and Biocompatibility of Polyesters Based on the Metabolic Synthon, Dihydroxyacetone. *Biomaterials* **2016**, *98*, 41–52.

(21) Burke, A.; Hasirci, N. Polyurethanes in Biomedical Applications. In *Biomaterials: From Molecules to Engineered Tissues*; Hasirci, N., Hasirci, V., Eds.; Springer Science+Business Media, LLC: New York, New York, 2004; pp 83–105.

(22) Zdrahala, R.; Zdrahala, I. Biomedical Applications of Polyurethanes: A Review of Past Promises, Present Realities, and a Vibrant Future. *J. Biomater. Appl.* **1999**, *14*, 67–90.

(23) Fernando, S.; McEnery, M.; Guelcher, S. A. Polyurethanes for Bone Tissue Engineering. In *Advances in Polyurethane Biomaterials*; Cooper, S. L., Guan, J., Eds.; Woodhead Publishing, Elsevier Ltd.: Duxford, UK Cambridge, MA, USA and Kidlington, UK, 2016; pp 481–496.

(24) Cherng, J. Y.; Hou, T. Y.; Shih, M. F.; Talsma, H.; Hennink, W. E. Polyurethane-Based Drug Delivery Systems. *Int. J. Pharm.* **2013**, *450*, 145–162.

(25) Lamba, N. M. K.; Woodhouse, K. A.; Cooper, S. L. *Polyurethanes in Biomedical Applications*; CRC Press: Boca Raton, London, New York, Washington, D.C., 1998.

(26) Pan, J.; Li, G.; Chen, Z.; Chen, X.; Zhu, W.; Xu, K. Alternative Block Polyurethanes Based on poly(3-Hydroxybutyrate-Co-4-Hydroxybutyrate) and Poly(ethylene Glycol). *Biomaterials* **2009**, *30*, 2975–2984.

(27) Broek, R. P. G. ten; Issa, Y.; van Santbrink, E. J. P.; Bouvy, N. D.; Kruitwagen, R. F. P. M.; Jeekel, J.; Bakkum, E. A.; Rovers, M. M.; Goor, H. van. Burden of Adhesions in Abdominal and Pelvic Surgery: Systematic Review and Met-Analysis. *BMJ* **2013**, *347*, f5588.

(28) Menzies, D.; Ellis, H. Intestinal Obstruction from Adhesions--How Big Is the Problem? *Ann. R. Coll. Surg. Engl.* **1990**, *72*, 60–63.

(29) Diamond, M. P.; Burns, E. L.; Accomando, B.; Mian, S.; Holmdahl, L. Seprafilm Adhesion Barrier: (2) A Review of the Clinical Literature on Intraabdominal Use. *Gynecol. Surg.* **2012**, *9*, 247–257.

(30) Huang, H.; Deng, M.; Jin, H.; Dirsch, O.; Dahmen, U. Preventing Intra-Abdominal Adhesions with a Sodium Hyaluronate Carboxymethylcellulose Membrane Enabled Visualization of Hepatic Microcirculation. *Int. J. Surg.* **2013**, *11*, 935–943.

(31) Jia, Y.; Li, J. Molecular Assembly of Schiff Base Interactions: Construction and Application. *Chem. Rev.* **2015**, *115*, 1597–1621.

(32) Denmark, S. E.; Eklov, B. M.; Yao, P. J.; Eastgate, M. D. On the Mechanism of Lewis Base Catalyzed Aldol Addition Reactions: Kinetic and Spectroscopic Investigations Using Rapid-Injection NMR. *J. Am. Chem. Soc.* **2009**, *131*, 11770–11787.

(33) Jo, S.; Engel, P. . S.; Mikos, A. G. Synthesis of Poly (ethylene Glycol)-Tethered Poly (propylene Fumarate) and Its Modification with GRGD Peptide. *Polymer (Guildf).* **2000**, *41*, 7595–7604.

(34) Kohler, N.; Fryxell, G. E.; Zhang, M. A Bifunctional Poly(ethylene Glycol) Silane Immobilized on Metallic Oxide-Based Nanoparticles for Conjugation with Cell Targeting Agents. *J. Am. Chem. Soc.* **2004**, *126*, 7206–7211.

APPENDIX A

SUPPLEMENTARY INFORMATION FOR CHAPTER 2: INSIGHT INTO THE UNEXPECTEDLY RAPID DEGRADATION OF DIHYDROXYACETONE-BASED HYDROGELS

(Contributors: Jonathan Mares and Daniel Petralia)

Figure A.1. Image of CC-DHA polymer shortly after synthesis, prior to purification. The lower left panel shows the stirbar immobilized within the cross-linked gel.

*Appendix A is reprinted with permission from Ricapito, N. G.; Mares, J.; Petralia, D.; Putnam, D. Insight into the Unexpectedly Rapid Degradation of Dihydroxyacetone-Based Hydrogels. *Macromol. Chem. Phys.* **2016.** DOI: 10.1002/macp.201600170. Copyright (2016) Wiley-VCH Verlag GmbH & Co. KGaA, Weinheim.

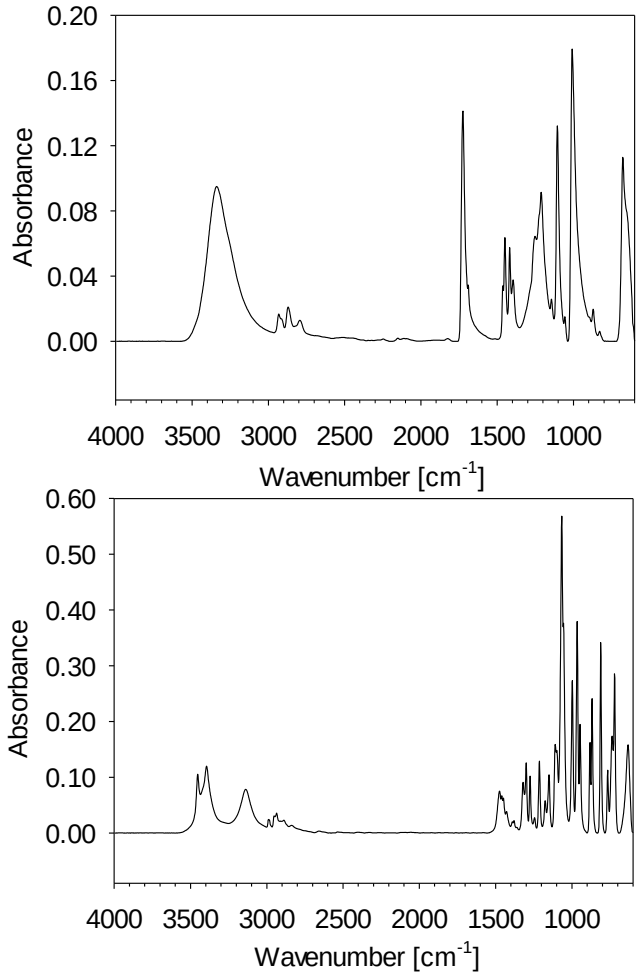

Figure A.2. FT-IR spectra of solid dihydroxyacetone monomer generated by recrystallization from 2-propanol (top) and dimer as purchased from Sigma-Aldrich (bottom). The peak at 1724 cm^{-1} corresponds to the ketone group of DHA, which does not appear in the dimer spectrum.

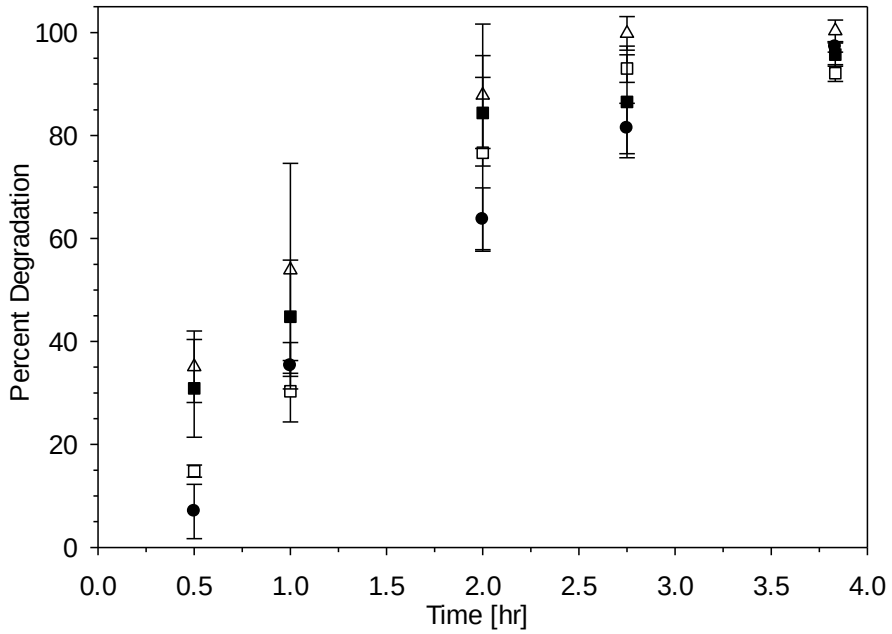

Figure A.3. Percent degradation of four different batches of CC-DHA hydrogels. N=3 per time point, for each batch. (■) Batch 1 (△) Batch 2 (●) Batch 3 (□) Batch 4.

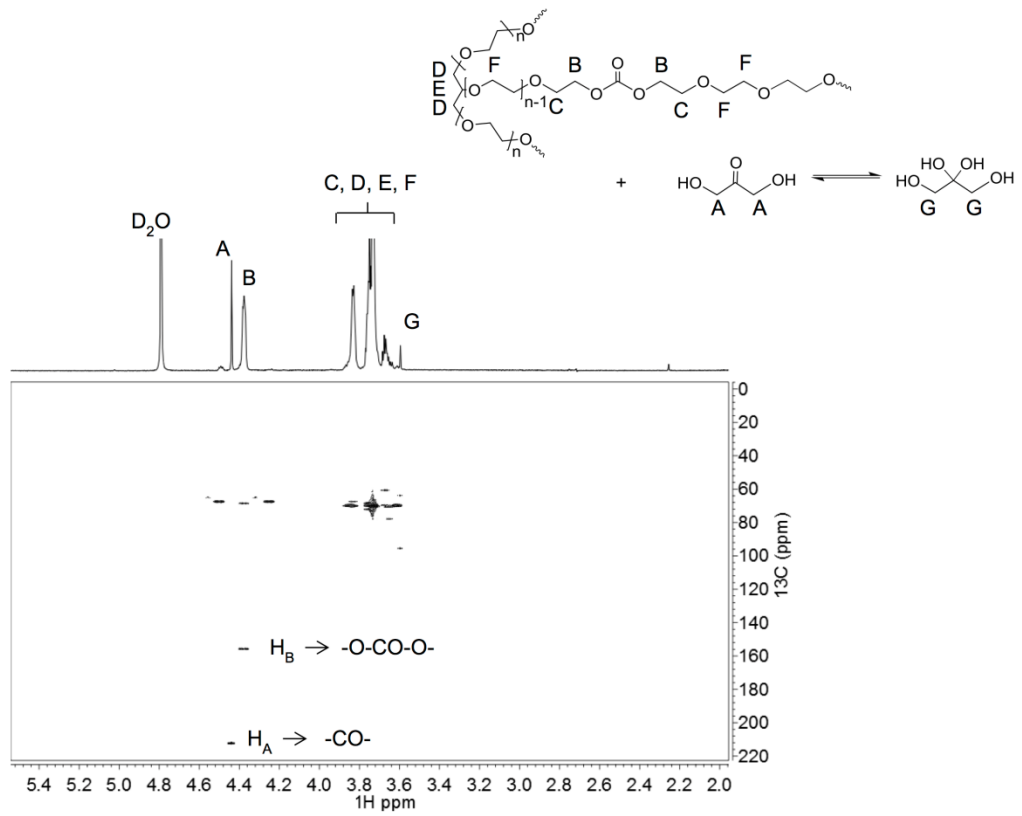

Figure A.4. ^{1}H-^{13}C HMBC NMR spectrum of hydrogel degradation products after 7 hours of rotation in D_2O/PBS at 37°C. The symbol (~) symbol serves to indicate the random and unknown sequence of GE and TEGBC repeat units in the backbone. The ^{1}H NMR trace is magnified (compared to Figure 7a) for more facile interpretation. The spectrum was recorded on a Varian INOVA spectrometer operating at 150 MHz for ^{13}C observation and 600 MHz for ^{1}H observation. The experiment was acquired with a 0.3 s acquisition time, 8 scans per increment, and 1.0 s relaxation delay.

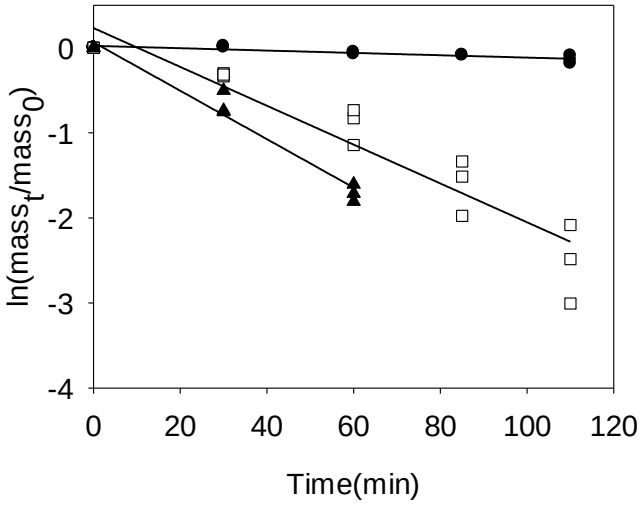

Figure A.5. Determination of fitting parameters for the degradation profiles of CC-DHA hydrogels in solutions of varying pH, at 37°C. The fraction of hydrogel mass remaining (dry, lyophilized) in time was fit to first order kinetics. Time points were measured in triplicate and all three samples at each time point are included. Parameters are as follows: (●) pH = 6, y = -0.0014x + 0.022, R^2=0.814, Std. error on slope: 0.0002, (□) pH= 7, y = -0.023x + 0.23, R^2=0.899, Std. error on slope: 0.002, (▲) pH = 8, y = -0.028x + 0.063, R^2=0.971, Std. error on slope: 0.002. At pH=8, a sample was observed to completely degrade in 85 minutes. Therefore, only the initial stages of degradation were evaluated for first order kinetics.

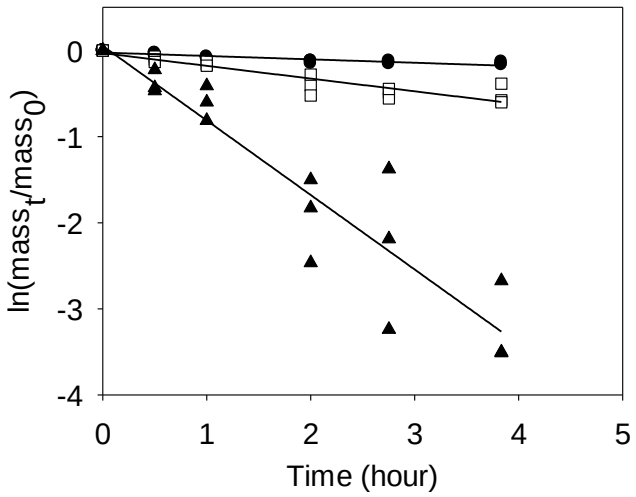

Figure A.6. Determination of fitting parameters for the degradation profiles of CC-DHA hydrogels in PBS, pH=7.4, at various temperatures. The fraction of hydrogel mass remaining (dry, lyophilized) in time was fit to first order kinetics. Time points were measured in triplicate and all three samples at each time point are included. Parameters are as follows: (●) 4°C: $y = -0.039x - 0.024$, R^2=0.836, Std. error on slope = .004 (□) Room temperature: $y = -0.1477x – 0.031$, $R^2 = 0.856$, Std. error on slope = 0.02, and (▲) 37°C: $y = -0.87x + 0.052$, R^2=0.883, std. error on slope = 0.08

APPENDIX B

SUPPLEMENTARY INFORMATION FOR CHAPTER 3: A BIODEGRADABLE INTRAPERITONEAL SHIELD WITH SHORT RESIDENCE TIME TO FACILITATE ABDOMINAL CLOSURE AFTER LAPAROTOMY

The research presented in this appendix was performed in collaboration with Dr. Jason A. Spector and his research team at the Laboratory of Bioregenerative Medicine and Surgery, in the Department of Surgery, Division of Plastic Surgery, at Weill Cornell Medical College, New York, NY. Contributors: Kerry A. Morrison and Dr. Omer Kaymakcalan.

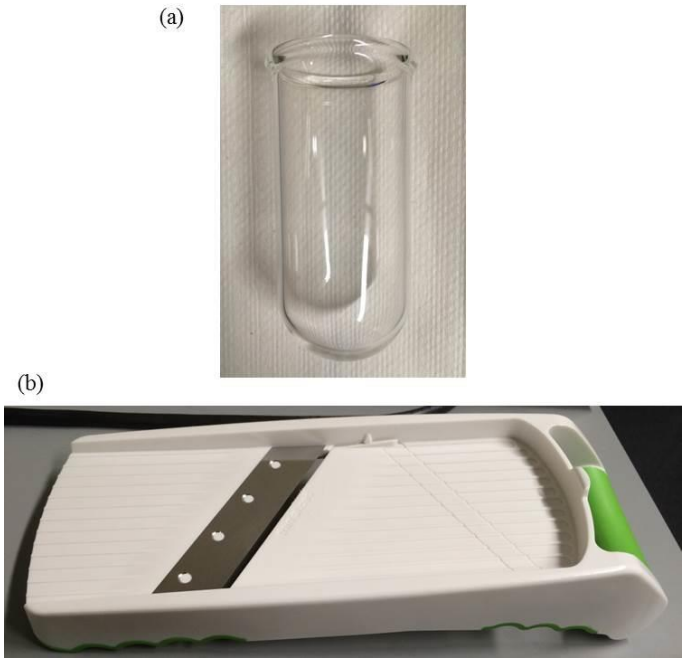

Figure B.1. (a) Reaction flask used for the synthesis of CC-DHA hydrogel disks of 20mm and 8mm diameter. (b) Progressive Prep Solutions Multi Slicer with the "thin slices" insert used for slicing of CC-DHA hydrogels.

Table B.1. CC-DHA hydrogel disk (8 mm diameter, approximately 2mm thickness) degradation results at various time points following in vivo intraperitoneal implantation into a mouse model. Results also include fluid volume within the abdominal cavity at each time point.

Evaluation Time (hr)	CC-DHA Initial Mass (mg)	CC-DHA Mass at Evaluation (mg)	Fluid in Abdomen at Evaluation Time (mL)
3	88.4	0	0.5
	82.6	0	0.5
	95.1	0	0.5
	101.6	0	0.5
6	94.1	0	0.3
	71.3	0	0.3
	94.4	0	0.3
	72.9	0	0.3
9	82.3	0	0
	62.6	0	0
	63.6	0	0
	90.1	0	0
24	58.4	0	0
	83.6	0	0
	62.1	0	0
	98.6	0	0
8 (days)	82.9	0	0

APPENDIX C

SUPPLEMENTARY INFORMATION FOR CHAPTER 4: KINETIC ANALYSIS OF THE REACTION BETWEEN DIHYDROXYACETONE AND ETHANOLAMINE

The ReactIR silicon-based sensor was tested for chemical compatibility using a silicon test chip provided by Mettler-Toledo AutoChem, Inc.

Procedure:

Phosphate buffered saline (5.0mL) was injected into a 10mL beaker, in a 37^{o}C water bath, stirred, and allowed 10min to reach the appropriate temperature. A pH probe was then inserted into the solution. Next, 200µL of a DHA monomer solution (Table C.2, line 3) was injected such that the final reaction concentration was 0.158M DHA (total, both ketone and hydrate forms). Next, ethanolamine (150µL) was injected to yield a final concentration of 0.465M ethanolamine. The resulting pH was immediately recorded, after which the pH probe and stir bar were removed and the silicon test chip (initial mass: 0.1743 g) was inserted. After 30 min, the chip was removed, washed with DI water, gently dried, and re-weighed. The process was repeated three times using the same chip to test for mass loss after repeated exposure. No mass loss was observed, as shown in table C.1.

Table C.1. Analysis of the chemical compatibility of the silicon-based ReactIR sensor with brief and repeated exposure (30 minutes per trial) to a solution of DHA (0.158M, total) and ethanolamine (0.465M), at 37^{o}C. Initial chip mass: 0.1743 g. No mass loss was observed in the allotted time.

Trial	pH	Final Mass (g)
1	11.02	0.1746
2	11.03	0.1744
3	11.06	0.1745

Table C.2. Preparation of concentrated DHA solutions in PBS (pH=7.4) for injection into IR-reaction vessel. Each preparation yields a different initial concentration of DHA for reaction with ethanolamine. Total volume (column C) was measured using a volumetric pipet. *The highest initial concentration of DHA (0.505M) was not obtainable at an injection volume of 200µL due to solubility, therefore 250µL was injected instead. In this case, the EA injection volume was reduced from 150µL to 100µL.

	Column A	Column B	Column C	Column D
Total Initial DHA (M)	**DHA (g) added to an empty 4mL glass scintillation vial**	**PBS (µL) added to DHA in column A**	**Total volume (µL) of DHA and PBS, when mixed (Column A + Column B)**	**Volume of column C solution injected into reaction (µL)**
0.050	0.0482	380	400	200
0.100	0.0964	352	400	200
0.158	0.1928	400	505	200
0.200	0.1928	284	400	200
0.296	0.2892	236	405	200
0.400	0.3856	190	400	200
0.505	0.4820	190	495	*250

Table C.3. Preparation of concentrated EA solutions in PBS (pH=7.4) for injection into IR-reaction vessel. Each preparation yields a different initial concentration of EA for reaction with DHA. To achieve the desired injection concentration, an arbitrary mass of EA was measured, volume was calculated according to density (EA density = 1.012g/mL), and remaining PBS needed was determined.

Initial EA in Reaction (M)	Concentration of EA in 0.15 mL injection-sample (g/mL)
0.050	0.109
0.100	0.218
0.200	0.436
0.300	0.653
0.400	0.871
0.465	1.012 (Pure EM)

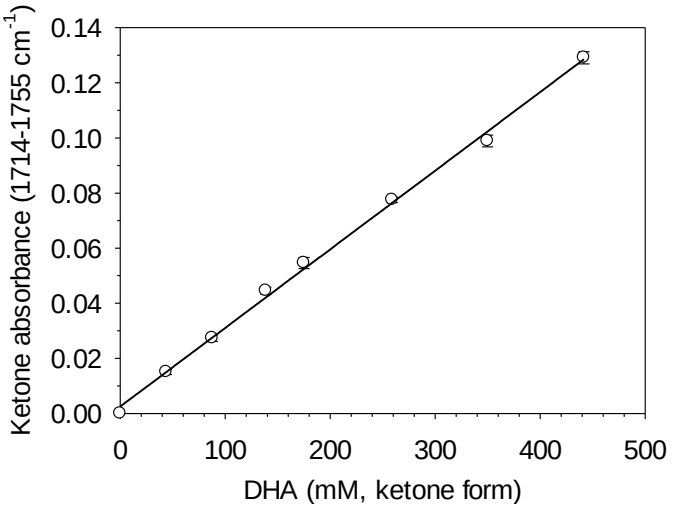

Figure C.1. Change in IR ketone absorbance vs. the concentration of DHA in monomeric ketone form, at 37°C, in PBS, pH=7.4. Data was collected using a ReactIR 4000. The concentration of DHA in ketone form was taken to be 85% of the total concentration of DHA monomer injected into solution. For DHA= 163mM (total), n=48 total individual measurements: 12 separate trials, where each trial has 4 data points collected. For all other DHA concentrations, n=8 data points: 2 trials with 4 points each. Linear fit: $y=2.85x10^{-4}x+0.0025$, $R^2=0.998$.